Einfluss pflanzlicher Toxine auf das Mikrobiom

von *Spodoptera littoralis*

Dissertation

zur Erlangung des akademischen Grades

Doctor rerum naturalium (Dr. rer. nat.)

Vorgelegt dem Rat der Biologisch-Pharmazeutischen Fakultät der
Friedrich-Schiller-Universität Jena

seit 1558

Von Master-Biochemiker

Novoselov Alexey Lvovich

geboren am 14.06.1984 in Moskau

Gutachter:

1. Prof. Dr. Wilhelm Boland

Abteilung für Bioorganische Chemie, Max-Planck-Institut für Chemische Ökologie, Jena

2. Prof. Dr. Erika Kothe

Institut für Mikrobiologie, Biologisch-Pharmazeutische Fakultät, Friedrich Schiller Universität, Jena

3. Prof. Dr. Alexander V. Oleskin

Abteilung für allgemeine Ökologie, Biologische Fakultät, Staatliche Universität Moskau, Vorobiev Berg, Moskau 119991, Russland

Datum der Verteidigung: 12.10.17

für meine Eltern

Impact of plant toxins on the gut microbial community of *Spodoptera littoralis*

Dissertation

Faculty for Biology and Pharmacy

Friedrich-Schiller-University in Jena

seit 1558

Master of Biochemistry

Novoselov Alexey Lvovich

Date of birth: 14 Jun 1984 in Moscow

Supervisors:

1. Prof. Dr. Wilhelm Boland

Department of Bioorganic Chemistry, Max Planck Institute for Chemical Ecology, Jena

2. Prof. Dr. Erika Kothe

Institute of Microbiology, Faculty for Biology and Pharmacy, Friedrich Schiller University of Jena, Jena

3. Prof. Dr. Alexander V. Oleskin

General Ecology Department, Biology School, Moscow State University, Vorobiev Hills, Moscow 119991, Russia

The date of defense: 12.10.17

TABLE OF CONTENTS

Abbreviations and symbols

MWAS   microbiome-wide association studies

PCA   principal component analysis

OTUs   operation taxonomic units

Aldh   Aldehyde dehydrogenase

8-MOP   8-methoxypsoralen

3-NPA   3-nitropropionic acid

LD50   Lethal Dose, 50%

FAAs   amides of fatty acids,

L-Val   L-valine

L-Ile   L-isoleucine

L-Leu   L-leucine

L-Phe   L-phenylalanine

L-Tyr   L-tyrosine

1. Introduction

In the last decade, the amount of publications on microbiome research hase increased enormously. In 2012, around 800 publications were published, while last year this number surpassed 2000 (fig. 1). Research on the microbiome has a significant effect on different fields of the life sciences, health care, agriculture, and the food industry (Arnold et al., 2016).
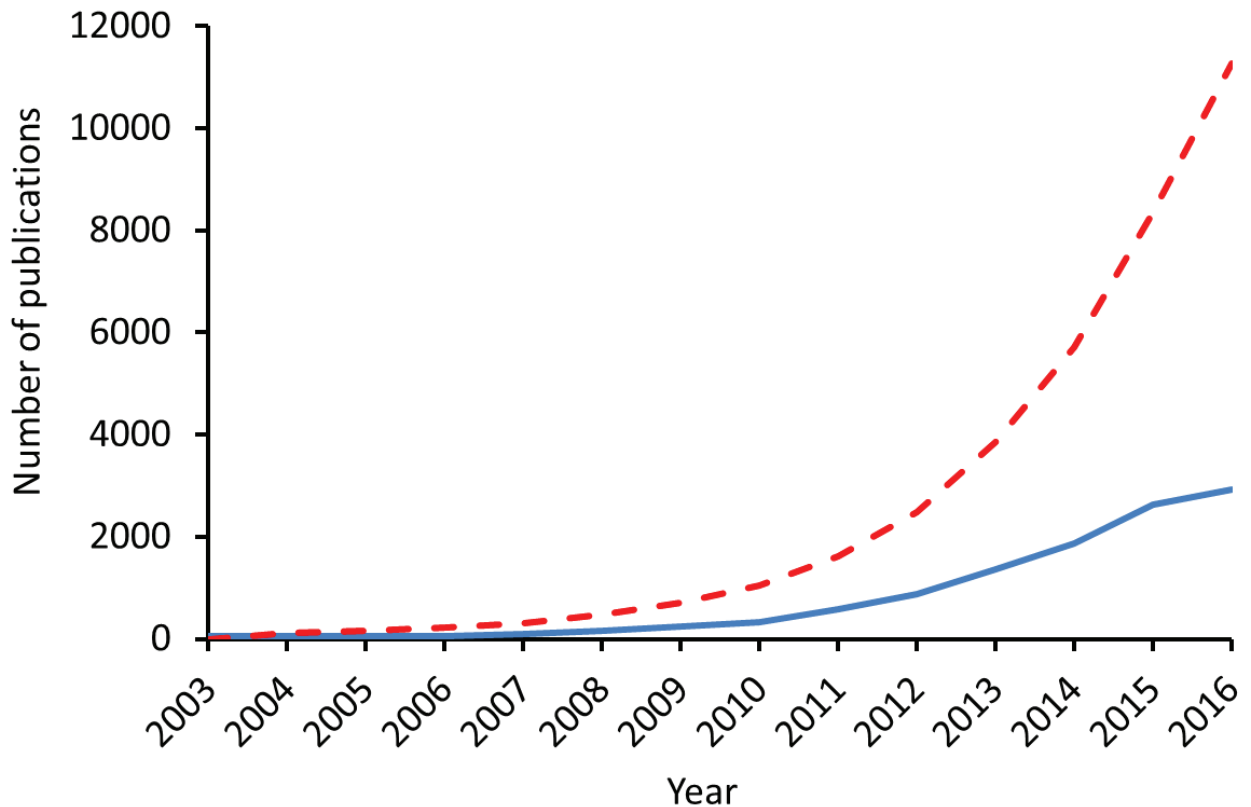

Figure 1. Source: Thomas Reuters Web of Science, accessed 23.12.2016., using the title search terms ("gut microbiota", "insect microbiome", "microbiome", "human microbial", "gut ecology") over the period of 2003 to 2016. ——— indicates number of publication, — — — indicates cumulative article types.

Guts of animals are populated by myriads of bacteria which are in close interaction with each other and the host. Some functions of microbiota have been known since decades. For example, vitamin biosynthesis and essential amino acid supplying. But some functions were recognized only recently.

Microbiome-wide association studies (MWAS) can link whole microbiomes to a variety of disorders like obesity, cardiovascular disease and colon cancer, among others. However, causal and network-based interactions remain unclear in many cases (Gilbert et al., 2016).

The gut microbial community could be rather stable and may be constantly presented in certain groups of the host population. Sequences of 39 individual metagenomes of Europeans from 6 countries have revealed 3 enterotypes in human population. The phylogenetic composition of the newly sequenced samples confirmed that the Firmicutes and Bacteroidetes phyla constitute the vast majority of a human gut microbiome. A principal component analysis (PCA) of 33 samples showed three distinct clusters, called enterotypes. Each of these three enterotypes was identifiable by the dominance of levels of one of three genera: *Bacteroides* (enterotype 1), *Prevotella* (enterotype 2) and *Ruminococcus* (enterotype 3). These enterotypes were densely populated areas in a multidimensional space of community composition. They were likely to characterize individuals, though they were not geographically specific as was recognized across subjects from different continents: Asia, Europe, and the Americas. In addition, individual host properties such as body mass index, age, and gender could not explain the observed enterotypes (Manimozhiyan et al., 2011).

The gut microbiome of animals significantly differs from communities of free living bacteria. Groups of researchers from Cornell University have collected 99,801 full length 16S rRNA gene sequences of 464 samples published in 181 studies. The library was obtained with a cloning of 16S rRNA gene in the plasmid followed by sequencing. The sampling resulted in only 500-900 sequences per sample and therefore was not a deep sequencing. However, different patterns were observed in the distribution of phyla in guts collected from organisms in different habitats. Across vertebrate and invertebrate gut samples, which included human, insect and worm guts, the Firmicutes and Bacteroidetes were numerically the most dominant phyla (fig. 2). Other phyla tended to have higher representation in non-gut samples. The operation taxonomic units (OTUs) shared between gut samples of humans and insects are Firmicutes, followed by a smaller number from the Bacteroidetes. In contrast, free-living communities shared OTUs from the Lentisphaerae, Actinobacteria, Acidobacteria phyla, as well as many others (Ley et al., 2008). Compared to humans and other vertebrates, microbiomes of insects have not been extensively studied.

Surprisingly, populations of honey bees from different geographical locations shared common cores of bacteria population. The core microbiome of the honey bee is represented by Lactobacillus and Ralstonia (Yuna et al., 2014). Gut microbial communities are closely associated with the host and play an essential role for the insects. Microbes carry out numerous biochemical functions and contribute to numerous processes.

Engel and Moran proposed several functions of bacteria in insect guts. It has been shown that the gut microbiomes of the bumble bee (*Bombus terrestri*), desert locust (*Schistocerca gregaria*), and various mosquito species provide colonization resistance against pathogens or parasites. Gut microbiota in the hindgut of termites are involved in the degradation of cellulose and in nutrient supplementation, such as the synthesis of vitamins and essential amino acids or in nitrogen fixation. Gut bacteria have also been shown to degrade toxins that are ingested with the diet. In a number of insects, gut bacteria produce molecules involved in intraspecific and interspecific communication, such as pheromones and kairomones (fig. 3). In *Drosophila melanogaster*, the commensal gut microbiota have been shown to be involved in intestinal cell renewal and promotion of systemic growth. Self-renewal operations of the *D. melanogaster* midgut epithelium are affected by gut bacteria. Agnotic *D. melanogaster* have reduced intestinal stem cell pools, slower epithelial cell turnover and abnormal intestine sizes. Some authors

indicate that the gut microbiome may have an effect on stem cell proliferation (Engel, Moran, 2013). Gut bacteria also could affect the germ lines of *D. melanogaster*. Flies with suppressed gut bacteria have repressed oogenesis. The offspring hase an expedited maternal-to-zygotic-transition. The agnotic flies are more sensitive to stress.
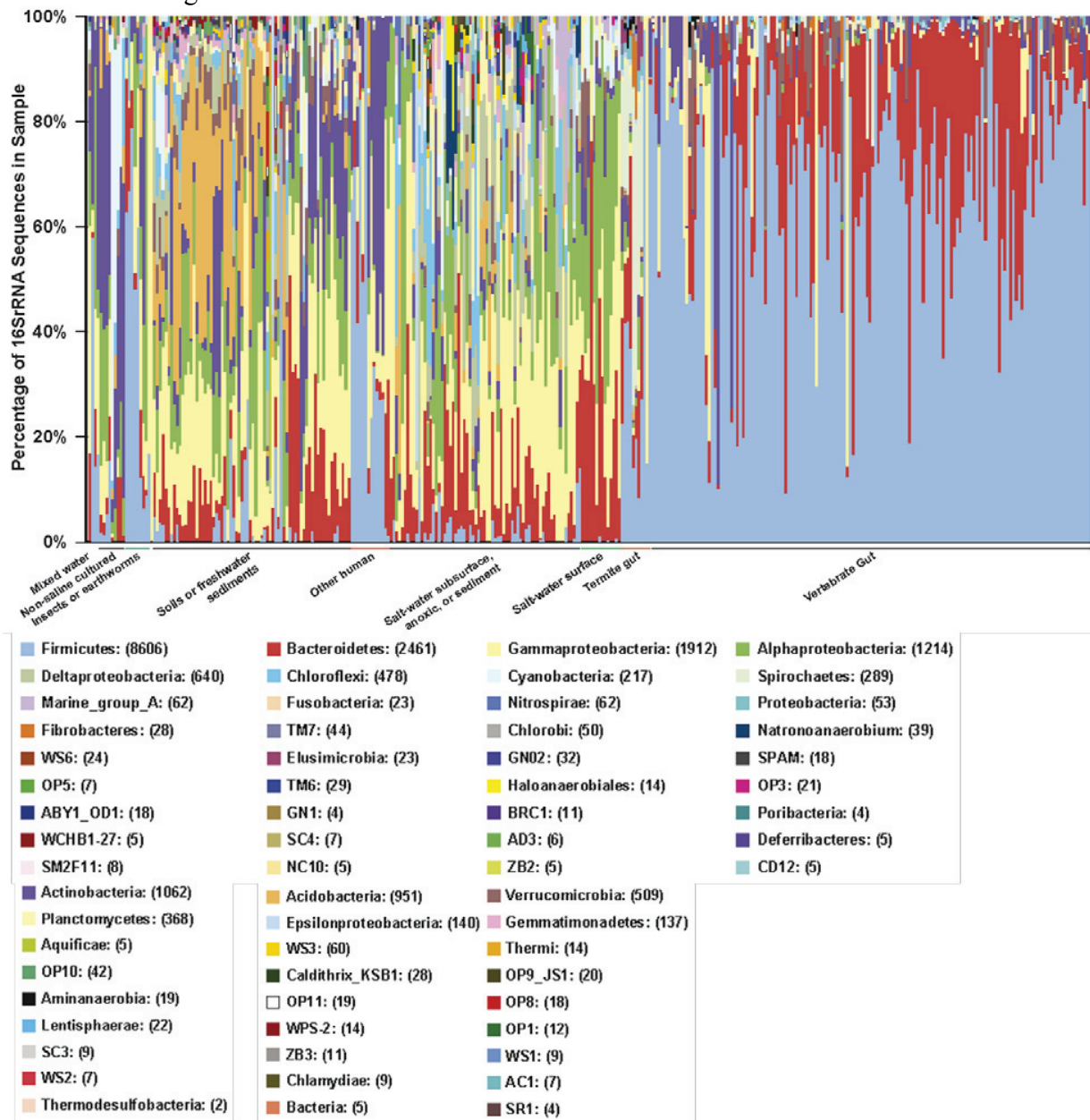

Figure 2. Relative abundances of phyla in samples. Bar graph shows the proportion of sequences from each sample that could be classified at the phylum level, together with color codes. Formatting preserved from Gordon et al. (Nature 2008).

Gut bacteria modulate gene expression in the host. Removal of Acetobacter species from the guts of *D. melanogaster* affected the expression of the Drosophila Aldehyde dehydrogenase (Aldh) gene (Elgart et al., 2016).

An optimal composition of gut microbiota is essential for normal development of the host. Several research groups made attempts to determine main factors which determine composition of gut microbiome. Large scale study of insects' populations was conducted in South Korea. Microbial communities of 305 individual insects belonging to 218 species in 21 taxonomic orders have been studied. Microbial composition was documented with 454 pyrosequencing technology. In total, 174,374 sequence reads were obtained. Authors indicated that the composition of insect gut microbial communities depends on environmental habitat, developmental stage, the host phylogeny and diet. (Yuna et al., 2014) Diet could be one of the major factors that influences on microbiome composition and functions. First of all, adaptation to a food source requires appropriate changes in the digestive tract.

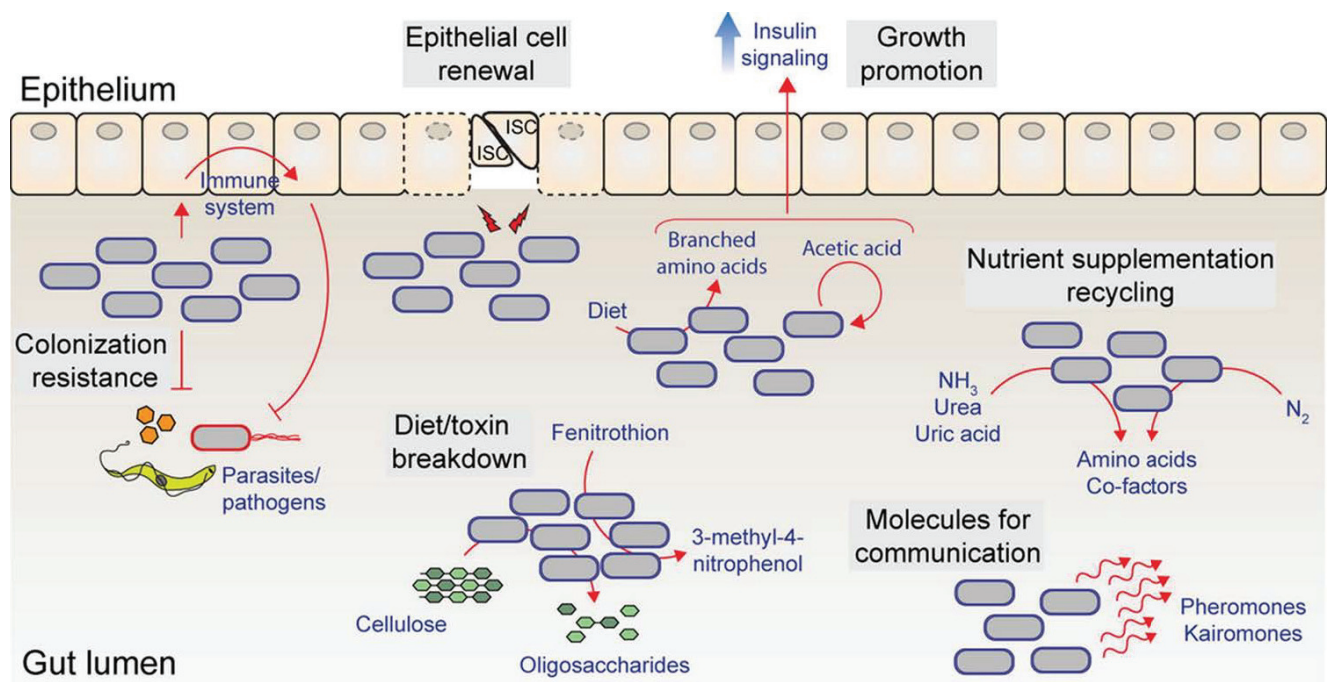Figure 3. Functions of the insect gut microbiome. Format conserved from Engel, Moran. (FEMS Microbiol Rev 2013).

It is clear that adaptation to plant sources represented challenges that most insect orders could not resolve, only eight of the 29 orders of insects have adapted to feeding on plants (Futuyma, Agrawal, 2009). Plant tissue significantly differs from other diet sources (Ortego, 2012).

Insects developed numerous morphological and physiological adaptations to exploit plant substrates (Ortego, 2012). In the Orthoptera order, crickets and mole crickets share unusual features in their gut structure that are not found in other groups of insects. These unusual features include a long segment of hindgut containing setae-bearing papillae. In the Blattodea order, termites are characterized by an increased compartmentalization of their intestinal tract. In the digestive systems of most insect orders, physiological adaptations can be found to help with the management of indigestible plant material. In Coleoptera, Hymenoptera and Lepidoptera, there is a specific spatial distribution of the digestive function. The enzymatic activity is mainly restricted to the midgut (Ortego, 2012). The physical and chemical conditions of the digestive tract are also adapted to assimilate plant material. The gut pH varies in different insects. The pH of the midgut of herbivorous insects is usually in the slightly acidic to neutral range, with the exception the alkaline midgut of lepidopteran larvae (Terra and Ferreira 1994; Köhler, 2012). In Lepidoptera, the goblet cells pump potassium into the lumen of the gut (Gomes et al. 2013). Not only do leaf proteins and cell wall polysaccharides become more soluble under an alkaline pH, but also tannins precipitate fewer enzymes (Ortego, 2012). Some authors indicate the existence of active regulation of acid–base transport to stabilize the lumen pH after feeding (Harrison, 2001). The insect's gut is an ecological niche, which could be colonized by diverse microbial communities. The physical and chemical conditions of the digestive tract determine specific composition of gut microbiome of herbivores insects (Tang et al., 2012).

In the crickets the setae provide a suitable habitat and substrate surface for the growth of numerous microorganisms. In the Termites each gut compartment is colonized by a specific microbial community. The alkaline compartment is inhabited by a 187 genera of bacteria. The most frequent sequences belonged to *Firmicutes*, *Spirochaetes* and *Actinobacteria*. This data are obtained with 454 sequencing.

Gut microbiota of *Lepidoptera* draw the attention of several research groups. Only several researches were focused on the questions of variability and robustness of the *Lepidoptera* larvae microbiome. Under field conditions the gut community of *Helicoverpa armigera* is highly variable and strong influenced by the host plant of the organism (Berenbaum, 1995; Priya et al., 2012). A group of researchers from India studied field population of *H. armigera*. Insects were sampled from host plants grown in different parts of India. Bacteria were isolated from the *H. armigera* gut. Authors reported presence of *Bacillus, Cellulomonas*, *Acinetobacter*, *Micrococcus*, *Enterobacter*, and *Enterococcus* bacteria orders. *Enterobacter* and *Enterococcus* were universally present in all *Helicoverpa* samples collected off of different crops and in different parts of India. The bacterial diversity varied greatly among insects that were from different host plants. Laboratory-made media significantly diverged from the natural diet of the crop plant. It was found that the *H. armigera* midgut bacterial community was similar to that of the leaf phyllosphere. Gypsy moth caterpillars' guts had communities that were highly dependent on their diet (Broderick et al., 2004). In cabbage white butterflys' guts widespread environmental taxa of bacteria were found (Robinson et al., 2010). Experiments demonstrated that not all environmental bacteria are able to colonize gut epithelium, but rather only several species. Gut microbial communities demonstrate robustness in the event of invasion by foreign bacterial species (Dillon, Dillon, 2004; Murphy, Teakle, Macrae, 1994). Feeding on antibiotics and sinigrin increased community susceptibility to the establishment of foreign strains (Robinson et al., 2010). Food-derived plant toxins can majorly alter the structure of gut microbial community.

Numerous environmental factors like concentration and composition of plant secondary metabolites, nutrient richness and suitability of plant material to feeding could influence the gut microbiome. Despite such researches, *Lepidoptera* gut microbiome were mainly studied under field conditions, researches under controlled laboratory conditions are still rare.

So we were interested to study effect of plant toxins on gut microbial community of *Lepidoptera* under controlled laboratory conditions. As model organism *Spodoptera littoralis* was selected.

Spodoptera littoralis belongs to the order of Lepidoptera. It host range covers over 40 plant families including 87 species of economically important plants. *S. littoralis* is widespread in the Mediterranean region of Europe (e.g. Spain, Italy, France), North Africa (e.g. Egypt) and Asia (e.g. Cyprus, Iran).

Spodoptera littoralis larvae feed on *Poaceae* (maize), *Solanaceace* (tomato, tobacco plants), *Brassicáceae*, and *Fabaceae* (lucerne, soybeans) (Davis et al., 2003). These and many other host plants produce toxic secondary metabolites. The detoxification process in the *S. littoralis* gut is unclear. Little is known about the dynamics of the microbial communities of *S. littoralis* and the effect of plant toxins on their gut microbial community.

S. littoralis and its gut microbiome are typically faced with several toxins. We were interested in coumarin, 8-methoxypsoralen (8-MOP), 3-nitropropionic acid (3-NPA), amygdalin and crotalin. These compounds belong to different class of chemical compounds, have different mechanism of toxic effects and are present in plants at different concentrations.

Coumarins are found in many plants. Several plants are rich in these compounds, among them *Melilotus* spp. (sweet clover), *Apiaceae* spp., *Citrus* spp. (orange), and *Acanthaceae* spp (Venugopala et al., 2013). Biosynthesis of coumarins can occur from several different processes, though it particularly arises from shikimic acid metabolism (Frasera, Clint, 2011). The concentration of coumarins depends on environmental factors such as shading, temperature and humidity (Bertolucci et al., 2013). Coumarin content in leaves ranges from 0.4% to 9.81% by m/m (Blahová, Svobodová, 2012). Coumarins are involved in various plant defense mechanisms against herbivores and fungi (Matern, 1991). Also, they are a group of molecules with a wide range of anti-microbial activity against gram negative bacteria. Their presence leads to hepatotoxicity, oxidative stress and apoptosis. Coumarin inhibited growth of *Pseudomonas spp* (de Souzaa et al., 2005). The mechanism of inhibition is unclear. In bacteria, coumarin antibiotics inhibit DNA replication. Their target for this inhibition is the enzyme DNA gyrase, an ATP-dependent bacterial type II topoisomerase. Coumarin antibiotics suppress the introduction of negative supercoils into circular genomic DNA. In eukaryotic cells, coumarins bind non-protein sulfhydryl groups and deplete glutathione (Andreza et al., 2004).

Furocoumarins are found in 15 plant families, though mainly distributed among *Apiaceae*, *Moraceae*, *Rutaceae* and *Fabaceae* (Dugrand-Judek et al. 2015). The route of biosynthesis is derived from the phenylpropanoid pathway and the mevalonate pathway (Hehmann et al., 2004). Biosynthesis of furocoumarins is induced by abiotic factors like mechanical damage, low temperature, insect feeding, and chemical presence of sodium hypochlorite and copper sulfate (Iriti, Faoro, 2009). In different plants of the *Apiaceae* family, furocoumarins can accumulate to concentrations of 50 – 2000 mg/kg (Dolan et al., 2010). Furocoumarins covalently bind DNA, fatty acids, and proteins (Studzian et al., 1999).

3-nitropropanoic acid (3-NPA) is a naturally occurring toxin with a profound effect on human health and domestic livestock (Francis et al., 2013). 3-NPA was isolated from a number of plant and fungi species, and recently has been shown to be synthesized by beetles. 3-NPA

producing plants are widely distributed. It was shown that 3-NPA is one of the major components responsible for the toxic effect of some weeds (Williams, 1994). In Legume species, 3-NPA is present in high concentrations: up to 2.6% of dry mass m/m (Burdock et al., 2001). Feeding on such Legumes causes lathyrism and other neuronal diseases for herbivores (Meldrum et al., 2000;). The neurotoxicity of 3-NPA comes from its irreversible inhibition of succinate dehydrogenase. It was shown that 3-NPA is 16-fold more toxic to neurons than to other cell types (Olsen et al., 1999; Tarazona, Sanz, 1987; Hipkin et al., 2004). Intoxication by 3-NPA leads to motor dysfunction and in some cases to death of cattle (Akopian et al., 2012, Francis et al., 2013; Parry et al., 2011; Mithöfer, Boland, 2012). Cases of 3-NPA poisoning were widely documented in livestock and lead to significant economic losses (Williams, 1994).

Mammals are highly susceptible to 3-NPA. It is estimated that median lethal dose (LD50) for rats equals 67 mg/kg of their body weight (Tarazona, Sanz, 1987). In contrast, insects are highly resistant to 3-NPA. The grasshopper species *Melanoplus bivittatus* survives after feeding on concentrations of 3-NPA that are lethal to mammals. In the frass of 3-NPA fed *Melanoplus bivittatus,* amides of 3-NPA, glycine, serine, and glutamine were detected (Majak et al., 1998). A large diversity of N-acyl amino acid conjugates have previously been described in Lepidoptera (e.g. amides of fatty acids, FAAs). FAAs have been shown to be involved in plant herbivore interactions (Alborn et al., 1997; Lait et al., 2003; Yoshinaga et al., 2005; Ping et al., 2007). In comparison to *Pieris rapae*, a specialized Cruciferae species, the phytophagous generalist *S. littoralis* has not been intensively studied in terms of its detoxification of small molecular toxins.

Cyanogenic glycosides are widely distributed among 100 families of flowering plants. All cyanogenic glycosides are biosynthesized from one of the six amino acids: L-valine (L-Val), L-isoleucine (L-Ile), L-leucine (L-Leu), L-phenylalanine (L-Phe), L-tyrosine (L-Tyr), and cyclopentenyl-glycine (cyclopentenyl-Gly). Two cytochromes-P450s enzymes and a Uridine 5'-diphospho -glucosyltransferase are involved in the biosynthesis of the cyanogenic glycosides. Plants produce cyanogenic glycosides, with amino acids that cannot be used for protein synthesis. Usually plants containing 0.02% of cyanogenic glycosides (m/m) are likely to be toxic, and highly poisonous plant may contain up to 0,6% cyanogenic glycosides (m/m) (Bryson, 1996). There is strong evidence that cyanogenesis is one of the mechanisms that can serve to protect the plant from predators such as herbivores. Cyanogenic glucosides are hydrolyzed by a glucosidase in the gut of herbivores and rely on toxic compounds to function. Amygdalin is one of those toxic compounds. First the amygdalin is split into prunasin by the amygdalin hydrolase. Then the prunasin hydrolase splits the prunasin into mandelonitrile, which is split into benzaldehyde and hydrogen cyanide (Beck et al., 2005). The released hydrogen cyanide anion binds the heme iron atom, so that the heme proteins are inactivated. The cyanide anion primarily inhibits cytochrome C oxidase and this inactivation of cytochrome C oxidase leads to suppression of a respiratory chain (Atta-Ur-Rahman, 2002).

More than 95% of investigated pyrrolizidine alkaloids are found in four plants families. Pyrolizidine alkaloids are mainly present in *Fabaceae* (e.g. *Crotalaria sp.*), *Boraginaceae*, *Asteraceae* and *Orchidaceae* (Rösemann, 2006). The synthesis of pyrrolizidine alkaloids takes place during amino acid metabolism. Biosynthesis starts with decarboxylation of the amino acids L-arginine and L-ornithine. Crotalin is one of the most common pyrrolizidine alkaloids. Pyrrolizidine alkaloids' concentrations in Crotalaria species range between 0.28% to 0.01% m/m (Colegate, 1999). In plants, the crotalin is mostly stored in the form of N-oxides. In the gut of the insects, the microsomale cytochrome P450 enzyme reduces the N-oxide form of crotalin to a

reactive derivate which is genotoxic. It reacts with DNA and damages the gut tissue (Bernays, 2004).

The effect of plant toxins on the gut microbial community is unclear and poorly investigated. The aim of this project thus was to evaluate the effect of plant toxins on *S. littoralis* gut microbiome.

To achieve the aim several objectives were addressed in the project. On the first step we have studied an effect of plant toxins and antibiotics on growth parameters of the larvae and on their survival rate. On the second step we have studied detoxification process in the larvae gut. On the third step we have studied an effect of plant toxins on composition and structure of gut microbiome.

2. Thesis outline – List of articles and manuscripts

Article I

Spodoptera littoralis detoxifies neurotoxic 3-nitropropanoic acid by conjugation with amino acids.

Novoselov A, Becker T, Pauls G, von Reuß SH, Boland W.

This manuscript describes the detoxification mechanism of 3-NPA in *S. littoralis*. It has been shown that growth in larvae fed in the artificial diet with a sublethal admixture of 3-NPA (4.2 μmol per g) was slowed significantly, but the larvae experienced no increase in mortality. In contrast, larvae injected with 25.2 μmol/g (bodyweight) 3-NPA experienced acute toxicity and death. Comparative analysis of 3-NPA-treated and -untreated control samples using HR-MS^2 revealed a group of differential signals that were identified as amino acid amides of 3-NPA with glycine, alanine, serine, and threonine. When sublethal amounts of stable isotope-labeled 3-NPA were injected into a larva's hemolymph, 3-NPA amino acid conjugates were identified as putative detoxification products. Bioassays with synthetic standards confirmed that the toxicity of the amides was negligible in comparison to the toxicity of free 3-NPA, demonstrating that amino acid conjugation in *S. littoralis* represents an efficient way to detoxify 3-NPA. Furthermore, biosynthetic studies using crude fractions of the gut tissue indicated that conjugation of 3-NPA with amino acids occurs in epithelial cells of the insect's gut. Taken together, these results suggest that the detoxification of 3-NPA in *S. littoralis* proceeds via conjugation to specific amino acids within the epithelial cells, followed by export of the nontoxic amino acid conjugates to the hemolymph via as yet uncharacterized mechanisms, most likely involving the Malpighian tubules.

Author contributions:

Designed experiments: N.A. (90%), B.T., P.G., von R.S.H., B.W.

Conducted experiments: N.A. (99%), B.T., P.G., von R.S.H., B.W.

Performed data analysis: N.A. (96%), B.T., P.G., von R.S.H., B.W.

Wrote the manuscript: N.A. (94%), B.T., P.G., von R.S.H., B.W.

Article II

Draft Genome Sequence of *Enterococcus mundtii* SL 16, an Indigenous Gut Bacterium of the Polyphagous Pest *Spodoptera littoralis*

Bosheng Chen, Chao Sun, Xili Liang, Xingmeng Lu, Qikang Gao, Pol Alonso-Pernas, Beng-Soon Teh, Alexey L. Novoselov, Wilhelm Boland and Yongqi Shao

The data report presents draft genome sequencing of *Enterococcus mundtii* from *S. littoralis*. Recent extensive surveys of its microbiome reveal that *Enterococcus mundtii* is one of the predominant gut microorganisms of *S. littoralis* and present at high frequency. Particularly, a stable isotope labeling-based approach suggested that this phylotype was also highly metabolically active inside the host across life history of *S. littoralis*, indicating the significant role played by *E. mundtii* in host biology. Therefore, the symbiotic *E. mundtii* probably constitutes a key factor for the success of this generalist herbivore in adapting to different environments and food sources. The aim of this study was to produce a genome sequence of the strain SL 16, which would assist in understanding of the coevolution of the microbe and the insect host. The dataset has been submitted to NCBI Whole Genome Shotgun (WGS) projects and is reported here, providing an overview of the genome sequence and relevant features of the gut symbiotic *E. mundtii*

Author contributions:

Designed experiments: B.C., C.S., X.L., X.L., Q.G., P.A-P., B-S. T, A.L.N.(6%), W.B. and Y. S.

Conducted experiments: B.C., C.S., X.L., X.L., Q.G., P.A-P., B-S. T, A.L.N., W.B. and Y. S.

Performed data analysis: B.C., C.S., X.L., X.L., Q.G., P.A-P., B-S. T, A.L.N. (10%), W.B. and Y. S.

Wrote the manuscript: B.C., C.S., X.L., X.L., Q.G., P.A-P., B-S. T, A.L.N. (4,5%), W.B. and Y. S.

Article III

Bacterial community and PHB-accumulating bacteria associated with the wall and specialized niches of the hindgut of the forest cockchafer (*Melolontha hippocastani*)

Pol Alonso-Pernas, Erika Arias-Cordero, Alexey Novoselov, Christina Große, Jürgen Rybak, Martin Kaltenpoth, Martin Westermann, Ute Neugebauer, Wilhelm Boland

In this manuscript the bacterial community of the forest cockchafer (*Melolontha hippocastani*) was characterized using amplicon sequencing of the 16S rRNA gene fragment. It was found that, in second-instar larvae, Caulobacteraceae and Pseudomonaceae showed the highest relative abundances, while in third-instar larvae, the dominant families were Porphyromonadaceae and Bacteroidales-related. In adults, an increase of the relative abundance of Bacteroidetes, Proteobacteria (γ- and δ- classes) and the family Enterococcaceae (Firmicutes) was observed. This suggests that the composition of the hindgut wall community may depend on the insect's life stage. Additionally, specialized bacterial niches hitherto very poorly described in the literature were spotted at both sides of the distal part of the hindgut chamber. We named these structures "pockets". Amplicon sequencing of the 16S rRNA gene fragment revealed that the pockets contained a different bacterial community than the surrounding hindgut wall, dominated by Alcaligenaceae and Micrococcoccaceae-related families. Poly-β-hydroxybutyrate (PHB) accumulation in the pocket was suggested in isolated *Achromobacter* sp. by Nile Blue staining, and confirmed by gas chromathography–mass spectrometry analysis (GC-MS) on cultured bacterial mass and whole pocket tissue. Raman micro-spectroscopy allowed to visualize the spatial distribution of PHB accumulating bacteria within the pocket tissue. The presence of this polymer might play a role in the colonization of these specialized niches.

Author contributions:

Designed experiments: P.A-P., E.A-C., A.N. (30%), C.G., J.R., M.K., M.W., U.N., W.B.

Conducted experiments: P.A-P., E.A-C., A.N. (20%), C.G., J.R., M.K., M.W., U.N., W.B.

Performed data analysis: P.A-P., E.A-C., A.N. (45%), C.G., J.R., M.K., M.W., U.N., W.B.

Wrote the manuscript: P.A-P., E.A-C., A.N. (25%), C.G., J.R., M.K., M.W., U.N., W.B.

3. Article I

Spodoptera littoralis detoxifies neurotoxic 3-nitropropanoic acid by conjugation with amino acids.

Novoselov A, Becker T, Pauls G, von Reuß SH, Boland W.

Spodoptera littoralis detoxifies neurotoxic 3-nitropropanoic acid by conjugation with amino acids

Alexey Novoselov, Tobias Becker, Gerhard Pauls, Stephan H. von Reuß, Wilhelm Boland[*]

Max Planck Institute for Chemical Ecology, Bioorganic Chemistry, Hans-Knoell-Straße 8, D-07745, Jena, Germany

ARTICLE INFO

ABSTRACT

Spodoptera littoralis is a phytophagous generalist. Its host range includes more than 40 plant species, some of which produce 3-nitropropanoic acid (3-NPA), an irreversible inhibitor of mitochondrial succinate dehydrogenase. Growth in larvae fed an artificial diet with a sublethal admixture of 3-NPA (4.2 μmol per g) was slowed significantly, but larvae experienced no increase in mortality. In contrast, larvae injected with 25.2 μmol/g (bodyweight) 3-NPA experienced acute toxicity and death. To study the detoxification mechanism of 3-NPA in *S. littoralis*, the insect frass was analyzed by HPLC-MS. Comparative analysis of 3-NPA-treated and -untreated control samples using HR-MS^2 revealed a group of differential signals that were identified as amino acid amides of 3-NPA with glycine, alanine, serine, and threonine. When sublethal amounts of stable isotope-labeled 3-NPA were injected into a larva's hemolymph, 3-NPA amino acid conjugates were identified as putative detoxification products. Bioassays with synthetic standards confirmed that the toxicity of the amides was negligible in comparison to the toxicity of free 3-NPA, demonstrating that amino acid conjugation in *S. littoralis* represents an efficient way to detoxify 3-NPA. Furthermore, biosynthetic studies using crude fractions of the gut tissue indicated that conjugation of 3-NPA with amino acids occurs in epithelial cells of the insect's gut. Taken together, these results suggest that the detoxification of 3-NPA in *S. littoralis* proceeds via conjugation to specific amino acids within the epithelial cells followed by export of the nontoxic amino acid conjugates to the hemolymph via as yet uncharacterized mechanisms, most likely involving the Malpighian tubules.

1. Introduction

3-Nitropropanoic acid (3-NPA) is a naturally occurring neurotoxin known as bovinocidin that has a profound effect on human health and domestic livestock (Burdock et al., 2001; Francis et al., 2013; Mithöfer and Boland, 2012; Xingjie et al., 1992). 3-NPA is a neurotoxin that irreversibly inhibits succinate dehydrogenase, a key enzyme of the citric acid cycle (Hipkin et al., 2004; Olsen et al., 1999; Tarazona and Sanz, 1987). Livestock exposed to 3-NPA suffers from motor dysfunction and in some cases death (Akopian et al., 2012; Francis et al., 2013; Parry et al., 2011). 3-NPA mainly occurs in legumes; in particular several *Astragalus* species contain high levels of this compound (Burdock et al., 2001) and also certain endophytic fungi are able to produce 3-NPA (Chomcheon et al., 2005). The compound has been shown to be responsible for the toxicity of some weeds (Meldrum, 2000; Williams, 1994), and cases of 3-NPA poisoning have been widely documented in livestock, leading to significant economic losses (Williams, 1994).

In contrast, some grasshoppers such as *Melanoplus bivittatus* survive feeding on concentrations of 3-NPA that are lethal to mammals (Majak et al., 1998; Tarazona and Sanz, 1987). In the frass of *M. bivittatus* larvae 3-NPA conjugates of the amino acids glycine, serine, and glutamine were detected and assumed to be putative detoxification products. However, no information concerning the properties and toxicity of 3-NPA amino acid amides in insects has been reported (Majak et al., 1998). Many *N*-acyl amino acid conjugates have been described in Lepidoptera (Alborn et al., 1997; Stauber et al., 2012). Glutamine amides of fatty acids are known to be involved in plant—herbivore interaction (Alborn et al., 1997; Lait et al., 2003; Ping et al., 2007; Yoshinaga et al., 2005). The conjugates with glycine are products of glucosinolate metabolism in *Pieris rapae* (Stauber et al., 2012). However, despite this, the metabolic pathways of 3-NPA detoxification in the phytophagous generalist *Spodoptera littoralis* are poorly understood (Grossa et al., 2008). Larvae of *S. littoralis* feed on more than 40 plant families,

including legumes that accumulate 3-NPA in concentration up to 100 μmol per g fresh weight (Hipkin et al., 2004). The aim of this study was to determine the metabolic pathways that facilitate the detoxification of 3-NPA in *S. littoralis*. We show that *S. littoralis* gains its resistance to 3-NPA by converting the free acid into several non-toxic amino acid amides.

2. Materials and methods

2.1. Insects and toxicity experiments

S. littoralis eggs were obtained from Syngenta Crop Protection Münchwilen AG (Switzerland) and cultivated (Tang et al., 2012). The eggs were placed in a box with artificial medium and hatched at 14 °C (Bergomaz and Boppre, 1986). The larvae were cultivated at room temperature (24 °C) (Tang et al., 2012). The insects were raised on an artificial medium prepared according to Spiteller et al. (2005), but without addition of the preservatives parabene and formaldehyde. Fresh food was provided to the *S. littoralis* larvae once a day. For the feeding experiments, 3-NPA or amino acid amides of 3-NPA were added to the artificial diet at different concentrations. The body weight and body length of each insect were determined every day during the experiment. The control group fed on the artificial medium (n = 20) and the experimental group fed on a medium containing 3-NPA (c = 4.2; 8.4; 16.8; 33.6 mmol/kg, n = 20). The experiments were repeated three times. For the injection experiments, a buffer was used (1.4 mM NaCl, 0.07 mM, Na_2HPO_4, 0.03 mM KH_2PO, 4 mM KCl, pH 7.4). The solutions were injected into 4th-instar larvae (n = 30). In the control group, only the buffer was injected into the insect. In the experimental group, a solution of 3-NPA (c = 8.4; 12.6; 16.8; 25.2; 33.6 μ mol/g b. w.) was dissolved in the buffer and injected into the larvae (1 μl/100 mg of larvae weight). After injection, the larvae were individually reared on an artificial diet in plastic boxes (25 °C ± 1 °C). Fifth-instar larvae were used for tissue sampling. The larvae were killed using CO_2 and dissected. Their guts were separated from the other tissue and hemolymph was sampled with a thin capillary after dissection. The regurgitate was sampled with a thin capillary after stimulation of the larvae by forceps as described by Turlings et al. (1993).

2.2. HPLC/MS analysis of the hemolymph and excrement samples

Samples of the hemolymph and the frass of treated and untreated control larvae were suspended in $MeOH/H_2O$ (1:1, v/v). The samples were centrifuged and analyzed by LC-MS and LC-HRMS experiments. The samples were analyzed on a Thermo Finnigan LCQ with atmospheric pressure chemical ionization (APCI) in the negative mode (vaporizer temperature: 450 °C; capillary temperature: 275 °C; source current: 4 uA; capillary voltage: −38 V; tube lens offset: −33 V). The mixture was separated on an Agilent HP1100 HPLC system equipped with a Hibar column (250 × 4 mm, Purospher STAR, RP-18 endcapped, 5 μm) using a flow of 1 ml min ^{1} with 97% of solvent A (0.1% formic acid in water) and 3% of solvent B (0.1% formic acid in acetonitrile) for 5 min, followed by a gradient up to 60% B over 30 min, then to 100% B for 5 min. Natural compounds were analyzed by using high-resolution (HRMS) and tandem mass spectrometry (BRUKER MAXIS) connected to an Dionex UltiMate 3000-system equipped with an Hibar column (250 × 4 mm, Purospher STAR, RP-18e, 5 μm).

The samples of subcellular fractions were separated isocratically on a Thermo Finnigan LCQ with electro spray ionization (ESI) in the negative mode (capillary temperature: 275 °C; source current: 100 μA; capillary voltage: −44 V; the tube lens offset: −53 V). The separation was achieved on an Agilent HP1100 HPLC system equipped with a LiChroCART (250 × 2 mm, Purospher STAR RP-18

endcapped, 5 μm). The samples were eluted at a flow of 0.380 ml min ^{1} with 80% solvent A (0.1% formic acid in water) and 20% solvent B (0.1 formic acid in acetonitrile) for 10 min.

2.3. General synthesis of the isotopic labeled 3-NPA and 3-NPA amides of amino acids

The synthesis of 3-[1—^{13}C,3—^{15}N]-nitropropionic acid was performed according to Baxter et al. (1985) using $Na^{15}NO_2$ to introduce a second stable isotope label.

The synthesis of the described amides of 3-NPA was performed using dicyclohexyl carbodiimide (DCC), 3-NPA, and free amino acids in an aqueous reaction medium (Neises and Steglich, 1978; Becker et al., 2015). For details see supplementary material (appendix I).

2.4. Subcellular fraction preparation

Gut tissue was cut open and washed with tris buffer, 50 mM tris base, 2 mM $MgCl_2$, and 250 mM sucrose according to Tiedtke et al. (1988). Washed gut tissue was mixed with 1 ml of homogenization buffer, prepared by mixing the tris buffer with 10 μl protease inhibitor mix (Serva) dissolved in phosphate buffer system (PBS), and 1 μl of 1 M dithiothreitol (DTT). Iron bits were added to the sample, which was homogenized using a GenoGrinder (SPEX SamplerPrep 2010) for 1 min at 1210 rpm. After homogenization, the debris was sedimented by centrifugation for 10 min at 500 g. Mitochondria were isolated by differential centrifugation, and microsomes were isolated by ultracentrifugation at 100,000 g (Firstenberg and Silhacek, 1973). Twice-washed mitochondria and microsomes were used in assays for the *in vitro* biosynthesis of 3-NPA amides of amino acids.

2.5. Assays for in vitro biosynthesis of 3-NPA amides of amino acids

Cytosolic proteins, and mitochondrial and microsomal fractions were added to 200 μl of homogenization buffer along with 1 mM coenzyme A (CoA), 25 mM adenosine triphosphate (ATP), 250 μg/ml glycine, and 250 μg/ml 3-NPA. The samples were incubated at room temperature for 20 h and lyophilized, and the residue was suspended in ethanol. The suspension was centrifuged, the supernatant was concentrated under reduced pressure, and the dry residue was taken up with MeOH and analyzed by LC-MS.

2.6. Assays for biosynthesis of 3-NPA amides in gut microorganisms

The gut content was separated from each insect's intestine, and diluted in 5 ml Todd-Hewitt-Bouillon (THB). 250 μg/ml 3-NPA and 250 μg/ml glycine was added, and the mixture was incubated overnight at 37 °C and shaken at 220 r.p.m. For cultivation under anaerobic conditions, the gut content in 2 ml THB was placed in a BBL GasPak anaerobic jar with Anaerocult A atmosphere generation kit (Merck)and incubated for 7 days at 27 °C in an anaerobic atmosphere composed of 18% CO_2 and traces of O_2.

3. Results

3.1. Toxicity of 3-nitropropanoic acid for S. littoralis by oral uptake

To study the susceptibility of *S. littoralis* larvae to the toxic host plant metabolite 3-NPA, feeding experiments were conducted.

3-NPA was added to the artificial diet of *S. littoralis* at 4.2 μmol 3-NPA per g (Chomcheon et al., 2005) to study the toxicological effects on the larvae. The body weight and length of *S. littoralis* larvae were determined over the time they fed on diet with 3-NPA

(experimental group) and without 3-NPA (control). Larvae of the experimental group grew significantly slower than those of the control group. After 16 days of feeding on the diet containing 3-NPA, a decrease of the average body length of 62% (Fig. 1B) and a decrease of the weight gain to 34% were observed (Fig. 1A). No effects on moulting or increase in mortality was detected in insects that fed on 4.2 μmol 3-NPA per g of the diet compared to insects in the control group.

To determine the overall resistance of S. littoralis to 3-NPA, increasing amounts of the toxin were added to the artificial diet of the larvae. After the application of 4.2, 8.4 16.8 and 33.6 μmol 3-NPA/g of artificial diet, the mortality of larvae in the experimental group was equal to that of larvae in the control group (data not shown). These data indicate that S. littoralis was highly resistant to 3-NPA upon feeding.

3.2. Toxicity of 3-nitropropanoic acid for S. littoralis after injection

The effect of directly injecting 3-NPA into the larval hemolymph of S. littoralis was studied. The following concentrations of buffered solutions of the toxin were injected: 8.4, 12.6, 16.8, 25.2, 33.6 μmol 3-NPA per g body weight. Mortality in insects fed with 3-NPA was lower than that in insects injected with ascending concentrations of 3-NPA (Fig. 2).

After injections of concentrations of 33.6 μmol 3-NPA per g body weight, all of the larvae died within 1 day, at concentrations of 12.6 μmol 3-NPA per g body weight 43% of the larvae survived (Fig. 2). These results show that S. littoralis larvae are more susceptible to injection than to oral administration of 3-NPA and suggest that S. littoralis is capable of detoxifying orally ingested 3-NPA.

3.3. Identification of 3-NPA derived metabolites

To study the detoxification of 3-NPA in the gut, the frass of larvae treated with 3-NPA was analyzed by HPLC-MS. Differential analysis
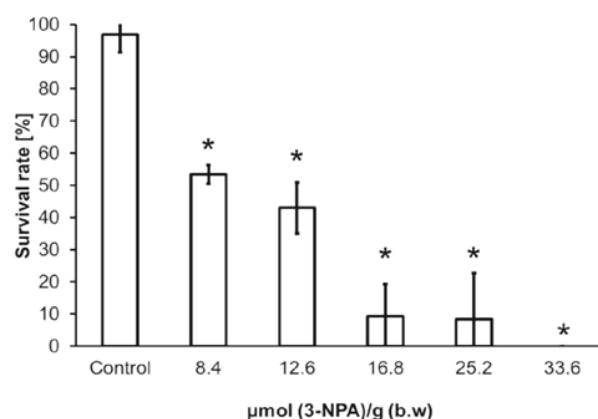
Fig. 2. Comparison of the survival rates of S. littoralis larvae determined 2 days after injection of increasing amounts of 3-NPA (one-way Anova, Dunnett's post test, *p < 0.05; ±1 SD, n = 3).

of the frass of treated larvae versus the frass of untreated control revealed a 3-NPA-dependent signal that might represent a metabolite derived from 3-NPA (Fig. 3A). Its mass spectrum showed a pseudo molecular ion at m/z 175 [M−H] along with signals for the formic acid adduct and the dimer. HR-MS/MS analysis revealed the formula $C_5H_7N_2O_5^-$, which suggested an amide-bound glycine conjugate of 3-NPA (**1**) (Fig. S1). To unambiguously establish that the detected compound originates from 3-NPA, the stable isotope labeled $[1-^{13}C,3-^{15}N]$-3-nitropropanoic acid was synthesized and injected into the hemolymph of S. littoralis larvae. HPLC-MS analysis of the putative 3-NPA metabolite in the insect frass revealed a mass shift of $\Delta m/z$ +2 for the molecular ion along with $\Delta m/z$ +1 for the fragment ion originating from neutral loss of $^{15}HNO_2$ and confirmed the structure assignment of (3-nitropropanoyl)glycine **1**
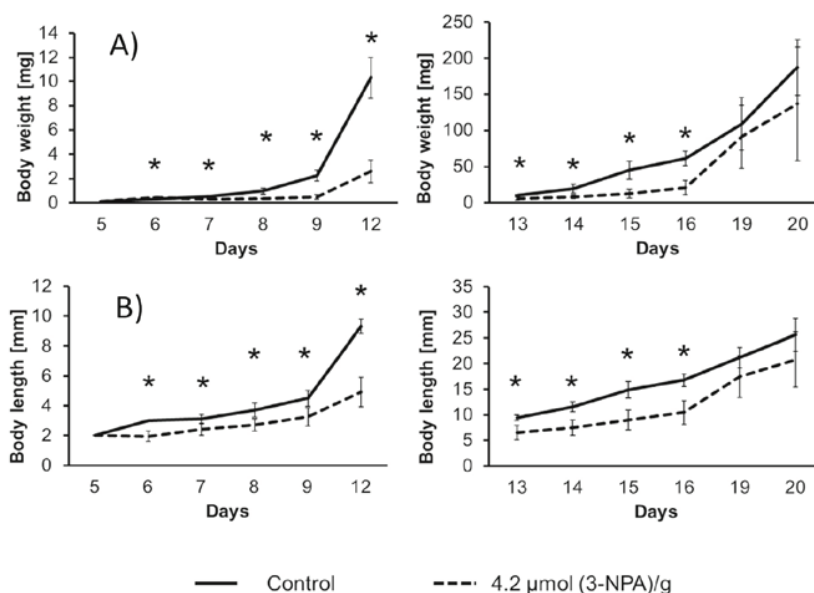
Fig. 1. Effect of the plant secondary metabolite 3-nitropropionic acid (3-NPA) on the body weight (A) and length (B) of S. littoralis larvae over time compared to the control (one-way Anova, Dunnett's post test, *p < 0.05; ±1 SD, n = 20).
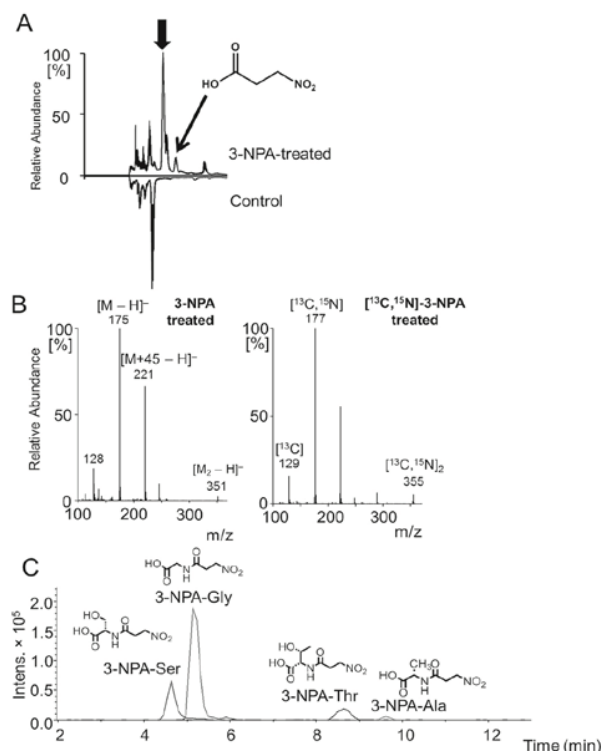
Fig. 3. (A): differential HPLC-MS analysis of the frass of 3-NPA treated and untreated control larvae; (B): Mass spectra of natural (3-nitropropanoyl)glycine **1** from *S. littoralis* after feeding on diet containing 3-NPA or $[1-^{13}C,3-^{15}N]$-3-NPA; (C): 3-NPA–amino acid conjugates **1—4** detected in the frass of larvae fed on diet containing 3-NPA.

(Fig. 3B). Screening for similar amino acid conjugates, we detected three additional differential signals in the chromatograms of the larval frass after the larvae had been injected with 3-NPA (Fig. 3C). Tandem- and HRMS analyses provided molecular formulas corresponding to amides of 3-NPA and alanine **2**, serine **3** as well as threonine **4**. The chromatograms of the frass of larvae treated with isotopically labeled 3-NPA showed a mass shift $\Delta m/z$ of $+2$. Consequently, amides of 3-NPA with glycine, alanine, and serine as well as threonine were synthesized and shown to be identical to the natural components (see supplemental material Fig. S2).

3.4. Toxicity experiments using amino acid amides 1—4

To determine the toxicity of the amino acid amides **1—4** to *S. littoralis*, solutions of the synthetic standards were injected into the larval hemolymph. The application of compounds **1—4** at 25.2 μmol per g body weight showed a survival rate of ca. 95%, whereas after injection of 3-NPA at the same concentration only 8% of the larvae survived (Fig. 4). The control group showed a survival rate of 95%. These results clearly indicate that in contrast to free 3-NPA, the amino acid amides **1—4** are not toxic when injected into *S. littoralis* larvae. This result confirms our assumption that the conjugation of 3-NPA to an amino acid represents an efficient detoxification pathway in *S. littoralis*. Moreover, the non-toxic compounds **1—4** could also be detected in the hemolymph after insects fed on an artificial diet containing 12.6 μ mol/g 3-NPA. The conjugates were also found in the frass after insects were injected with 8.4 μ mol 3-NPA per g body weight (data are not shown).

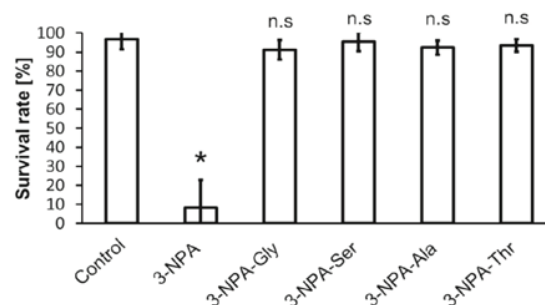**Fig. 4.** Survival of *S. littoralis* larvae. Survival was determined 2 days after the injection of 3-NPA and 3-NPA amino acid conjugates at 25.2 μmol/g body weight. (one way Anova, Dunnett's post test, *$p < 0.05$; n.s. = no significant difference; ± 1 SD, n = 3).

3.5. Determination of detoxification activity in the gut tissue

The formation of amino acid amides of 3-NPA has been shown to be a major detoxification reaction of this plant toxin in *S. littoralis* larvae. To determine where the detoxification occurs after insects feed on 3-NPA containing diet, different parts of the insect were isolated and incubated with 3-NPA and glycine.

At first, the gut content was isolated to investigate any conjugation activity of the gut microbiota. For this purpose, the gut liquid was separated from gut tissue and incubated for 24 h with a mixture of 3-NPA and glycine under aerobic or anaerobic conditions. However, none of the conjugation products could be detected, indicating that the gut microbes are not responsible for detoxifying 3-NPA in *S. littoralis*.

The enzymes that catalyze the amide formation may also be excreted by the insect's epithelial tissue into the gut lumen. To study whether the amide formation is carried out by secreted enzymes, the regurgitate of the larvae was collected and incubated with 3-NPA and glycine for 24 h; however, the conjugates were not detected (Fig. 5A). Since incubation experiments with the gut liquid failed, the tissue of the gut cells was separated from the gut content and adjacent tissues, homogenized, and the debris was filtered. 3-NPA, glycine, adenosine triphosphate (ATP), and coenzyme A (CoA) were added to the filtrate, and after 24 h of incubation, the 3-NPA-glycine conjugate **1** could be detected by LC-MS. This finding indicates that the conjugation activity is closely associated with the gut tissue. In addition, the fat body was separated from the other tissue and shown to catalyze the production of amino acid amides (Fig. 5B). To determine the conjugation activity in different subcellular organelles, the gut tissue was homogenized and fractionated. After centrifugation, the mitochondrial fraction was separated from the supernatant. Glycine and 3-NPA were added to both samples along with adenosine triphosphate (ATP), and coenzyme A (CoA). After incubation for 24 h, the 3-NPA-glycine conjugate **1** was detected in the supernatant but not in the mitochondrial fraction (Fig. 5C). To determine if the corresponding enzymes are present in the cytosol or in vesicles, cytosolic proteins were separated from the microsomes by ultracentrifugation. After the addition of 3-NPA, glycine, ATP, and CoA to both fractions and incubation for 24 h, compound **1** was detected in the cytosolic fraction (Fig. 5D). This finding shows that the enzymes involved in 3-NPA detoxification are present in the cytosol of epithelial cells in *S. littoralis*.

4. Discussion

The application of biologically relevant concentrations of toxic 3-NPA were shown to significantly reduce the growth rate of
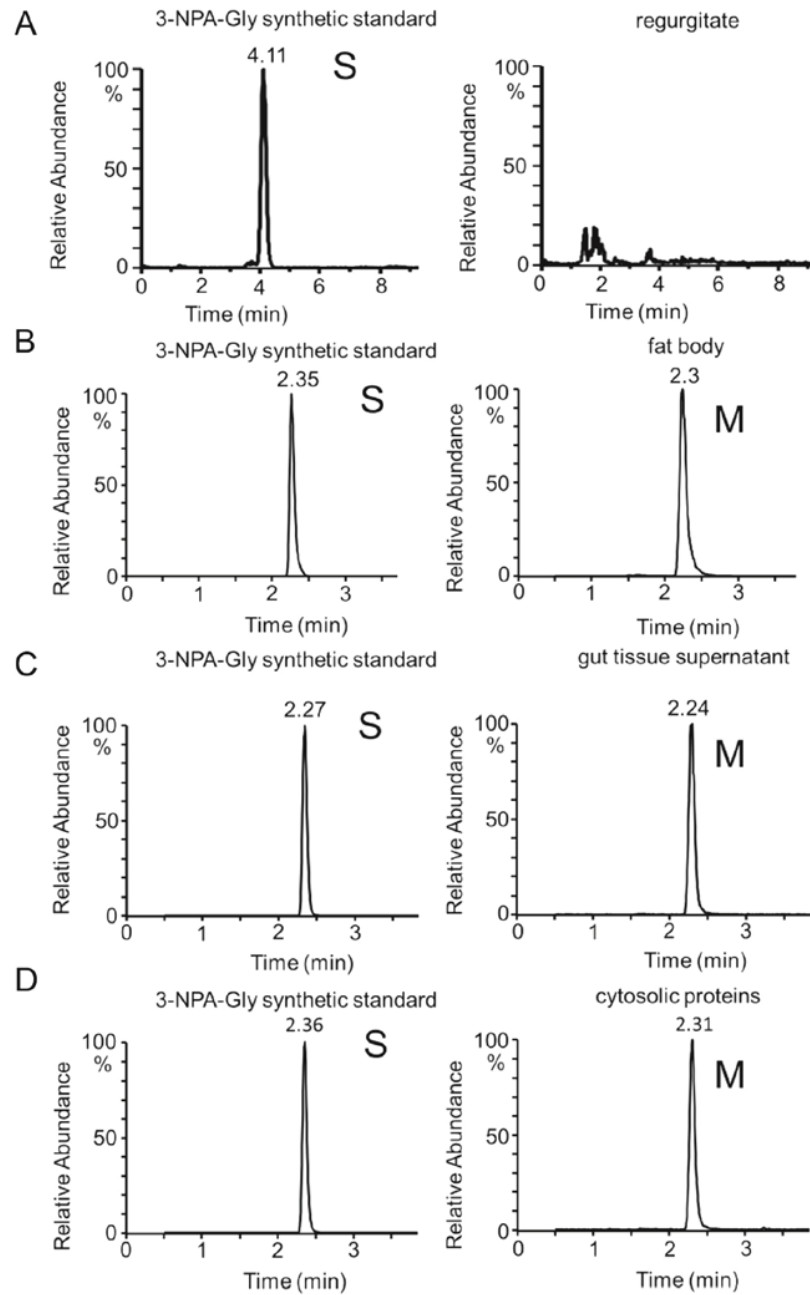
Fig. 5. The regurgitate (A), fat body tissue (B), and crude homogenized gut tissue (C), and isolated cytosolic proteins (D) were tested for conjugation activity. Samples were incubated with 3-NPA, glycine, ATP, and CoA for 24 h. The conjugate of 3-NPA with glycine was analyzed by LC-MS. (S- synthetic standard, M-metabolite).

S. littoralis larvae (Fig. 1A, B). Inhibition of larval growth by secondary metabolites is a frequent strategy how plants defend themselves against herbivores (Ibanez et al., 2012; Byers et al., 1977). Observed growth rate reduction by 3-NPA in S. littoralis suggests that 3-NPA, in fact, inhibits the growth of Lepidoptera (Cipollini et al., 2008; Wang et al., 2010).

Although larval growth is decreased after S. littoralis feeds on 3-NPA (Fig. 1A, B), its ingestion is not lethal; concentrations of 3-NPA

up to 33.6 μ mol/g did not result in higher mortality compared to insects in the control group, demonstrating that S. littoralis is highly resistant to oral uptake of 3-NPA. In contrast, injecting the same amounts of 3-NPA into the insect's hemolymph resulted in mortality and death, suggesting that the total detoxification capacity of S. littoralis is based on conjugation of 3-NPA in the gut epithelium and the fat body.

Comparative analysis of the frass of S. littoralis larvae fed on a

diet with or without 3-NPA revealed the presence of new components shown to originate from 3-NPA by feeding stable isotope labeled precursors. Molecular structures of these 3-NPA conjugation products were deduced from HR-MS/MS data and confirmed by total synthesis (see supporting information). In the frass of 3-NPA fed *S. littoralis* larvae amino acid amide of 3-NPA was detected, but no glutathione derivative was detected. 3-Nitropropanoyl glycine (**1**) and 3-nitropropanoyl serine (**3**) have previously been described as metabolites in the grasshopper *M. bivittatus*. The grasshopper also produces a glutamine derivative which is absent in *S. littoralis* (Majak et al., 1998). Homologous 3-nitropropanoyl alanine (**2**) and (3-nitropropanoyl) threonine (**4**) were exclusively detected in *S. littoralis* and represent novel compounds. Although 3-NPA amino acid conjugates have previously been identified as putative detoxification products from *M. bivittatus*, no data concerning the toxicity of these compounds have been reported (Majak et al., 1998). We found that in *S. littoralis* the injection of the amides **1**–**4** into the hemolymph is not toxic. However, the injection of the same amount of free 3-NPA causes mortality in 92% of the larvae (Figs. 4 and 5) demonstrating that conjugation with amino acids represents an efficient way to cope with 3-NPA. Amino acid conjugation represents a common detoxification mechanism in insects and, as such, is similar to glycosylation or reaction with glutathione (Schramm et al., 2012) which force excretion.

Conjugation to amino acids is well known from Lepidoptera. Glycine conjugates have been described as products of glucosinolate metabolism (Stauber et al., 2012).

Conjugation of long chain fatty acids to glutamine is mainly facilitated by gut tissue or membrane-associated enzymes (Alborn et al., 1997; Lait et al., 2003; Yoshinaga et al., 2005). However, occasionally the insect gut microbial community exhibited conjugation activity, as in the case of *N*-linolenoyl glutamine biosynthesis by *Microbacterium arborescens* in *Spodoptera exigua* (Ping et al., 2007). In *S. littoralis*, however, no 3-NPA conjugation activity of the gut microbes under aerobic or anaerobic conditions has been detected (Fig. 5). In contrast, cytosolic proteins, isolated from the *S. littoralis* gut tissue, were shown to catalyze the formation of 3-NPA amino acid amides in the presence of ATP and CoA (Figs. 4 and 5C). Dedicated enzymes catalyzing the conjugation of 3-NPA to amino acids from this or other organisms have not been described previously.

Taken together, these results indicate that amino acid conjugation via amide formation represents an important detoxification pathway in *S. littoralis*. Although the exact mechanisms of 3-NPA conjugation remains to be elucidated our results allow us to propose a functional model.

The epithelial cells protect the larval hemolymph from the free toxin taken up with the food (Fig. 6), as was previously shown for tannins (Appel and Michael, 1990; Engel and Moran, 2013; Giordana et al., 1989). Due to the high consumption rate of *S. littoralis* (consumed diet passes the gut within 2 h), larvae may accumulate a large amount of 3-NPA in the gut that can pass the membrane barriers via different membrane carriers (Lamp et al., 2011). Once taken up by the epithelium, as-yet unidentified cytosolic proteins detoxify 3-NPA by converting it to non-toxic amino acid conjugates. From the cytosol, the detoxification products **1**–**4** can be transported back into the gut lumen via apocrine secretion or passed onto the hemolymph (Cristofoletti et al., 2001; Ratzka et al., 2002; Terra and Ferreira, 1994; Wittstock et al., 2004) (Fig. 6). Compounds **1**–**4** were detected in the hemolymph after insects fed on a high concentration of 3-NPA (12.6 μ mol/g of artificial diet weight). In addition, compounds **1**–**4** were detected in the frass of the larvae after sublethal doses of 3-NPA (8.4 μ mol 3-NPA per g body weight) were injected into the hemolymph. When the toxin reaches the hemolymph after larvae have
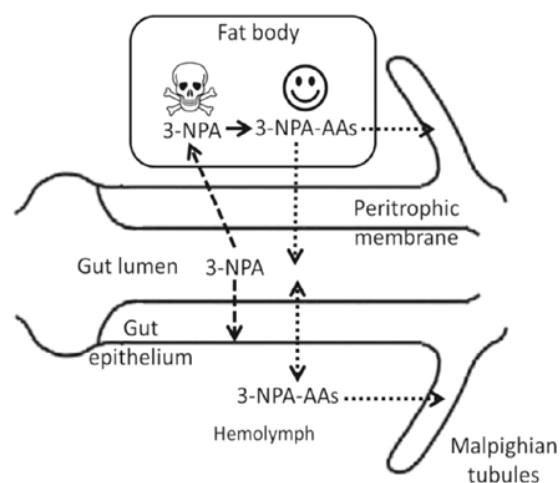

Fig. 6. Detoxification of 3-NPA and flux of metabolites in *S. littoralis*. 3-NPA can pass through membranes via different carriers. In the epithelial cells, the detoxification of 3-NPA proceeds via conjugation to amino acids by as-yet unidentified cytosolic proteins. 3-NPA conjugates are exported to the hemolymph, or retransported into the gut lumen by unknown mechanims. Also the fat body is able to produce amino acid amides. Conjugates reaching the hemolymph may be excreted via the malpighian tubules.

consumed high amounts of plant material, the fat body is also able to produce amino acid amides. Once amino acid amides are produced, they can be transported from the hemolymph to the hind gut via the malpighian tubules and finally excreted from the system.

In conclusion, we demonstrated that the formation of 3-NPA amides of glycine, serine, threonine and alanine by cytosolic enzymes of the insect epithelium represents an important detoxification pathway in *S. littoralis*. Details of 3-NPA metabolism and the responsible enzymes in *S. littoralis* remain to be identified.

Acknowledgments

Appendix A. Supplementary data

Supplementary data related to this article can be found at http://dx.doi.org/10.1016/j.ibmb.2015.05.013.

References

Akopian, G., Crawford, C., Petzinger, G., Jakowec, M.W., Walsh, J.P., 2012. Brief mitochondrial inhibition causes lasting changes in motor behavior and corticostriatal synaptic physiology in the Fischer 344 rat. Neuroscience 215, 149–159.
Alborn, H.T., Turlings, T.C.J., Jones, T.H., Stenhagen, G., Loughrin, J.H., Tumlinson, J.H., 1997. An elicitor of plant volatiles from beet armyworm oral secretion. Science 276, 945–949.
Appel, H.M., Michael, M.M., 1990. Gut redox conditions in herbivorous lepidopteran larvae. J. Chem. Ecol. 16, 3277–3290.
Baxter, R.L., Abbot, E.M., Greenwood, S.L., McFarlane, I.J., 1985. Conservation of the carbon-nitrogen bond of aspartic acid in the biosynthesis of 3-nitropropanoic acid. Chem. Soc. Chem. Commun. 564–566.
Becker, T., Kartikeya, P., Paetz, C., von Reuß, S.H., Boland, W., 2015. Synthesis and photosensitivity of isoxazolin-5-one glycosides. Org. Biomol. Chem. 13, 4025–4030.

Bergomaz, R., Boppre, M., 1986. A simple instant diet for rearing Arctiidae and other moths. J. Lepidopterists' Soc. 40, 131—137.

Burdock, G.A., Carbin, I.G., Soni, M.G., 2001. Safety assessment of β-nitropropionic acid: a monograph in support of an acceptable daily intake in humans. Food Chem. 75, 1—27.

Byers, R.A., Gustine, D.L., Moyer, B.G., 1977. Toxicity of β-nitropropionic acid to Trichoplusia ni. Environ. Entomol. 6, 167—171.

Chomcheon, P., Wiyakrutta, S., Scriubolmas, N., Kittakoop, P., 2005. 3-Nitropropionic acid (3-NPA), a potent antimycobacterial agent from endophytic fungi: is 3-NPA in some plants produced by endophytes? J. Nat. Prod. 68, 1103—1105.

Cipollini, D., Stevenson, R., Enright, S., Eyles, A., Bonello, P., 2008. Phenolic metabolites in leaves of the invasive shrub, Lonicera maackii, and their potential phytotoxic and anti-herbivore effects. J. Chem. Ecol. 34, 144—152.

Cristofoletti, P.T., Ribeiro, A.F., Terra, W.R., 2001. Apocrine secretion of amylase and exocytosis of trypsin along the midgut of Tenebrio molitor larvae. J. Insect Physiol. 47, 143—155.

Engel, P., Moran, A.N., 2013. The gut microbiota of insects — diversity in structure and function. FEMS Microbiol. Rev. 37, 699—735.

Firstenberg, D.E., Silhacek, D.L., 1973. Juvenile hormone regulation of oxidative metabolism in isolated insect mitochondria. Experientia 29, 1420—1422.

Francis, K., Smitherman, C., Nishino, S.F., Spain, J.C., Gadda, G., 2013. The biochemistry of the metabolic poison propionate 3-nitronate and its conjugate acid, 3-nitropropionate. Int. Union Biochem. Mol. Biol. Life 65, 759—768.

Giordana, B., Sacchi, V.F., Parenti, P., Hanozet, G.M., 1989. Amino acid transport systems in intestinal brush-border membranes from lepidopteran larvae. Am. J. Physiol. 257, 494—500.

Grossa, E.M., Brune, A., Walenciak, O., 2008. Gut pH, redox conditions and oxygen levels in an aquatic caterpillar: potential effects on the fate of ingested tannins. J. Insect Physiol. 54, 462—471.

Hipkin, C.R., Simpson, D.J., Wainwright, S.J., Salem, M.A., 2004. Nitrification by plants that also fix nitrogen. Nature 430, 98—101.

Ibanez, S., Gallet, C., Després, L., 2012. Plant insecticidal toxins in ecological networks. Toxins 4, 228—243.

Lamp, J., Keyser, B., Koeller, D.M., Kurt, U., Braulke, T., Mühlhausen, C., 2011. Glutaric aciduria type 1 metabolites impair the succinate transport from astrocytic to neuronal cells. J. Biol. Chem. 286, 17777—17784.

Lait, C.G., Alborn, H.T., Teal, E.A., Tumlinson, J.H., 2003. Rapid biosynthesis of N-linolenoyl-L-glutamine, an elicitor of plant volatiles, by membrane-associated enzyme(s) in Manduca sexta. Proc. Natl. Acad. Sci. U. S. A. 100, 7027—7032.

Majak, W., Johnson, D.L., Benn, M.H., 1998. Detoxification of 3-nitropropionic acid and karakin by melanopline grasshoppers. Phytochemistry 49, 419—422.

Meldrum, B.S., 2000. Glutamate as a neurotransmitter in the brain: review of physiology and pathology. J. Nutr. 130, 1007—1015.

Mithöfer, A., Boland, W., 2012. Plant defense against herbivores: chemical aspects. Annu. Rev. Plant Biol. 63, 431—450.

Neises, B., Steglich, W., 1978. Simple method for the esterification of carboxylic acids. Angew. Chem. Int. Ed. 17, 522.

Olsen, C., Rustad, A., Fonnum, F., Paulsen, R.E., Hassel, B., 1999. 3-Nitropropionic

acid: an astrocyte-sparing neurotoxin in vitro. Brain Res. 850, 144—149.

Parry, R., Nishino, S., Spain, J., 2011. Naturally-occurring nitro compounds. Nat. Prod. Rep. 28, 152—167.

Ping, L., Büchler, R., Mithöfer, A., Svatoš, A., Spiteller, D., Dettner, K., Gmeiner, S., Piel, J., Schlott, B., Boland, W., 2007. A novel Dps-type protein from insect gut bacteria catalyses hydrolysis and synthesis of N-acyl amino acids. Environ. Microbiol. 9, 1572—1583.

Ratzka, A., Vogel, H., Kliebenstein, D.J., Mitchell-Olds, T., Kroymann, J., 2002. Disarming the mustard oil bomb. Proc. Natl. Acad. Sci. U. S. A. 99, 11223—11228.

Schramm, K., Vassão, D.G., Reichelt, M., Gershenzon, J., Wittstock, U., 2012. Metabolism of glucosinolate-derived isothiocyanates to glutathione conjugates in generalist lepidopteran herbivores. Insect Biochem. Mol. Biol. 42, 174—182.

Spiteller, D., Dettner, K., Boland, W., 2005. Gut bacteria may be involved in interactions between plants, herbivores and their predators: microbial biosynthesis of N-acylglutamine surfactants as elicitors of plant volatiles. Biol. Chem. 381, 755—762.

Stauber, E.J., Kuczka, P., van Ohlen, M., Vogt, B., Janowitz, T., Piotrowski, M., Beuerle, T., Wittstock, U., 2012. Turning the 'Mustard Oil Bomb' into a 'Cyanide Bomb': aromatic glucosinolate metabolism in a specialist insect herbivore. PLoS ONE 7, e35545.

Tang, X., Freitak, D., Vogel, H., Ping, L., Shao, Y., Cordero, E.A., Andersen, G., Westermann, M., Heckel, D.G., Boland, W., 2012. Complexity and variability of gut commensal microbiota in polyphagous lepidopteran larvae. PLoS ONE 7, e36978.

Tarazona, J.V., Sanz, F., 1987. Aliphatic nitro compounds in Astragalus lusitanicus Lam. Vet. Hum. Toxicol. 29, 437—439.

Terra, W.R., Ferreira, C., 1994. Insect digestive enzymes: properties, compartmentalization and function. Comp. Biochem. Physiol. 109, 1—62.

Tiedtke, A., Rasmussen, L., Florin-Christensen, J., Florin-Christensen, M., 1988. Release of lysosomal enzymes in Tetrahymena: a Ca²⁺-dependent secretory process. J. Cell. Sci. 89, 167—171.

Turlings, T.C.J., McCall, P.J., Alborne, H.T., Tumlinson, J.H., 1993. An elicitor in caterpillar oral secretions that induces corn seedlings to emit chemical signals attractive to parasitic wasps. J. Chem. Ecol. 19, 412—425.

Wang, S.D., Liu, W., Xue, C.B., Luo, W.C., 2010. The effects of luteolin on phenoloxidase and the growth of Spodoptera exigua (Hubner) larvae (Lepidoptera: Noctuidae). J. Pestic. Sci. 35, 483—487.

Williams, M.C., 1994. Impact of poisonous weeds on livestock and humans in North America. Rew. Weed Sci. 6, 1—27.

Wittstock, U., Agerbirk, N., Stauber, E.J., Olsen, C.E., Hippler, M., Mitchell-Olds, T., Gershenson, J., Vogel, H., 2004. Successful herbivore attack due to metabolic diversion of a plant chemical defense. Proc. Natl. Acad. Sci. U. S. A. 101, 4859—4864.

Xingjie, L., Xueyun, L., Wenjuan, H., 1992. Studies on the epidemiology and etiology of moldy sugarcane poisoning in China. Biomed. Environ. Sci. 5, 161—177.

Yoshinaga, N., Morigaki, N., Matsuda, F., Nishida, R., Mori, N., 2005. In vitro biosynthesis of volicitin in Spodoptera litura. Insect Biochem. Mol. Biol. 35, 175—184.

4. Article II

Draft Genome Sequence of *Enterococcus mundtii* SL 16, an Indigenous Gut Bacterium of the Polyphagous Pest *Spodoptera littoralis*

Bosheng Chen, Chao Sun, Xili Liang, Xingmeng Lu, Qikang Gao, Pol Alonso-Pernas, Beng-Soon Teh, Alexey L. Novoselov, Wilhelm Boland and Yongqi Shao

frontiers
in Microbiology

Draft Genome Sequence of *Enterococcus mundtii* SL 16, an Indigenous Gut Bacterium of the Polyphagous Pest *Spodoptera littoralis*

Bosheng Chen[1†], Chao Sun[2†], Xili Liang[1], Xingmeng Lu[1], Qikang Gao[2],
Pol Alonso-Pernas[3], Beng-Soon Teh[3], Alexey L. Novoselov[3], Wilhelm Boland[3] and
Yongqi Shao[1*]

[1] Laboratory of Invertebrate Pathology, College of Animal Sciences, Zhejiang University, Hangzhou, China, [2] Analysis Center
of Agrobiology and Environmental Sciences, Zhejiang University, Hangzhou, China, [3] Department of Bioorganic Chemistry,
Max Planck Institute for Chemical Ecology, Jena, Germany

Keywords: *Enterococcus mundtii*, genome sequencing, symbiosis, *Spodoptera littoralis*, intestinal tract

INTRODUCTION

Insects are the most abundant and diverse animal class on Earth, and they are associated with an amazing variety of symbiotic microorganisms, which participate in many relationships with the hosts (Douglas, 2015). For example, the fungal symbiont (*Leucoagaricus gongylophorus*) of leaf-cutting ants produces diverse enzymes for the degradation of plant material (Kooij et al., 2016). Similarly, *Bacillus pumilus* isolated from the gut of wood boring *Mesomorphus* sp. (Coleoptera: Tenebrionidae) exhibits significant cellulolytic and xylose isomerase activities (Balsingh et al., 2016).

The Lepidoptera, including moths and butterflies, is one of the most widespread and widely recognizable insect orders in the world. Although butterflies and moths play an important role in the natural ecosystem as pollinators and as food in the food chain, their leaf-chewing larvae are often problematic in agriculture, as their main source of food is live plants (Mithöfer and Boland, 2012). The leafworm *Spodoptera littoralis* (Lepidoptera: Noctuidae) is a highly polyphagous lepidopteran pest found worldwide and also an important model system used in a variety of biological research. Recent extensive surveys of its microbiome reveal that *Enterococcus mundtii* is one of the predominant gut microorganisms of *S. littoralis* and present at high frequency (Tang et al., 2012; Chen et al., 2016; Teh et al., 2016). Particularly, a stable isotope labeling-based approach suggested that this phylotype was also highly metabolically active inside the host across life history of *S. littoralis*, indicating the significant role played by *E. mundtii* in host biology (Shao et al., 2014). Therefore, the symbiotic *E. mundtii* probably constitutes a key factor for the success of this generalist herbivore in adapting to different environments and food sources. The aim of this study was to produce a genome sequence of the strain SL 16, which would assist in understanding of the
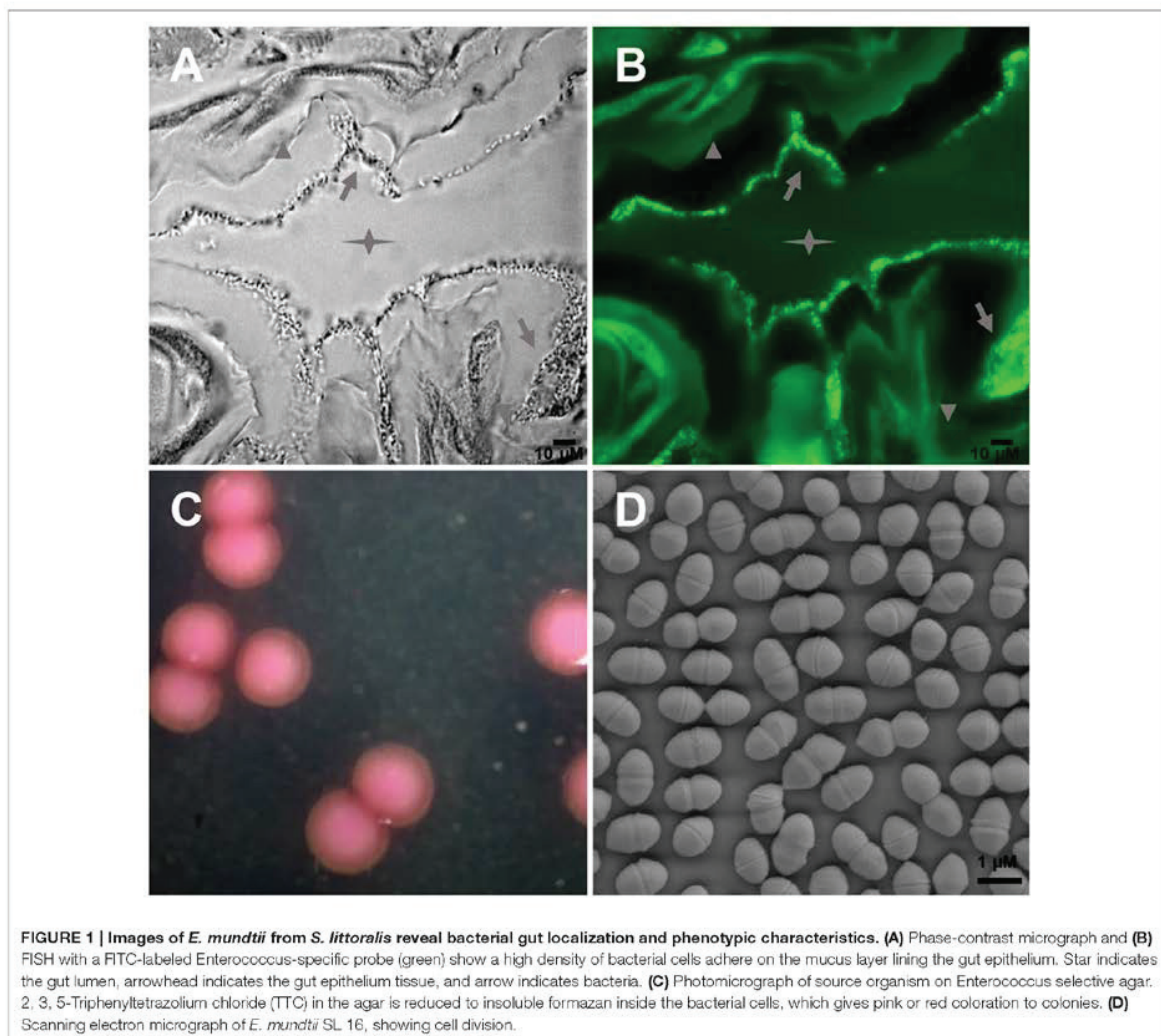
coevolution of the microbe and the insect host. The dataset has been submitted to NCBI Whole Genome Shotgun (WGS) projects and is reported here, providing an overview of the genome sequence and relevant features of gut symbiotic *E. mundtii*.

MATERIALS AND METHODS

Isolation of the Bacterial Strain

E. mundtii strain SL 16 was isolated from the mature 5th instar larva using standard microbiology methods. Briefly, the normal larvae were washed and sedated on ice for at least 1 h to anesthetize them. Then the whole gut sections were dissected from larvae using a fine Vannas scissor and forceps under a binocular microscope (Shao et al., 2013). The fresh gut

tissues were put into phosphate buffered saline (PBS: 137 mM NaCl, 10 mM Na_2HPO_4, 2 mM KH_2PO_4, and 2.7 mM KCl) and homogenized by hand with a sterile pestle. Bacterial isolates were made by plating the homogenized gut tissues on the *Enterococcus* Selective Agar (45183, Fluka). After incubation for 24 h at 30°C, the growing bacterial colonies were sub-cultured twice on the same agar medium. 2, 3, 5-Triphenyltetrazolium chloride (TTC) in the medium is reduced to insoluble formazan inside the bacterial cells, which gives pink or red coloration to enterococcal colonies. These purified enterococcal colonies were tested for key phenotypic traits including carbohydrate fermentation capability, motility, and pigment production as previously described (Manero and Blanch, 1999). Furthermore, the taxonomy was validated by colony PCR and sequencing of the amplified 16S rRNA gene. The representative *E. mundtii*

FIGURE 1 | Images of *E. mundtii* from *S. littoralis* reveal bacterial gut localization and phenotypic characteristics. (A) Phase-contrast micrograph and (B) FISH with a FITC-labeled Enterococcus-specific probe (green) show a high density of bacterial cells adhere on the mucus layer lining the gut epithelium. Star indicates the gut lumen, arrowhead indicates the gut epithelium tissue, and arrow indicates bacteria. (C) Photomicrograph of source organism on Enterococcus selective agar. 2, 3, 5-Triphenyltetrazolium chloride (TTC) in the agar is reduced to insoluble formazan inside the bacterial cells, which gives pink or red coloration to colonies. (D) Scanning electron micrograph of *E. mundtii* SL 16, showing cell division.

isolate, designated strain SL 16, was selected for this WGS project.

Fluorescence in situ Hybridization (FISH) was applied to localize the dominant enterococci as previously described (Shao et al., 2014). Shortly, FISH was performed on 5 μm thin cross sections of the cold polymerizing resin (Technovit 8100, Heraeus Kulzer GmbH, Wehrheim, Germany) embedded gut tissue. The specificity of probes was tested and hybridization condition was achieved as described (Tang et al., 2012). The sample was hybridized with 1.5 mM FITC-labeled *Enterococcus*-specific probe in hybridization buffer containing 900 mM NaCl, 20 mM Tris-HCl (pH 8.0), 20% formamide, 1% SDS. And images were taken with an Axio Imager Z1 microscope (Carl Zeiss, Jena, Germany). For scanning electron microscopy (SEM), cells were fixed in paraformaldehyde (1%), and glutaraldehyde (0.25%), dehydrated by ascending alcohol series and dried. After coating samples with gold, scanning electron micrographs were taken with a LEO 1525 instrument (Carl Zeiss, Jena, Germany).

Genomic DNA Isolation, Library Preparation and Sequencing

The genomic DNA was extracted from the cultured bacterium according to Pospiech and Neumann (1995). DNA quality was examined by 1% agarose gel electrophoresis and quantified using a NanoDrop™ spectrophotometer. The DNA library was constructed using the TruSeq™ DNA Sample Preparation Kit (Illumina Inc., San Diego, CA), and 5 μg of pure genomic DNA was prepared for a standard Illumina shotgun library construction. Briefly, genomic DNA was first sheared to a size ranging between 400 and 500 bp using the Covaris M220 per the manufacturer's recommendations. The fragmented DNA sample was end-repaired, dA-tailed, and ligated to multiplex adapters according to the manufacturer's instructions. The ligated products were purified and further enriched using PCR. The quality of the final amplified libraries were checked by running an aliquot (1 μL) on a high-sensitivity Bioanalyzer 2100 DNA Chip (Agilent Technologies). Paired-end sequencing was performed by using an Illumina MiSeq platform (Illumina Inc., San Diego, CA) at Majorbio Bio-pharm Technology Co., Ltd (Shanghai, China) according to the manufacturer's instructions (Zhang et al., 2016).

Preprocessing and Genome Assembly

The quality of sequence reads was evaluated using the FastQC tool as previously described (Balsingh et al., 2016). Reads with >10% Ns and/or 25–35 bases of low quality (≤Q20) were filtered out, and adapter and duplication contamination were removed as well as read ends were trimmed off. The filtered reads were assembled with Short Oligonucleotide Analysis Package (SOAP) *de novo* version 2.04 using a range of *k*-mer sizes (Li et al., 2009). Then GapCloser version 1.12 was used to close any internal gaps in the optimal scaffolded assembly. Repeats were predicted by RepeatMasker and Tandem Repeats Finder (TRF) tools (Rédou et al., 2016). Barrnap version 0.4.2 and tRNAscan-SE version 1.3.1 were employed to predict rRNAs and tRNAs respectively. The genome was annotated using Glimmer version 3.02

(Xu et al., 2014). The Clusters of Orthologous Groups of proteins (COG) categories were assigned to the SL 16 genome annotation using blastp (BLAST 2.2.28+) against the COG genes collection (Von Mering et al., 2005). The translations of the identified coding sequences (CDSs) were also used to search against the Protein family (Pfam) database with *E*-value cut-off of 1-e5. The metabolic pathway analysis was constructed using the Kyoto Encyclopedia of Genes and Genomes (KEGG) (Kanehisa et al., 2014).

INTERPRETATION OF DATA SET

Whole Genome Sequencing of *E. mundtii* SL 16

Large amounts of *E. mundtii* closely adhere to the mucosal layer of *S. littoralis* gut epithelium, where they form a biofilm-like structure (**Figures 1A,B**). Strain SL 16 displays characteristic phenotypes of *E. mundtii*. It grows well on Slanetz and Bartley medium (Slanetz and Bartley, 1957), producing smooth, circular, glistening colonies (**Figure 1C**). The bacterial cells are 0.5–1.0 μm in diameter, and occur in the form of pairs (**Figure 1D**). Strain SL 16 could utilize various carbon sources, including xylose, cellobiose, and sucrose (**Table 1**).

Sequencing the genome of *E. mundtii* SL 16 produced a raw data set of 1,764,821,160 total bases. During the quality control, Illumina PCR adapter reads and low-quality reads were removed, and a total of 3,469,570 mate-pair reads (total bases 1,698,525,052 bp) were retained. The cleaned sequence reads were assembled with a *k*-mer setting of 125, which was determined by the optimal assembly result. The resulting genome sequence has an estimated size of 3,296,585 bp and a G+C content of 38.36%. 43,977 bp were repeats as predicted by RepeatMasker and TRF tools, which constituted 1.33% of the entire assembled genome.

TABLE 1 | *E. mundtii* SL 16 genome resources and characteristics.

	Name	Genome resources/characteristics
1	NCBI Bioproject ID	PRJNA337899
2	NCBI Biosample ID	SAMN05513637
3	NCBI Genome Accession Number	MCRG00000000
4	Sequence type	Illumina Miseq
5	Total number of Reads	3,515,580
6	Overall coverage	>100x
7	Estimated genome size (bp)	3,296,585
8	GC content (%)	38.36
9	Average of gene length (bp)	889
10	Protein coding genes	2939
11	tRNA coding genes	59
12	Motility	Non-motile
13	Cellobiose metabolism	Positive
14	Xylose metabolism	Positive
15	Arabinose metabolism	Positive
16	Sucrose	Positive

A total of 3125 genes with sequence length of 2,780,928 bp were predicted, which account for 84.4% of the genome, and 59 tRNA genes were identified by tRNAscan-SE. CDSs were searched against the NR, GO, string, Swiss-Prot, COG, and KEGG databases to analyze gene functions and metabolic pathways. In all, 1493 CDSs were assigned to COG families and 1411 CDSs were included in 154 pathways. Several physiological traits that may explain the successful adaptation of this bacterium to the environment of the gut have been found. In particular, a large amount of the coding capacity encountered in the genome of SL 16 (almost 12%) is dedicated to genes assigned to functions related to carbohydrate transport and metabolism, which matches well with the observed physiological characteristics of this strain (**Table 1**). This feature is shared with other colonic inhabitants, such as *Bacteroides fragilis* (Flint et al., 2008), and reflects the ecological niche of the organism presented inside a herbivore gut. The genome encodes several ABC-type sugar transporters, sugar-binding proteins, and a rich suite of glycosyl hydrolases, such as β-N-acetylhexosaminidase, α-galactosidase, β-glucosidase, β-galactosidase, and α-glucosidase. Moreover, the pyruvate dissipation pathways predicted for SL 16 include the capacity to produce L-lactate and several other fermentation metabolites, like short-chain fatty acids formate and acetate. This metabolic flexibility is expected to aid in efficient digestion and conversion of plant saccharides, thus promoting host development.

In conclusion, here we report a 3.30 Mbp draft genome sequence of *E. mundtii* strain SL 16, isolated from the generalist herbivore *S. littoralis*. The final *de novo* assembly is based on 1765 Mbp of Illumina data which provides an average coverage of 535 ×. Analysis of the genome shows high correlation between the genotypes and the phenotypes.

Direct Link to Deposited Data and Information to Users

The dataset submitted to NCBI include the assembled consensus sequence of *E. mundtii* SL 16 in Fasta format. The genome sequence can be accessed at DDBJ/EMBL/GenBank under the accession no. MCRG00000000. This paper describes the first version of the genome (https://www.ncbi.nlm.nih.gov/nuccore/MCRG00000000).

AUTHOR CONTRIBUTIONS

Work was planned by YS and WB, and executed jointly by BC and CS. XLi and BT were associated with isolation of the bacterium. AN and PA performed bioinformatics analyses. QG and XLu contributed to the DNA sequencing.

ACKNOWLEDGMENTS

REFERENCES

Balsingh, J., Radhakrishna, S., and Ulaganathan, K. (2016). Draft genome sequence of *Bacillus pumilus* ku-bf1 isolated from the gut contents of wood boring *Mesomorphus* sp. *Front. Microbiol.* 7:1037. doi: 10.3389/fmicb.2016.01037

Chen, B., Teh, B. S., Sun, C., Hu, S., Lu, X., Boland, W., et al. (2016). Biodiversity and activity of the gut microbiota across the life history of the insect herbivore *Spodoptera littoralis*. *Sci. Rep.* 6:29505. doi: 10.1038/srep29505

Douglas, A. E. (2015). Multiorganismal insects: diversity and function of resident microorganisms. *Annu. Rev. Entomol.* 60, 17–34. doi: 10.1146/annurev-ento-010814-020822

Flint, H. J., Bayer, E. A., Rincon, M. T., Lamed, R., and White, B. A. (2008). Polysaccharide utilization by gut bacteria: potential for new insights from genomic analysis. *Nat. Rev. Microbiol.* 6, 121–131. doi: 10.1038/nrmicro1817

Kanehisa, M., Goto, S., Sato, Y., Kawashima, M., Furumichi, M., and Tanabe, M. (2014). Data, information, knowledge and principle: back to metabolism in KEGG. *Nucleic Acids Res.* 42, D199–D205. doi: 10.1093/nar/gkt1076

Kooij, P. W., Pullens, J. W., Boomsma, J. J., and Schiøtt, M. (2016). Ant mediated redistribution of a xyloglucanase enzyme in fungus gardens of *Acromyrmex echinatior*. *BMC Microbiol.* 16:81. doi: 10.1186/s12866-016-0697-4

Li, R., Yu, C., Li, Y., Lam, T. W., Yiu, S. M., Kristiansen, K., et al. (2009). SOAP2: an improved ultrafast tool for short read alignment. *Bioinformatics* 25, 1966–1967. doi: 10.1093/bioinformatics/btp336

Manero, A., and Blanch, A. R. (1999). Identification of *Enterococcus* spp. with a biochemical key. *Appl. Environ. Microbiol.* 65, 4425–4430.

Mithöfer, A., and Boland, W. (2012). Plant defense against herbivores: chemical aspects. *Annu. Rev. Plant Biol.* 63, 431–450. doi: 10.1146/annurev-arplant-042110-103854

Pospiech, A., and Neumann, B. (1995). A versatile quick-prep of genomic DNA from gram-positive bacteria. *Trends Genet.* 11, 217–218. doi: 10.1016/S0168-9525(00)89052-6

Rédou, V., Kumar, A., Hainaut, M., Henrissat, B., Record, E., Barbier, G., et al. (2016). Draft genome sequence of the deep-sea basidiomycetous yeast *Cryptococcus* sp. strain Mo29 reveals its biotechnological potential. *Genome Announc.* 4:e00461-16. doi: 10.1128/genomeA.00461-16

Shao, Y., Arias-Cordero, E., Guo, H., Bartram, S., and Boland, W. (2014). In vivo Pyro-SIP assessing active gut microbiota of the cotton leafworm, *Spodoptera littoralis*. *PLoS ONE* 9:e85948. doi: 10.1371/journal.pone.0085948

Shao, Y., Arias-Cordero, E. M., and Boland, W. (2013). Identification of metabolically active bacteria in the gut of the generalist *Spodoptera littoralis* via DNA stable isotope probing using 13C-glucose. *J. Vis. Exp.* e50734. doi: 10.3791/50734

Slanetz, L. W., and Bartley, C. H. (1957). Numbers of enterococci in water, sewage, and feces determined by the membrane filter technique with an improved medium. *J. Bacteriol.* 74, 591–595.

Tang, X., Freitak, D., Vogel, H., Ping, L., Shao, Y., Cordero, E. A., et al. (2012). Complexity and variability of gut commensal microbiota in polyphagous lepidopteran larvae. *PLoS ONE* 7:e36978. doi: 10.1371/journal.pone.0036978

Teh, B. S., Apel, J., Shao, Y., and Boland, W. (2016). Colonization of the intestinal tract of the polyphagous pest *Spodoptera littoralis* with the GFP-Tagged indigenous gut bacterium *Enterococcus mundtii*. *Front. Microbiol.* 7:928. doi: 10.3389/fmicb.2016.00928

Von Mering, C., Jensen, L. J., Snel, B., Hooper, S. D., Krupp, M., Foglierini, M., et al. (2005). STRING: known and predicted protein-protein associations, integrated and transferred across organisms. *Nucleic Acids Res.* 33, D433–D437. doi: 10.1093/nar/gki005

Xu, G., Hu, J., Fang, X., Zhang, X., Wang, J., Guo, Y., et al. (2014). Genome sequence of *Pseudomonas aeruginosa* strain LCT-PA220, which was selected after space flight by using biolog's powerful carbon source utilization technology. *Genome Announc.* 2:e00169-14. doi: 10.1128/genomeA.00169-14

Zhang, X., Li, G.-X., Chen, S.-C., Jia, X.-Y., Wu, K., Cao, C.-L., et al. (2016). Draft genome sequence of *Desulfitobacterium hafniense* strain DH, a sulfate-reducing bacterium isolated from paddy soils. *Genome Announc.* 4:e01693-15. doi: 10.1128/genomeA.01693-15

5. Article III

Bacterial community and PHB-accumulating bacteria associated with the wall and specialized niches of the hindgut of the forest cockchafer (*Melolontha hippocastani*)

Pol Alonso-Pernas, Erika Arias-Cordero, Alexey Novoselov, Christina Große, Jürgen Rybak, Martin Kaltenpoth, Martin Westermann, Ute Neugebauer, Wilhelm Boland

Bacterial Community and PHB-Accumulating Bacteria Associated with the Wall and Specialized Niches of the Hindgut of the Forest Cockchafer (*Melolontha hippocastani*)

Pol Alonso-Pernas[1*†], Erika Arias-Cordero[1†], Alexey Novoselov[1], Christina Ebert[2,3], Jürgen Rybak[4], Martin Kaltenpoth[5], Martin Westermann[6], Ute Neugebauer[2,3] and Wilhelm Boland[1*]

[1] Department of Bioorganic Chemistry, Max Planck Institute for Chemical Ecology, Jena, Germany, [2] Center for Sepsis Control and Care, Jena University Hospital, Jena, Germany, [3] Leibniz Institute of Photonic Technology, Jena, Germany, [4] Department of Evolutionary Neuroethology, Max Planck Institute for Chemical Ecology, Jena, Germany, [5] Department of Evolutionary Ecology, Institute of Zoology, Johannes Gutenberg University Mainz, Mainz, Germany, [6] Electron Microscopy Center, Jena University Hospital, Jena, Germany

A characterization of the bacterial community of the hindgut wall of two larval and the adult stages of the forest cockchafer (*Melolontha hippocastani*) was carried out using amplicon sequencing of the 16S rRNA gene fragment. We found that, in second-instar larvae, Caulobacteraceae and Pseudomonadaceae showed the highest relative abundances, while in third-instar larvae, the dominant families were Porphyromonadaceae and Bacteroidales-related. In adults, an increase of the relative abundance of Bacteroidetes, Proteobacteria (γ- and δ- classes) and the family Enterococcaceae (Firmicutes) was observed. This suggests that the composition of the hindgut wall community may depend on the insect's life stage. Additionally, specialized bacterial niches hitherto very poorly described in the literature were spotted at both sides of the distal part of the hindgut chamber. We named these structures "pockets." Amplicon sequencing of the 16S rRNA gene fragment revealed that the pockets contained a different bacterial community than the surrounding hindgut wall, dominated by Alcaligenaceae and Micrococcaceae-related families. Poly-β-hydroxybutyrate (PHB) accumulation in the pocket was suggested in isolated *Achromobacter* sp. by Nile Blue staining, and confirmed by gas chromatography–mass spectrometry analysis (GC-MS) on cultured bacterial mass and whole pocket tissue. Raman micro-spectroscopy allowed to visualize the spatial distribution of PHB accumulating bacteria within the pocket tissue. The presence of this polymer might play a role in the colonization of these specialized niches.

Keywords: hindgut, *Melolontha hippocastani*, gut bacteria, poly-β-hydroxybutyrate, PHB, *Achromobacter*, Raman microscopy

35

INTRODUCTION

Bacteria not only thrive as free-living organisms in the environment, they also engage in complex symbiotic relationships with higher organisms (Wells and Varel, 2011). Insects, in particular, are associated with a large diversity of microorganisms that play important roles for their host's physiology, ecology, and evolution. The insect gut is colonized by a wide range of bacterial phylotypes that interact with the host and allow it to subsist on nutritionally imbalanced diets. The recycling of nitrogen, the provisioning of essential amino acids and cofactors, and the digesting of recalcitrant polymers in the host's diet are among the functions for which symbiotic microorganisms play an integral role (Potrikus and Breznak, 1981; Douglas, 2009; Watanabe and Tokuda, 2010), increasing the overall fitness of the insect host.

Typically, the insect gut is divided into three regions, i.e., foregut, midgut and hindgut. The symbiotic bacteria are either attached to the gut wall or colonize the gut as free-living organisms, usually mostly in the mid- and hindgut regions. The structure of these communities differs among insect species, influenced by the host's diet and taxon (Egert et al., 2003, 2005; Colman et al., 2012; Jones et al., 2013). In the Scarabaeidae family, the hindgut region is of special importance. It is anatomically modified to serve as fermentation chamber. This chamber, in addition to its original function, namely, absorbing water and salts from the gut content, is also devoted to aiding digestion, probably with the help of the fermentative bacteria that colonize it (Egert et al., 2005; Huang et al., 2010; Arias-Cordero et al., 2012; Engel and Moran, 2013). These microbial associates are transmitted either vertically, directly from mother to offspring, or horizontally, that is, being taken anew from the environment by each host generation (Bright and Bulgheresi, 2010). In horizontally transmitted symbiosis, the host usually ingests the symbiont along with unwanted microbes that may compete for the colonization of the gut. The selection of the right symbiont may depend on its phenotypic traits. Kim et al. (2013) showed that poly-β-hydroxybutyrate (PHB) accumulation by the symbiont is crucial for the maintenance of host–microbe relationship.

In this study, we investigate the forest cockchafer (*Melolontha hippocastani*). This scarabaeid constitutes an interesting model due to its particular life cycle, consisting in two well-differentiated stages: the rhizophagous larvae spend up to 4 years underground, while the adults, after pupation, emerge from the soil and shift to a diet based exclusively on foliage. To date, there is a lack of comparative studies on the variation of the gut bacterial community associated with the transition from larva to adult. Only one study addressed this question, a study conducted by Arias-Cordero et al. (2012), focused on the midgut of *M. hippocastani*. Surprisingly, they found a group of bacterial phylotypes that seems to always be stable. This core community is maintained through metamorphosis and is unaffected by the radical change of the host diet from roots to leaves, when the shift occurs from a below-ground (larval) to an above-ground (adult) stage (Arias-Cordero et al., 2012).

In view of this unexpected stability of the gut microbial community, we considered appropiate to characterize the bacterial communities inhabiting the hindgut wall of both below- and above-ground stages of the forest cockchafer, thus complementing the above-mentioned midgut-based study (Arias-Cordero et al., 2012). We put our focus on the hindgut wall itself, and also on particular bacterial niches attached and connected to it, at both sides of the distal part of the larval hindgut. These small structures, called from now on "pockets," have been hitherto only once described in the literature (Wildbolz, 1954). They consist of several tubular poles connected to the hindgut chamber, which contain bacterial phylotypes that are minor or not detected in the hindgut wall. We detected the presence of PHB within the pockets, and *Achromobacter* sp., one of the major pocket bacterial species, is able to accumulate PHB in pure culture. This suggests that some of the pocket symbionts may be horizontally transmitted, as previous studies found this type of inclusions in symbiotic *Burkholderia* of environmental origin harbored in the midgut crypts of the midgut of *Riptortus pedestris* (Kim et al., 2013). The question of whether PHB plays a role in host nutrition remains unknown.

MATERIALS AND METHODS

Sample Collection and DNA Extraction

Second-instar (L2) and third-instar (L3) larvae of *M. hippocastani* and actively flying adults were collected in forests of red oak in Mannheim (49°29′20″N 8°28′9″E), and Graben-Neudorf (49°9′55″N 8°29′21″E), respectively, between December 2010 and May 2014. Beetles were collected at the same sites. The insects were transported alive in boxes with soil or tree leaves. Before dissection, the insects were kept at −20°C for 20 min to kill them, and then rinsed three times alternately with sterile distilled water and 70% ethanol. Dissection was performed on ice in a phosphate-buffered saline (PBS) solution. Hindguts, as shown between dotted lines in **Figure 1D** (top for larva and bottom for adult), were excised, cut open, and carefully washed three times with sterile PBS in order to remove any unattached bacteria. The pockets were separated from the hindgut wall, and as much of the surrounding epithelium was removed as possible. Samples were stored at −20°C before DNA extraction. The day of the extraction, frozen samples were thawed on ice and dried at 45°C for 90 min in a Speedvac (Concentrator 5301, Eppendorf), then crushed in a 1.5 ml tube with a sterile pestle. For 454-pyrosequencing, DNA extractions of the tissue were carried out using the PowerSoil™ DNA Isolation Kit (MO BIO Laboratories Inc., Carlsbad, CA, USA) according to the protocol provided by the manufacturer. Final DNA concentrations were determined using a Nanovue device (GE Healthcare, Little Chalfont, UK). In order to test for the quality of the extracted DNA and confirm the presence of DNA from bacteria, a diagnostic PCR reaction was carried out as described (Arias-Cordero et al., 2012).

Transmission Electron Microscopy (TEM)

Dissected hindguts and pockets of larvae were fixed in a solution of 2.5% glutaraldehyde and 2% paraformaldehyde in 0.1 M

36

sodium cacodylate buffer (pH 7.2). Immediately afterward, the tissue was transferred to the same solution for overnight fixation. Next day, the fixative was removed, and the tissue was post fixed with 1% osmium tetroxide in cacodylate buffer for 2 h. During the following ascending ethanol series samples were stained with 2% uranyl acetate. The samples were embedded in Araldite CY212 epoxy resin (Agar Scientific Ltd, Stansted, United Kingdom) according to manufacturer's instruction. Semi-thin sections (1 μm thickness) were stained with Richardson's methylene blue in order to localize the right position for the examination. Hindgut areas were further trimmed down to 500 μ × 500 μm. Ultra-thin sections of 80 nm thickness were cut using an ultramicrotome Ultracut E (Reichert–Jung, Vienna, Austria) and mounted on Formvar-carbon coated grids (100 meshes, Quantifoil GmbH, Großlöbichau, Germany). Finally, sections were contrasted with lead citrate for 4 min and analyzed in a transmission electron microscope EM900 (Zeiss AG, Oberkochen, Germany).

Light Microscopy, Richardson Staining, and Autofluorescence Visualization

In all cases the tissue was fixed as described above for transmission electron microscopy (TEM). The tissues employed were larvae hindgut walls and pockets. For the Richardson staining, semi-thin sections of 0.3–0.6 μm (embedded as for TEM) were immersed in a 60°C staining solution for 3–5 min. Afterward, the tissue was washed twice with sterile water. Finally, the sections were placed on a glass slide, dried and mounted for microscopic observation. For the autofluorescence visualization, a excised complete hindgut pocket was placed onto a glass slide and covered with PBS. Visualization was carried out using a LeicaTCS-SP2 confocal microscope using a 10× dry or 40× oil Leica objective (HC PL APO 10×/0.4, Leica, Bensheim, Germany) in both cases. For autofluorescence, laser line employed was 488 nm.

Bacterial Tag-Encoded FLX Amplicon Pyrosequencing (bTEFAP) and Data Analysis

For pyrosequencing, a sample was composed of the extracted DNA of six insects collected during the same year, pooled together in equal amounts for a single run. A total of four samples were sequenced (L2 pocket, L2 hindgut wall, L3 hindgut wall, and adult hindgut wall). DNA was sent to an external service provider (Research and Testing Laboratories, Lubbock, TX, USA) for bTEFAP with 16S rRNA primers Gray28F (5′-GAGTTTGATCNTGGCTCA-3′) and Gray519R (5′-GTNTTACNGCGGCKGCTG -3′) (Ishak et al., 2011). A sequencing library was generated through one-step PCR with 30 cycles, using a mixture of HotStar and HotStar HiFidelity *Taq* polymerases (Qiagen, Hilden, Germany). Sequencing extended from Gray28F, using a Roche 454 FLX instrument with Titanium reagents and procedures at Research and Testing Laboratory (RTL, Lubbock, TX, USA[1]). Quality control and analysis of

454 reads, including calculation of rarefaction curves and community richness and diversity indexes, was done in QIIME version 1.8.0 (Caporaso et al., 2011). Low-quality ends of the sequences were trimmed with a sliding window size of 50 and an average quality cut-off of 25. Subsequently, all low-quality reads (quality cut-off = 25) and sequences <200 bp were removed, and the remaining reads were denoised using the "denoiser" algorithm as implemented in QIIME (Reeder and Knight, 2010). Denoised high-quality reads were clustered into operational taxonomic units (OTUs) using a multiple OTU picking strategy with cdhit (Li and Godzik, 2006) and uclust (Edgar, 2010), with 97% similarity cut-offs, respectively. For each OTU, the most abundant sequence was chosen as a representative sequence and aligned to the Greengenes core set[2] using PyNast (Caporaso et al., 2010). RDP classifier was used for taxonomy assignment (Wang et al., 2007). An OTU table was generated describing the occurrence of bacterial phylotypes within the samples.

qPCR Analysis of Pocket and Hindgut Wall Tissue

For the quantitative real-time PCR (qPCR) analysis, third-instar larvae were used. A sample was composed of the pooled DNA from hindgut wall, or pockets, of three different larval individuals. Three samples from each tissue (hindgut wall and pockets) were considered, and each one was analyzed per triplicate. Specific primers were designed using Geneious 6.0.5[3] for the five most consistently found bacterial taxa in the pocket (*Achromobacter, Citrobacter, Bosea, Brevundimonas,* and *Pseudomonas*), based on the alignment of the representative set of sequence data for all OTUs available from the 454-pyrosequencing. PCR conditions for each primer pair were optimized using gradient PCRs (Salem et al., 2013). Their specificity was verified *in silico* against the SILVA ribosomal RNA database[4] and *in vitro* by sequencing. Briefly, PCR products from pocket DNA were analyzed on 1% agarose gels (150 V, 30 min). The products were purified from the gel with Invisorb Fragment CleanUp kit (Stratec Molecular, Berlin, Germany) and cloned in pCR 2.1 vector using the Original TA Cloning kit (Invitrogen, Carlsbad, CA, USA). Ninety clones with positive inserts were selected according to the manufacturer's protocol and sequenced on a 3730 XL DNA Analyzer (Applied Biosystems, Foster City, CA, USA) with BD 3.1 chemistry. If the sequence matched the expected OTU, the primer pair was assumed to specifically amplify the target OTU within the gut and pocket. The sequences of the primers are listed in Supplementary Table S2. Quantitative PCRs for individual bacterial taxa were performed on a CFX96 Real Time System (Bio-Rad, Munich, Germany), in final reaction volumes of 10 μL containing 1 μL of template DNA (usually a 1:10 dilution of the original DNA extract), 0.6 μL of each primer (10 pM) and 5 μL of SYBR Green Mix (Rotor-Gene SYBR Green kit, Qiagen, Hilden, Germany). Standard curves were established using 10^{-6}–10^{-2} ng of specific

37

PCR product as templates for the qPCR. A NanoDrop ND-1000 spectrophotometer (Peqlab Biotechnology Limited, Darmstadt, Germany) was used to measure template DNA concentration for the standard curve. Five different replicates of the standard concentrations for each bacterial taxon were used to calculate a correction factor and determine equitation parameters. PCR conditions were as follows: 95°C for 3 min, followed by 40 cycles of denaturation at 95°C for 10 s, annealing for 30 s and elongation at 72°C for 10 s. Then, a melting curve analysis was performed to ensure that amplicons were the same across samples for each primer assay, by increasing the temperature from 65 to 95°C within 5 min. The annealing temperature was specific for each primer pair: for *Achromobacter* and *Citrobacter*, 60°C; for *Bosea*, 63°C; for *Brevundimonas*, 55°C; for *Pseudomonas*, 68°C. Based on the standard curves, the 16S copy number could be calculated for each individual sample from the qPCR threshold values (Ct) by the absolute quantification (Lee et al., 2006, 2008), taking the dilution factor and the absolute volume of DNA extract into account. The quantitative differences in the microbial community abundances of the pocket were tested using SPSS 17.0 (Tukey HSD test, confidence interval of 0.05).

Isolation and Identification of Pocket Bacteria

Four second-instar pockets from different larvae were dissected as mentioned above and incubated together in a 0.8% NaOCl aqueous solution for 3 min on ice for surface sterilization. Then, the tissue was transferred in Ringer+ppi buffer (Cazemier et al., 1997) and sonicated using a Sonorex Super RK 102h sonicator (Bandelin, Germany) for 7 min at RT. After sonication, the tubes were incubated 15 min on ice and gently tapped from time to time. Ten-fold dilutions of the supernatant were plated on LB agar (Carl Roth, Germany) and ATCC agar in order to enrich for *Achromobacter* sp. The ATCC agar contained (per liter): 7.32 g K_2HPO_4, 4.6 g ammonium tartrate, 1.09 g KH_2PO_4, 0.04 g $MgSO_4$ $7H_2O$, 0.04 g $FeSO_4$ $7H_2O$, 0.014 g $CaCl_2$ $2H_2O$, and 35 g agar. Plates were incubated at 30°C for 48 h. Morphologically different colonies were subcultured three times before identification. Colony PCR targeting the small ribosomal subunit gene was performed on a GeneAmp 9700 Thermocycler (Applied BioSystems) using the general bacterial primers 27f and 1492r (Arias-Cordero et al., 2012). The 50 μL reaction mixture contained 1x buffer, 1.5 mM $MgCl_2$, 10 mM of the four deoxynucleotide triphosphates (dNTPs), 2.5 U Taq DNA polymerase (Invitrogen) and 0.5 mM of each primer. The PCR program was as follows: initial denaturation at 94°C for 3 min followed by 32 cycles of denaturation at 94°C for 45 s, annealing at 55°C for 30 s and elongation at 72°C for 1 min, and a final elongation step at 72°C for 10 min. Amplicon size was confirmed in a 1% agarose gel; then the PCR product was purified using the Invisorb Fragment CleanUp kit (STRATEC Molecular GmbH, Berlin, Germany). Sequencing was performed at Macrogen Europe (Amsterdam, The Netherlands), and the taxonomy of resulting sequences was assigned using Basic Local Alignment Search Tool (BLAST) (Tatusova and Madden, 1999).

Metabolic Testing of Bacterial Isolates

Nile Blue agar was prepared as described (Luellen and Schroth, 1994). A representative of each bacterial isolate was plated and incubated for 48 to 72 h at 30°C. The plates were then viewed under UV light to detect putative PHB production based on the fluorescence of the colonies. Nitrate reduction test was purchased from Sigma and conducted following the instructions provided by the manufacturer. A representative of each bacterial isolate was inoculated at high density, and tubes were sealed with liquid paraffin to create oxygen-poor conditions and incubated at 30°C up to 5 days.

Gas Chromatography – Mass Spectrometry

Twenty-five third-instar larvae were dissected as described, and their 50 pockets were analyzed as one single sample. *Achromobacter* sp. isolated from the pocket was cultured for 3 days in PHB inducing broth at 30°C for 72 h. The composition of PHB inducing broth is the same as Nile Blue agar (Luellen and Schroth, 1994) without Nile Blue or agar. The bacterial mass was recovered by centrifugation and washed twice with sterile distilled water prior to drying [45°C for 90 min in a Speedvac (Concentrator 5301, Eppendorf)]. 5 mg (dry weight) of bacterial mass was used for the analysis. Poly[(*R*)-3-hydroxybutyric acid] standard was obtained from Sigma (Germany), and 1 mg was used for the analysis. Derivatization was performed as described (Riis and Mai, 1988), using methanol instead of propanol for the esterification. GC analysis was performed in a ThermoQuest, Finnigan Trace GC-MS 2000 series (Egelsbach, Germany), equipped with a fused-silica capillary Phenomenex ZB-5 column (15 m × 0.25 mm, film thickness 0.25 μm) with a split ratio of 10:1. Helium was used as carrier gas at a flow rate of 1.5 ml/min. The oven temperature was programmed as follows: the initial temperature of 60°C was held for 3 min, then increased to 230°C at 30°C/min and held for 2 min. The inlet temperature was 250°C and the injection volume 1 μL. Mass spectra were measured in electron impact (EI) at 70 eV under full scan mode (m/z 35–575). Acquired data were further processed using the software Xcalibur (Thermo Scientific). 3-hydroxybutyric acid methyl esters were identified by comparison of the mass spectrum and retention time with poly[(*R*)-3-hydroxybutyric acid] standard.

Raman Micro-Spectroscopy

One pocket was used for each Raman measurement. CaF_2 slides suitable for Raman spectroscopy were poly-L–lysine coated by being soaked overnight in 0.1% poly-L–lysine solution (Sigma) at 4°C prior to measurement. The pocket tissue was fixed overnight with 4% paraformaldehyde solution in 0.9% NaCl at 4°C. After fixation, the paraformaldehyde was removed and the tissue was washed three times for 10 min with 0.9% NaCl solution under mild agitation. Then the pocket tissue was embedded in a mounting medium for cryotomy, OCT compound (VWR Chemicals, Radnor, PA, USA) and sliced in 12-μm thick sections using a Microm HM 560 cryomicrotome (Thermo Scientific, Waltham, MA, USA). The tissue slices were put onto the

38

poly-L–lysine coated CaF$_2$ slide, washed carefully with 0.9% NaCl to remove the remains of the mounting medium and viewed under a bright-field microscope to check for the characteristic round-shaped cross-sections of the pocket poles. The Raman spectra were acquired with a confocal Raman microscope alpha 300R (WITec, Ulm, Germany) using a 532 nm Nd:YAG solid laser with a power of 15 mW for excitation. The samples were measured in 0.9% NaCl using a 60× water immersion objective with NA 1.0 (Nikon, Tokyo, Japan). Collection of backscattered photons occurred through a back-illuminated CCD camera (DV401-BV-352, Andor, Belfast, UK). For spectral grating, 600 lines/mm were used for 532 nm. A multimode fiber of 25 μm diameter served as pinhole for confocal imaging. The Raman spectra were recorded by using 1 s integration time. Characteristic spectra and compartments in the pocket poles were detected by analyzing the Raman scans with the N-FINDR unmixing algorithm (Winter, 1999; Hedegaard et al., 2011) using Matlab software (MathWorks). The PHB was detected by identifying specific peaks through comparison with measured reference spectrum of pure PHB compound.

Nucleotide Sequence Accession Numbers

The 16S RNA gene sequences obtained by colony PCR have been deposited at the NCBI GenBank under accession numbers from KY178280 to KY178284 (**Table 1**). Pyrosequencing data from L2 hindgut wall, adult hindgut wall, L2 pocket and L3 hindgut wall have been deposited under accession numbers SRR5059348, SRR5059349, SRR5059340, and SRR5059351, respectively.

RESULTS

Localization and Morphology of the Pockets

During the dissection of larval individuals (**Figure 1A**), two small structures ["pockets," colored either white or black (**Figures 1F,G**)] attached outside the terminal point of the hindgut chamber (**Figures 1B,C,D,E, 2A**) were spotted. The pockets have a diameter of around 500 μm, and showed high autofluorescence when illuminated with a 488 nm laser (**Figure 2B**). They are covered by a fine layer of muscle tissue (Supplementary Figure S1). Their anatomy is composed by poles connected to the hindgut lumen (Supplementary Figure S2). Further anatomical investigation by TEM revealed that each pole
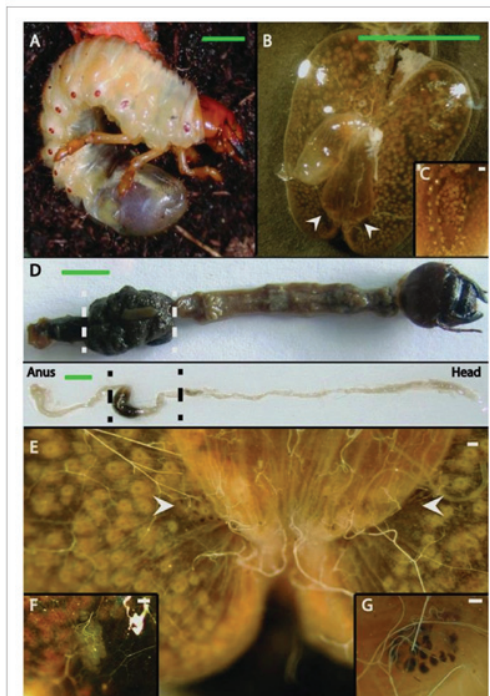

FIGURE 1 | Gut anatomy of larvae and adults of *Melolontha hippocastani*. (A) L3 larval instar living in the soil. **(B)** Hindgut fermentation chamber. White arrowheads point to the position of the pockets. **(C)** Close-up of a hindgut lobe. **(D)** Whole gut preparation of an L3 larval instar (top image) and an adult beetle (bottom image). The hindgut section used for microscopy and pyrosequencing is between the dashed lines. **(E)** The fermentation chamber and the pocket position (pointed with arrows). **(F)** Close-up of the *M. melolontha* pocket and **(G)** close-up of the *M. hippocastani* pocket. Scale bars: green 5 mm., white 100 μm.

was surrounded by a thick acellular tissue layer (possibly mucous-like, **Figure 2C**). Additionally, it was observed that each pole was lined with large numbers of bacterial cells (**Figure 2C**). These cells showed a high number of cytoplasmatic inclusions (**Figure 2D**).

TABLE 1 | Bacterial isolates from *Melolontha hippocastani*'s pockets with their metabolic capabilities.

| Closest taxonomic affiliation	Identity percentage	Nile blue staining	Denitrification	Accession number
Citrobacter murliniae	99	Negative	Nitrate to nitrite	KY178281
Achromobacter marplatensis	99	Positive	Nitrate to nitrogen	KY178280
Ochrobactrum thiophenivorans	100	Negative	Negative	KY178282
Phyllobacterium myrsinacearum	99	Positive	NT	KY178283
Stenotrophomonas maltophilia	99	Positive	NT	KY178284

NT, not tested.

39
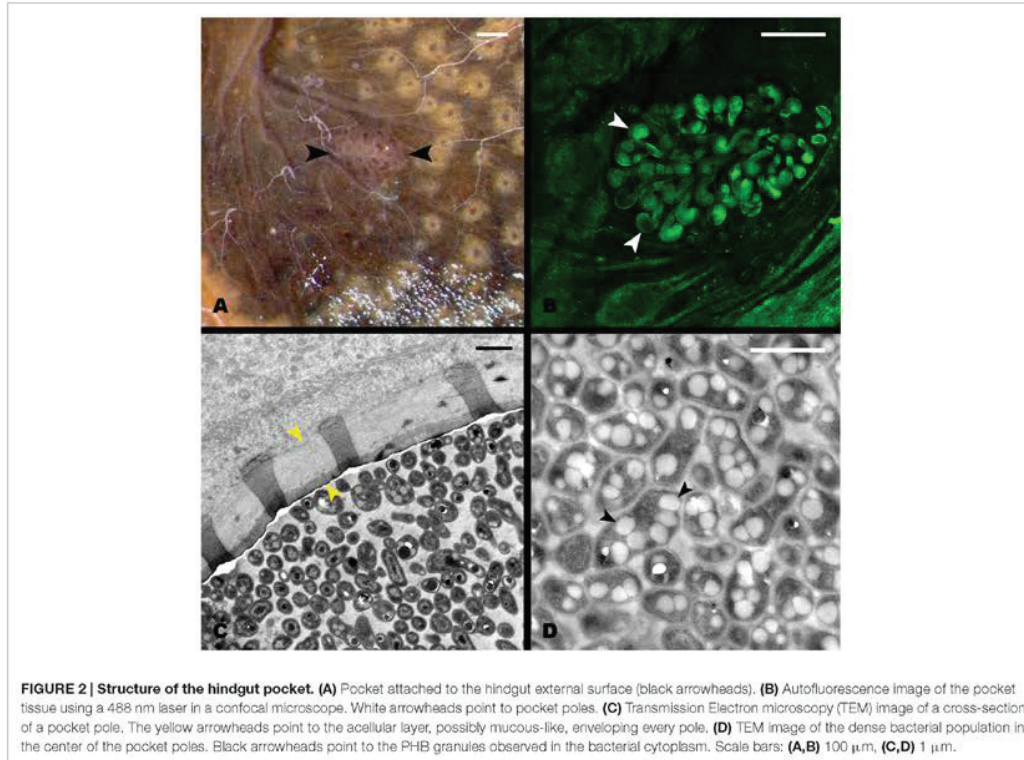
FIGURE 2 | Structure of the hindgut pocket. (A) Pocket attached to the hindgut external surface (black arrowheads). **(B)** Autofluorescence image of the pocket tissue using a 488 nm laser in a confocal microscope. White arrowheads point to pocket poles. **(C)** Transmission Electron microscopy (TEM) image of a cross-section of a pocket pole. The yellow arrowheads point to the acellular layer, possibly mucous-like, enveloping every pole. **(D)** TEM image of the dense bacterial population in the center of the pocket poles. Black arrowheads point to the PHB granules observed in the bacterial cytoplasm. Scale bars: **(A,B)** 100 µm, **(C,D)** 1 µm.
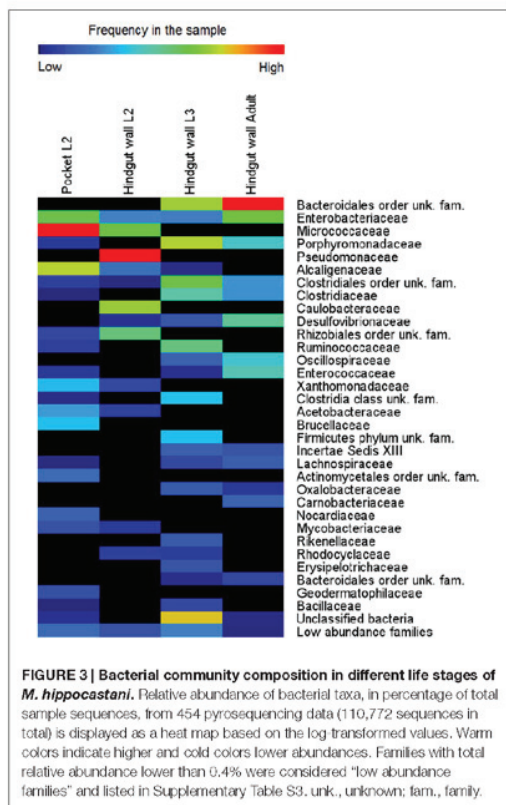
Pyrosequencing of the Bacterial Community from the Hindgut Wall of Adult Insects and Larvae, and Pockets

To establish the dynamics of the hindgut wall community across different host's life stages, the bacterial communities of the hindgut wall of L2 and L3 larvae and adults were compared. DNA from six different insects of each life stage was used, pooled together in a single pyrosequencing run. In the final output, 110,772 high quality reads were obtained (Supplementary Table S1). It was found that, in the L2 hindgut wall, the main bacterial phyla were Pseudomonadaceae, Caulobacteraceae and Micrococcaceae, while in L3 hindgut wall, those were Bacteroidetes phylum and Clostridia, with a large proportion of unknown bacteria. In the adults, an increase of the relative abundance of the Bacteroidales order, Proteobacteria (γ- and δ- classes) and the family Enterococcaceae (Firmicutes) was observed (**Figure 3**). Estimation of alpha-diversity in these samples was done using rarefaction methods, and richness and diversity indexes were also calculated (Supplementary Figure S3 and Table S1).

Amplicon sequencing revealed considerable differences in microbial communities between the L3 and L2 hindgut walls.

In L2, approximately 47% of the sequences obtained belong to the family Pseudomonadaceae and 30% to the family Caulobacteraceae, taxa that were not detected in the L3 hindgut wall; the L3 hindgut wall, in turn, had families at high abundances which were not or only at low abundances detected in L2 (e.g., Porphyromonadaceae, Bacteroidales, and Ruminococcaceae) (**Figure 3**). This may reflect the changes that the bacterial community undergoes throughout the different stages of the insect's life, suggesting that the hindgut wall is a dynamic environment.

A pooled sample of DNA extracted from 12 excised pockets (from 6 L2 larvae) was also sequenced, in order to compare their bacterial communities with the surrounding hindgut wall. It was found that the main bacterial phyla of the pocket tissue were Actinobacteria and Proteobacteria (α- and β- classes). Within the β-Proteobacteria, *Achromobacter* sp., which accounted for 85% of sequences from the family Alcaligenaceae, was the genus with the overall highest relative abundance in the pockets. The classification at genus level of the family Micrococcaceae was not achieved. These two families were present in low abundance in the L2 and L3 hindgut wall, as well as in the hindgut wall of adult beetles (**Figure 3**).

40

FIGURE 3 | Bacterial community composition in different life stages of *M. hippocastani*. Relative abundance of bacterial taxa, in percentage of total sample sequences, from 454 pyrosequencing data (110,772 sequences in total) is displayed as a heat map based on the log-transformed values. Warm colors indicate higher and cold colors lower abundances. Families with total relative abundance lower than 0.4% were considered "low abundance families" and listed in Supplementary Table S3. unk., unknown; fam., family.

Estimation of Absolute Abundances of Main Bacterial Genera in the Pockets and the Hindgut Wall

In order to compare the absolute abundances of key genera inhabiting the pocket and the hindgut wall of L3 larvae, namely *Achromobacter* (family Alcaligenaceae), *Bosea* (family Bradyrhizobiaceae), *Brevundimonas* (family Caulobacteraceae), *Citrobacter* (family Enterobacteriaceae) and *Pseudomonas* (family Pseudomonadaceae), qPCR with genus-specific primers was performed. In the pocket, *Achromobacter* was the most dominant of the genera, with an abundance about 10 times greater than that of *Pseudomonas* (Figure 4). *Citrobacter*, *Brevundimonas*, and *Bosea* showed lower abundances, with that of *Bosea* being three orders of magnitude lower than that of *Achromobacter*. The abundances of all four lower-abundant genera in the pockets differed significantly from that of *Achromobacter* (ANOVA, Tukey HSD test, $p < 0.05$). This is in line with the outcome of the 454-pyrosequencing, in which *Achromobacter* sp. (85% of family Alcaligenaceae sequences) was the most dominant of the identified genera in the pocket

(Figure 3). However, since it was not possible to classify the family Micrococcaceae at the genus level, it must be taken into account that *Achromobacter* sp. may be overcome by a Micrococcaceae-related genus.

In the hindgut wall, the abundances of *Pseudomonas*, *Brevundimonas*, and *Bosea* spp. (*Pseudomonas > Brevundimonas > Bosea*) were in good agreement with their respective family abundances showed by the 454 pyrosequencing approach. The occurrences of *Citrobacter* and *Achromobacter* spp., respectively, the first and second most ubiquitous genera according to the qPCR outcome, matched their respective abundances in the L3 hindgut wall pyrosequencing (families Enterobacteriaceae and Alcaligenaceae, respectively), but were significantly higher than their abundances in L2 hindgut wall pyrosequencing (**Figure 3**). This outcome fits with the abovementioned idea that the relative abundances of the gut bacterial community members are dynamic depending on the larval instar.

PHB Detection in Pocket Isolates and Pocket Tissue by Nile Blue Staining and GC-MS

Considering the relatively close phylogenetic relationship between the major genus in *M. hippocastani* pockets, *Achromobacter* sp., and the PHB-accumulating bacterium that colonizes the *R. pedestris* midguts crypts, *Burkholderia* sp. (Kim et al., 2013), we speculated that PHB accumulation could also take place in the pocket symbionts. To test this hypothesis, pocket symbionts were isolated in selective media. The bacterial species that were retrieved are listed in **Table 1**. PHB accumulation was suggested in *Achromobacter marplatensis*, *Stenotrophomonas maltophilia*, and *Phyllobacterium myrsinacearum* by its positive fluorescence under UV light when cultured in Nile Blue agar (**Table 1**) (Ostle and Holt, 1982).

Gas chromatography coupled with mass spectrometry (GC-MS) of pocket tissue as well as isolated *A. marplatensis* was conducted in order to confirm PHB presence. For the analysis, pockets and bacterial mass were derivatized through *trans*-esterification with methanol in the presence of acid (see Materials and Methods) prior to injection into the gas chromatograph. The resulting chromatograms (**Figure 5**) showed a peak corresponding to 3-hydroxybutyric acid methyl ester, the derivatized 3-hydroxybutyric acid monomeric unit of PHB, with a retention time of 2.21 min (± 0.01 min). Its identification was carried out by comparing the obtained mass spectrum and the retention time with the commercially available reference compound.

Raman Micro-Spectroscopy of the Pocket Tissue

In order to determine the spatial distribution of PHB-accumulating bacteria within the pocket pole, Raman micro-spectroscopy was performed. The Raman spectroscopic scans and spectra obtained are shown in **Figure 6**. Spectral unmixing using the N-FINDR algorithm revealed false-color images that showed different constituents by identifying different Raman spectral signatures. In the pocket poles containing
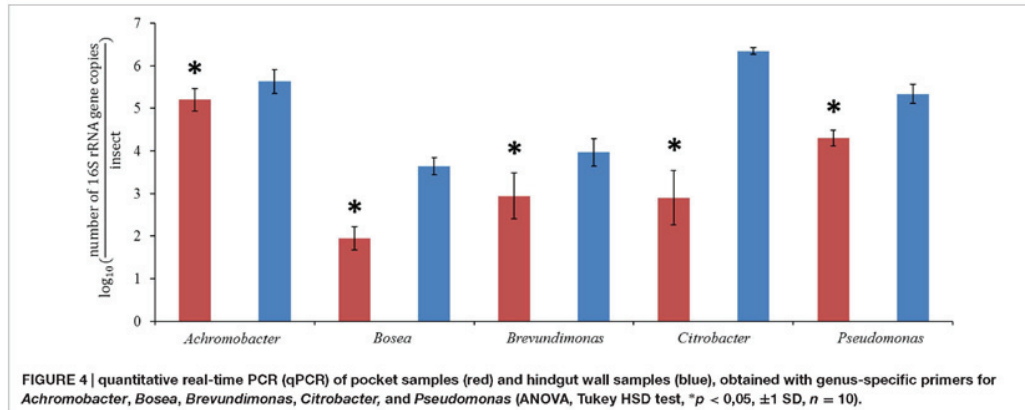
41

FIGURE 4 | quantitative real-time PCR (qPCR) of pocket samples (red) and hindgut wall samples (blue), obtained with genus-specific primers for *Achromobacter, Bosea, Brevundimonas, Citrobacter,* and *Pseudomonas* (ANOVA, Tukey HSD test, $*p < 0,05$, ±1 SD, $n = 10$).
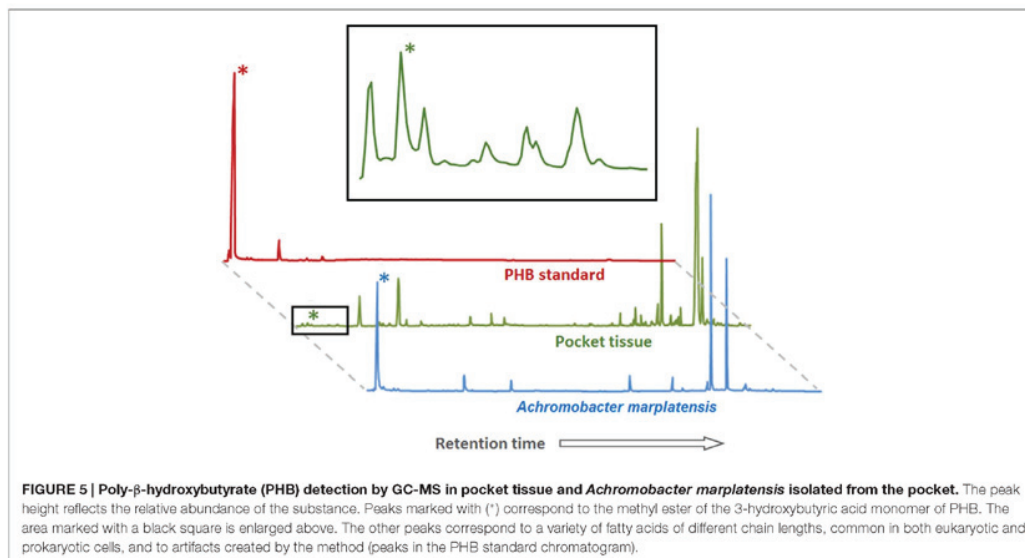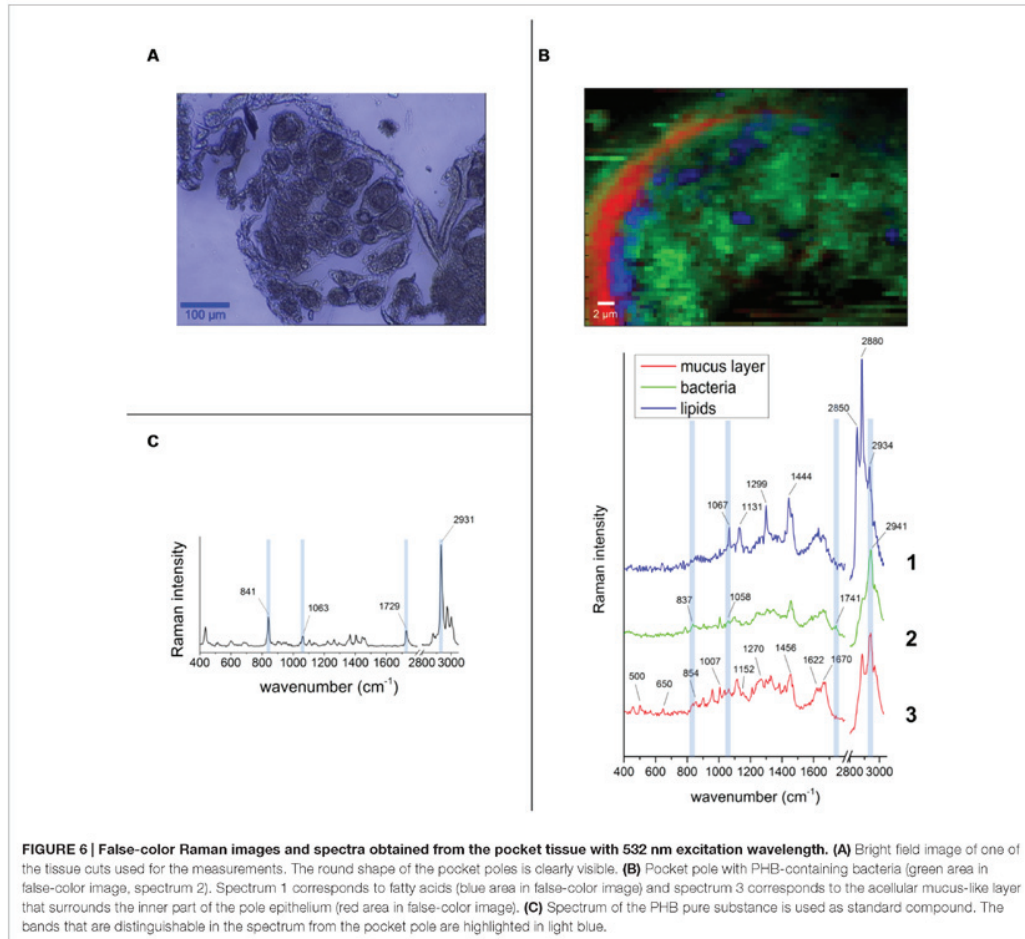

FIGURE 5 | Poly-β-hydroxybutyrate (PHB) detection by GC-MS in pocket tissue and *Achromobacter marplatensis* isolated from the pocket. The peak height reflects the relative abundance of the substance. Peaks marked with (*) correspond to the methyl ester of the 3-hydroxybutyric acid monomer of PHB. The area marked with a black square is enlarged above. The other peaks correspond to a variety of fatty acids of different chain lengths, common in both eukaryotic and prokaryotic cells, and to artifacts created by the method (peaks in the PHB standard chromatogram).

PHB-accumulating bacteria, they were distributed uniformly throughout the inner area of the pole as dots of approximately 1 μm diameter (spectrum 2 of **Figure 6B**, green area in false-color image). Within a typical bacterial Raman spectrum (Ciobotă et al., 2010; Majed and Gu, 2010), the presence of PHB granules was indicated by the bands at 837 and 1058 cm^{-1} (C-C stretching), and especially by the highly significant band at 1741 cm^{-1} (C=O stretching; compare PHB reference spectrum in **Figure 6C** with spectrum 2 in **Figure 6B**). The spectrum showing mainly C-C stretching (1067, 1131 cm^{-1}), CH$_2$ twisting (1299 cm^{-1}), and CH$_2$ bending (1444 cm^{-1}) vibrations (spectrum 1 in **Figure 6B**, blue area in false-color image),

were likely derived from fatty acids, probably of a saturated nature as the bands that provide evidence of unsaturation were missing (1260, 1650, and 3023 cm^{-1}), whereas the bands that support saturation were strong (1299, 1444, CH stretch region at 2800 – 3000 cm^{-1}) (Wu et al., 2011). Finally, the spectrum of the mucus-like layer (**Figure 2C**) surrounding the inner part of the pole (spectrum 3 of **Figure 6B**, red area in false-color image) revealed a complex composition, consisting mainly of proteins with disulphide bridges (S-S stretch, band 500 and 505 cm^{-1}, respectively), high tyrosine (Tyr) content with bands at 650 cm^{-1} (C-C twist Tyr), 854 and 859 cm^{-1} (ring vibration Tyr), 1270 cm^{-1} (protein amide

42

FIGURE 6 | False-color Raman images and spectra obtained from the pocket tissue with 532 nm excitation wavelength. (A) Bright field image of one of the tissue cuts used for the measurements. The round shape of the pocket poles is clearly visible. **(B)** Pocket pole with PHB-containing bacteria (green area in false-color image, spectrum 2). Spectrum 1 corresponds to fatty acids (blue area in false-color image) and spectrum 3 corresponds to the acellular mucus-like layer that surrounds the inner part of the pole epithelium (red area in false-color image). **(C)** Spectrum of the PHB pure substance is used as standard compound. The bands that are distinguishable in the spectrum from the pocket pole are highlighted in light blue.

III), 1456 cm^{-1} (CH$_2$ deformation), 1622 and 1626 cm^{-1}, respectively (C=C stretching Tyr and Trp), 1670 cm^{-1} (protein amide I or C=C stretching) (Tuma, 2005), and lipids (band 1270 cm^{-1} CH bend), and 1456 cm^{-1} (CH$_2$ deformation). For more detailed band assignment information, see Supplementary Table S4.

DISCUSSION

Bacterial Communities of the Hindgut Wall and the Pockets

Four hundred and fifty-four-pyrosequencing revealed that, in L2 larvae, the bacterial community of the hindgut wall was dominated by the families Pseudomonadaceae and Caulobacteraceae. These families, however, were overgrown in L3 by representatives of the family Porphyromonadaceae and the orders Bacteroidales and Clostridiales. Since these taxa are anaerobic, their proliferation in late larval instars may reflect a thickening of the bacterial layer attached to the hindgut wall, allowing the symbionts to reach more anaerobic areas toward the hindgut lumen, or a pronounced decrease in oxygen concentration due to high bacterial density. Similar shifts in bacterial abundances depending on the maturity of the larvae have been previously reported by Zheng et al. (2012) in *Holotrichia parallela* larvae. The hindgut wall of these larvae is populated by a reduced amount of coccoid cells in the L1 stage, although in the L3 stage, the density of bacteria is largely increased, with bacteroid cells dominating (Zheng et al., 2012).

43

In the adults, the relative abundances of Bacteroidetes, Proteobacteria (γ- and δ- classes) and the family Enterococcaceae (Firmicutes) were increased. Nevertheless, the overall composition of the adult hindgut wall community remained fairly constant compared to L3. This is in line with previous observations on *M. hippocastani* (Arias-Cordero et al., 2012). It was noted that the similarity between larval and adult bacterial communities becomes more evident in the later larval instars, suggesting that L3 larvae possess a community that is more closely related to that of the adults than to the L2 larvae. In addition, they noticed that the abundance of Enterobacteriaceae in the midgut increased continuously throughout the L2, L3, and adult stages (L2 < L3 < adult). In line with these findings is the presently observed increase of the genus *Citrobacter* from L2 to L3 (**Figures 3, 4**). Such increase in abundance of *Citrobacter* representatives toward latter larval instars may be related to the increasing amount of ingested food as the larvae grow, as previously isolated *Citrobacter* sp. from the gut of *M. hippocastani* showed the ability to degrade xylan and starch in pure culture (Arias-Cordero et al., 2012). Furthermore, in adults, the high abundance of Enterococcaceae and Enterobacteriaceae representatives might be related to the shift to leaf-based diet, as these families showed resistance to tannins, an ubiquitous plant defense compound (Smith and Mackie, 2004; Singh et al., 2011).

The abundances of the bacterial genera in the L3 hindgut wall showed by qPCR (**Figure 4**) are in good agreement with the pyrosequencing result, being *Citrobacter* sp. dominant over *Achromobacter* sp., just as the Enterobacteriaceae family is more abundant than Alcaligenaceae in **Figure 3**. Contrary, *Achromobacter* sp. dominates in the pocket. This is also in line with the 454-pyrosequencing, where the sequences obtained clustered mainly within Actinobacteria and α- and β-Proteobacteria, taxa that showed very low abundances in the hindgut wall. This result highlights the singularity of the pocket bacterial community and suggest that they function as specialized symbiotic niches, analogously to previously described structures in other insects (Kikuchi et al., 2005; Grünwald et al., 2010).

Significance of the PHB Inclusions

Transmission electron microscopy unveiled a number of white cytoplasmatic inclusions in the pocket bacteria [potential poly-3-hydroxybutyrate (PHB)]. By GC-MS analyses, it was possible to confirm the presence of poly-3-hydroxybutyrate. Raman micro-spectroscopy revealed that PHB-accumulating bacteria are widely distributed throughout the lumen of the pocket pole. PHB is commonly accumulated by Eubacteria and Archaea and serves as a carbon reserve, stored in the form of water insoluble droplets in the cytoplasm (Rehm, 2003). Its presence is probably linked to the white cytoplasmatic inclusions observed in TEM. Likewise, PHB inclusions also are present in the endosymbiont *Burkholderia* sp. colonizing the midgut crypts of the bean bug *R. pedestris*. Each generation of this insect orally acquire the *Burkholderia* bacterium *de novo* from the environment, and the accumulation of PHB by the symbiont is crucial to ensure proper colonization of the crypts and correct development of the insect host (Kim et al., 2013). The colonization success by

the PHB-accumulating symbiont could be related to its enhanced ability to cope with stress, as previous studies linked PHB accumulation to an increase of bacterial colonization efficiency and to tolerance to a variety of stresses such heat, reactive oxygen species, osmotic imbalance and nutritional depletion, among others (Kadouri et al., 2003; Kim et al., 2013). The high lipidic content within the pocket pole revealed by Raman micro-spectroscopy (**Figure 6**), suggests that the pockets are a nutritionally imbalanced habitat with a high C:N ratio that may favor the colonization by bacteria with the ability of accumulate PHB (Rehm, 2003). Also, oxygen limitation might contribute on selecting PHB-accumulating bacterial species over non-accumulating ones (Trainer and Charles, 2006). Symbiont sorting mechanisms in order to discard potentially pathogenic bacteria from the soil have been reported in the bean bug *R. pedestris* (Kim et al., 2013; Ohbayashi et al., 2015). However, in *M. hippocastani*, this putative discriminative process would not be as specific as in *R. pedestris*, since more than one bacterial phylotype are established in the pockets.

The presence of PHB is uncommon in vertically transmitted bacterial symbionts. Its accumulation is displayed mainly by free-living microorganisms, or by symbionts of environmental origin (Kim et al., 2013). This suggests that the PHB-accumulating pocket symbionts (*A. marplatensis* and possibly *S. maltophilia* and *P. myrsinacearum*; see **Table 1**) might be acquired from the environment. These genera, along with *Ochrobactrum thiophenivorans* (which is not likely to accumulate PHB; see **Table 1**), have been previously detected in the rhizosphere (Bertrand et al., 2000; Kämpfer et al., 2008; Ryan et al., 2009). Moreover, the BLAST alignments of the pocket isolates belonging to these taxa matched those of bacteria previously isolated from roots and soil (data not shown). Considering that, an environmental origin for these pocket symbionts is more plausible than a vertical transmission from mother to offspring. This latter possibility, nevertheless, cannot be totally discarded (Engel and Moran, 2013).

Physiological Role of the Pockets

The pockets in *M. hippocastani* have been only once described in literature (Wildbolz, 1954). Nonetheless, symbioses between insect and bacteria is a common and disparate phenomenon in nature (Douglas, 2009; Hansen and Moran, 2014) and analogous structures harboring symbiotic microorganisms have been found in other insects. Bugs belonging to the family Alydidae are associated with ectosymbiotic bacteria of the genus *Burkholderia*. It this case, the bacterium colonizes the crypts located in the distal section of the midgut (Kikuchi et al., 2005). Similarly, stinkbugs of the families Pentatomidae and Cydnidae harbor Gammaproteobacteria related bacteria in crypts located in the same region of the midgut (Prado and Almeida, 2009; Hosokawa et al., 2012). Other structures containing endosymbiotic bacteria and yeasts have been characterized in the proximal midgut of cerambycid beetles (Grünwald et al., 2010). The role of these symbionts within the insect gut and their involvement in host's nutrition, however, remains largely unknown.

In *M. hippocastani*, the pockets might be sites for denitrification processes. *A. marplatensis* isolated from these

44

small structures showed full denitrifying capabilities in a commercial nitrate reduction assay (**Table 1**). Moreover, the abundance of lipids within the pocket pole unveiled by Raman micro-spectroscopy (**Figure 6**) makes possible that these compounds are used by the pocket symbionts as electron donors for respiratory processes using nitrate as an electron acceptor (NO_3^-). Denitrification has already been reported in other rhizophagous white grubs (Majeed and Miambi, 2014). The presence of pockets could be also related to the rhizophagous diet of the larvae, as they were spotted in the rhizophagous larvae of *M. melolontha* as well (**Figure 1F**), but no similar structure was found in *Pachnoda marginata* (Supplementary Figure S4), whose grub-like larvae thrive not on roots but on humic acids. Host's diet and taxonomy have been pointed as key determinants of the composition of the gut symbiotic community by previous studies (Egert et al., 2003, 2005; Colman et al., 2012; Jones et al., 2013). Either way, it is possible that the pocket symbionts produce some kind of beneficial compound for the insect host. This hypothesis, however, remains for future research.

CONCLUSION

Our data revealed a complex and dynamic microbial community attached to the hindgut wall of the forest cockchafer. The composition of this community may be dependent on host's life stage. L3 larvae showed a more close community to the adults than L2 larvae. In addition, the presence of particular bacterial niches attached to the larval hindgut (pockets) is reported. Regarding the surrounding hindgut wall, these niches harbored a differentiated bacterial community in which the families Micrococcaceae and Alcaligenaceae were dominant. These structures could be related to denitrification processes. Furthermore, the presence of poly-β-hydroxybutyrate (PHB) granules among pocket bacteria is demonstrated. Further research is needed to fully understand the function of the pockets, and especially to determine the role(s) of the cytoplasmatic inclusions.

AUTHOR CONTRIBUTIONS

PA-P performed DNA extraction, light microscopy, pyrosequencing data analysis, gas chromatography measurements,

isolation, identification and metabolic testing of symbiotic bacteria and prepared the samples for Raman analysis. Also wrote the manuscript. EA-C spotted the pockets in the gut. Performed light microscopy, DNA extraction, fluorescence *in situ* hybridization, pyrosequencing data analysis and TEM data analysis. Also contributed in writing the manuscript. AN designed and performed qPCR experiments and analyzed the data. Also contributed in writing the manuscript. CE performed the Raman micro-spectroscopy analysis and analyzed the data. Also contributed in writing the manuscript. JR contributed in the design of TEM experiments and in the analysis of the data. MK contributed in the analysis of pyrosequencing data and calculated richness indexes and rarefaction curves. Also contributed in writing the manuscript. MW prepared samples for TEM, performed analysis and contributed in the analysis of the data. Spotted PHB inclusions in TEM images. UN contributed in the analysis of the Raman data. Also contributed in writing the manuscript. WB had the main idea of the project and supervised it. Also contributed in writing the manuscript.

FUNDING

ACKNOWLEDGMENTS

SUPPLEMENTARY MATERIAL

The Supplementary Material for this article can be found online at: http://journal.frontiersin.org/article/10.3389/fmicb.2017.00291/full#supplementary-material

REFERENCES

Arias-Cordero, E., Ping, L., Reichwald, K., Delb, H., Platzer, M., Boland, W., et al. (2012). Comparative evaluation of the gut microbiota associated with the below- and above-ground life stages (larvae and beetles) of the forest cockchafer, *Melolontha hippocastani*. *PLoS ONE* 7:e51557. doi: 10.1371/journal.pone.0051557

Bertrand, H., Plassard, C., Pinochet, X., Touraine, B., Normand, P., Cleyet-Marel, J. C., et al. (2000). Stimulation of the ionic transport system in Brassica napus by a plant growth-promoting rhizobacterium (*Achromobacter* sp.). *Can. J. Microbiol.* 46, 229–236. doi: 10.1139/cjm-46-3-229

Bright, M., and Bulgheresi, S. (2010). A complex journey: transmission of microbial symbionts. *Nat. Rev. Microbiol.* 8, 218–230. doi: 10.1038/nrmicro2262

Caporaso, J. G., Bittinger, K., Bushman, F. D., DeSantis, T. Z., Andersen, G. L., Knight, R., et al. (2010). PyNAST: a flexible tool for aligning sequences to a template alignment. *Bioinformatics* 26, 266–267. doi: 10.1093/bioinformatics/btp636

Caporaso, J. G., Kuczynski, J., Stombaugh, J., Bittinger, K., Bushman, F. D., Costello, E. K., et al. (2011). QIIME allows analysis of high-throughput community sequencing data. *Nat. Methods* 7, 335–336. doi: 10.1038/nmeth.f.303

Cazemier, A. E., Hackstein, J. H. P., Op den Camp, H. J. M., Rosenberg, J., and van der Drift, C. (1997). Bacteria in the intestinal tract of different species of arthropods. *Microb. Ecol.* 33, 189–197. doi: 10.1007/s002448990021

Ciobotă, V., Burkhardt, E. M., Schumacher, W., Rösch, P., Küsel, K., and Popp, J. (2010). The influence of intracellular storage material on bacterial identification

45

by means of Raman spectroscopy. *Anal. Bioanal. Chem.* 397, 2929–2937. doi: 10.1007/s00216-010-3895-1

Colman, D. R., Toolson, E. C., and Takacs-Vesbach, C. D. (2012). Do diet and taxonomy influence insect gut bacterial communities? *Mol. Ecol.* 21, 5124–5137. doi: 10.1111/j.1365-294X.2012.05752.x

Douglas, A. E. (2009). The microbial dimension in insect nutritional ecology. *Funct. Ecol.* 23, 38–47. doi: 10.1111/j.1365-2435.2008.01442.x

Edgar, R. C. (2010). Search and clustering orders of magnitude faster than BLAST. *Bioinformatics* 26, 2460–2461. doi: 10.1093/bioinformatics/btq461

Egert, M., Stingl, U., Bruun, L. D., Pommerenke, B., Brune, A., and Friedrich, M. W. (2005). Structure and topology of microbial communities in the major gut compartments of *Melolontha melolontha* larvae (Coleoptera: Scarabaeidae). *Appl. Environ. Microbiol.* 71, 4556–4566. doi: 10.1128/AEM.71.8.4556-4566.2005

Egert, M., Wagner, B., Lemke, T., Brune, A., and Friedrich, M. W. (2003). Microbial community structure in midgut and hindgut of the humus-feeding larva of *Pachnoda ephippiata* (Coleoptera: Scarabaeidae). *Appl. Environ. Microbiol.* 69, 6659–6668. doi: 10.1128/AEM.69.11.6659-6668.2003

Engel, P., and Moran, N. A. (2013). The gut microbiota of insects – diversity in structure and function. *FEMS Microbiol. Rev.* 37, 699–735. doi: 10.1111/1574-6976.12025

Grünwald, S., Pilhofer, M., and Höll, W. (2010). Microbial associations in gut systems of wood- and bark-inhabiting longhorned beetles [Coleoptera: Cerambycidae]. *Syst. Appl. Microbiol.* 33, 25–34. doi: 10.1016/j.syapm.2009.10.002

Hansen, A. K., and Moran, N. A. (2014). The impact of microbial symbionts on host plant utilization by herbivorous insects. *Mol. Ecol.* 23, 1473–1496. doi: 10.1111/mec.12421

Hedegaard, M., Matthäus, C., Hassing, S., Krafft, C., Diem, M., and Popp, J. (2011). Spectral unmixing and clustering algorithms for assessment of single cells by Raman microscopic imaging. *Theor. Chem. Acc.* 130, 1249–1260. doi: 10.1007/s00214-011-0957-1

Hosokawa, T., Kikuchi, Y., Nikoh, N., and Fukatsu, T. (2012). Polyphyly of gut symbionts in stinkbugs of the family cydnidae. *Appl. Environ. Microbiol.* 78, 4758–4761. doi: 10.1128/AEM.00867-12

Huang, S.-W., Zhang, H.-Y., Marshall, S., and Jackson, T. A. (2010). The scarab gut: a potential bioreactor for bio-fuel production. *Insect Sci.* 17, 175–183. doi: 10.1111/j.1744-7917.2010.01320.x

Ishak, H. D., Plowes, R., Sen, R., Kellner, K., Meyer, E., Estrada, D. A., et al. (2011). Bacterial diversity in solenopsis invicta and *Solenopsis geminata* ant colonies characterized by 16S amplicon 454 pyrosequencing. *Microb. Ecol.* 61, 821–831. doi: 10.1007/s00248-010-9793-4

Jones, R. T., Sanchez, L. G., and Fierer, N. (2013). A cross-taxon analysis of insect-associated bacterial diversity. *PLoS ONE* 8:e61218. doi: 10.1371/journal.pone.0061218

Kadouri, D., Jurkevitch, E., and Okon, Y. (2003). Involvement of the reserve material poly-β-hydroxybutyrate in *Azospirillum brasilense* stress endurance and root colonization. *Appl. Environ. Microbiol.* 69, 3244–3250. doi: 10.1128/AEM.69.6.3244-3250.2003

Kämpfer, P., Sessitsch, A., Schloter, M., Huber, B., Busse, H. J., Scholz, H. C., et al. (2008). *Ochrobactrum rhizosphaerae* sp. nov. and *Ochrobactrum thiophenivorans* sp. nov., isolated from the environment. *Int. J. Syst. Evol. Microbiol.* 58, 1426–1431. doi: 10.1099/ijs.0.65407-0

Kikuchi, Y., Meng, X., and Fukatsu, T. (2005). Gut symbiotic bacteria of the genus *Burkholderia* in the broad-headed bugs *Riptortus clavatus* and *Leptocorisa chinensis* (Heteroptera: Alydidae). *Appl. Environ. Microbiol.* 71, 4035–4043. doi: 10.1128/AEM.71.7.4035-4043.2005

Kim, J. K., Won, Y. J., Nikoh, N., Nakayama, H., Han, S. H., Kikuchi, Y., et al. (2013). Polyester synthesis genes associated with stress resistance are involved in an insect-bacterium symbiosis. *Proc. Natl. Acad. Sci. U.S.A.* 110, E2381–E2389. doi: 10.1073/pnas.1303228110

Lee, C., Kim, J., Shin, S. G., and Hwang, S. (2006). Absolute and relative QPCR quantification of plasmid copy number in *Escherichia coli.* *J. Biotechnol.* 123, 273–280. doi: 10.1016/j.jbiotec.2005.11.014

Lee, C., Lee, S., Shin, S. G., and Hwang, S. (2008). Real-time PCR determination of rRNA gene copy number: absolute and relative quantification assays with

Escherichia coli. *Appl. Microbiol. Biotechnol.* 78, 371–376. doi: 10.1007/s00253-007-1300-6

Li, W., and Godzik, A. (2006). Cd-hit: a fast program for clustering and comparing large sets of protein or nucleotide sequences. *Bioinformatics* 22, 1658–1659. doi: 10.1093/bioinformatics/btl158

Luellen, P., and Schroth, M. N. (1994). Detection of *Pseudomonas* colonies that accumulate poly-β-hydroxybutyrate on nile blue medium. *Plant Dis.* 78, 683–685. doi: 10.1094/PD-78-0683

Majed, N., and Gu, A. Z. (2010). Application of Raman microscopy for simultaneous and quantitative evaluation of multiple intracellular polymers dynamics functionally relevant to enhanced biological phosphorus removal processes. *Environ. Sci. Technol.* 44, 8601–8608. doi: 10.1021/es1016526

Majeed, M., and Miambi, E. (2014). Contribution of white grubs (Scarabaeidae: Coleoptera) to N 2 O emissions from tropical soils. *Soil Biol. Biochem.* 75, 37–44. doi: 10.1016/j.soilbio.2014.03.025

Ohbayashi, T., Takeshita, K., Kitagawa, W., Nikoh, N., Koga, R., Meng, X. Y., et al. (2015). Insect's intestinal organ for symbiont sorting. *Proc. Natl. Acad. Sci. U.S.A.* 112, E5179–E5188. doi: 10.1073/pnas.1511454112

Ostle, A. G., and Holt, J. G. (1982). Nile blue as a fluorescent stain for poly-β-hydroxybutyrate. *Appl. Environ. Microbiol.* 44, 238–241.

Potrikus, C. J., and Breznak, J. A. (1981). Gut bacteria recycle uric acid nitrogen in termites: a strategy for nutrient conservation. *Proc. Natl. Acad. Sci. U.S.A.* 78, 4601–4605. doi: 10.1073/pnas.78.7.4601

Prado, S. S., and Almeida, R. P. P. (2009). Phylogenetic placement of pentatomid stink bug gut symbionts. *Curr. Microbiol.* 58, 64–69. doi: 10.1007/s00284-008-9267-9

Reeder, J., and Knight, R. (2010). Rapid denoising of pyrosequencing amplicon data: exploiting the rank-abundance distribution. *Nat. Methods* 7, 668–669. doi: 10.1038/nmeth0910-668b

Rehm, B. H. A. (2003). Polyester synthases: natural catalysts for plastics. *Biochem. J.* 376(Pt 1), 15–33. doi: 10.1042/bj20031254

Riis, V., and Mai, W. (1988). Gas chromatographic determination of poly-β-hydroxybutyric acid in microbial biomass after hydrochloric acid propanolysis. *J. Chromatogr.* 445, 285–289. doi: 10.1016/S0021-9673(01)84535-0

Ryan, R. P., Monchy, S., Cardinale, M., Taghavi, S., Crossman, L., Avison, M. B., et al. (2009). The versatility and adaptation of bacteria from the genus *Stenotrophomonas. Nat. Rev. Microbiol.* 7, 514–525. doi: 10.1038/nrmicro2163

Salem, H., Kreutzer, E., Sudakaran, S., and Kaltenpoth, M. (2013). Actinobacteria as essential symbionts in firebugs and cotton stainers (Hemiptera, Pyrrhocoridae). *Environ. Microbiol.* 15, 1956–1968. doi: 10.1111/1462-2920.12001

Singh, B., Chaudary, L. C., Agarwal, N., and Kamra, D. N. (2011). Phenotypic and phylogentic characterisation of tannin degrading/tolerating bacterial isolates from the rumen of goats fed on pakar (*Ficus infectoria*) leaves. *J. Appl. Anim. Res.* 39, 120–124. doi: 10.1080/09712119.2011.558682

Smith, A. H., and Mackie, R. I. (2004). Effect of condensed tannins on bacterial diversity and metabolic activity in the rat gastrointestinal tract. *Appl. Environ. Microbiol.* 70, 1104–1115. doi: 10.1128/AEM.70.2.1104-1115.2004

Tatusova, T. A., and Madden, T. L. (1999). BLAST 2 SEQUENCES, a new tool for comparing protein and nucleotide sequences. *FEMS Microbiol. Lett.* 174, 247–250. doi: 10.1111/j.1574-6968.1999.tb13575.x

Trainer, M. A., and Charles, T. C. (2006). The role of PHB metabolism in the symbiosis of rhizobia with legumes. *Appl. Microbiol. Biotechnol.* 71, 377–386. doi: 10.1007/s00253-006-0354-1

Tuma, R. (2005). Raman spectroscopy of proteins: from peptides to large assemblies. *J. Raman Spectrosc.* 36, 307–319. doi: 10.1002/jrs.1323

Wang, Q., Garrity, G. M., Tiedje, J. M., and Cole, J. R. (2007). Naïve Bayesian classifier for rapid assignment of rRNA sequences into the new bacterial taxonomy. *Appl. Environ. Microbiol.* 73, 5261–5267. doi: 10.1128/AEM.00062-07

Watanabe, H., and Tokuda, G. (2010). Cellulolytic systems in insects. *Annu. Rev. Entomol.* 55, 609–632. doi: 10.1146/annurev-ento-112408-085319

Wells, J., and Varel, V. (2011). "Symbiosis of plants, animals and microbes," in *Animal Welfare in Animal Agriculture*, eds W. Pond, F. Bazer, and B. Rollin (Boca Raton, FL: CRC Press), 185–204.

Wildbolz, T. (1954). Beitrag zur anatomie, histologie und physiologie des darmkanals der larve von melo-lontha *Melolontha* L. *Mitt. schweiz. entomol. Ges.* 27, 193–240.

46

Winter, M. E. (1999). "N-FINDR: an algorithm for fast autonomous spectral end-member determination in hyperspectral data," in *Proceedings of the SPIE's International Symposium on Optical Science, Engineering, and Instrumentation*, Vol. 3753, Bellingham, WA, 266–275. doi: 10.1117/12.366289

Wu, H., Volponi, J. V., Oliver, A. E., Parikh, A. N., Simmons, B. A., and Singh, S. (2011). In vivo lipidomics using single-cell Raman spectroscopy. *Proc. Natl. Acad. Sci. U.S.A.* 108, 3809–3814. doi: 10.1073/pnas.1009043108

Zheng, W., Zhao, Y., and Zhang, H. (2012). Morphology and ultrastructure of the hindgut fermentation chamber of a melolonthine beetle *Holotrichia parallela* (Coleoptera: Scarabaeidae) during larval development. *Micron* 43, 638–642. doi: 10.1016/j.micron.2011.11.009

Conflict of Interest Statement: The authors declare that the research was conducted in the absence of any commercial or financial relationships that could be construed as a potential conflict of interest.

6. Unpublished results Part I

Plant secondary metabolites serve as defense tools for the plants and could affect performance of the pest. Effects of plant toxins on growth parameters of *S. littoralis* larvae were studied. The Plant toxins were added to artificial diet as an admixture. The experimental group was reared on a toxic diet, and body weights and body lengths were determined over the time. The effects of amygdalin, coumarin, methoxypsoralen (8-MOP), crotaline were studied. A plant cyanogenic glycoside, amygdalin was added in a typical environmental concentration of 0.87 µmol/g of diet. Amygdalin had significant effect on the *S. littoralis* larvae (fig. 1 a, b). The intoxicated larvae were significantly lighter compared to the control group. The body lengths were also significantly smaller as compared to the control group (fig. 1 b). No dead larvae were found in the experimental group.
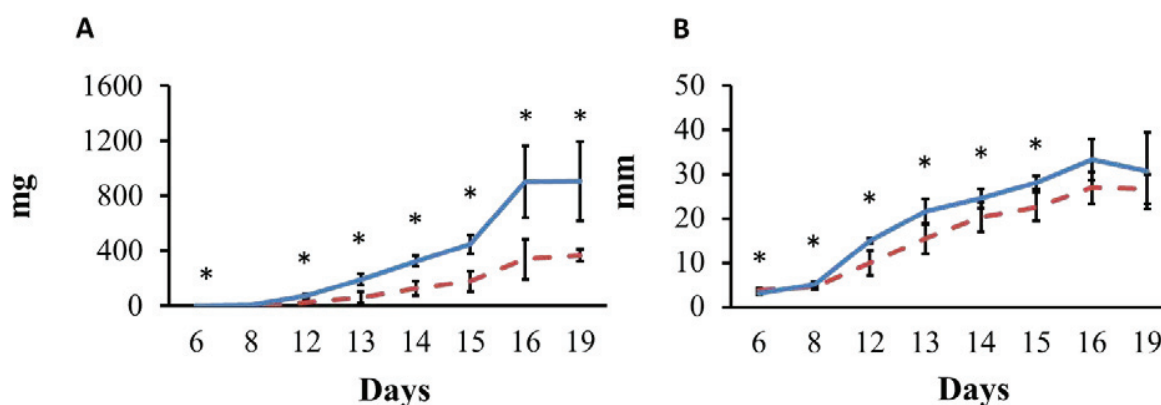

Figure 1. Effect of the plant secondary metabolite amygdalin 0.87 µmol/g on the body weight (A) and length (B) of *S. littoralis* larvae over time (—————), compared to the control (—————), one-way Anova, Dunnett's post test, *p < 0.05; ±1 SD, n = 20.

The effect of the plant secondary metabolite coumarin on *S. littoralis* larvae was studied. The change in body length and body weight was determined over the time. Coumarin was added to the artificial diet in a nature relevant concentration of 6.84 µmol/g of diet. Significant decrease in body weight was observed after 14 days (fig. 2 a), decrease of length was observed after 8 days of treatment (fig. 2 b). No dead larvae were detected after feeding on coumarin.
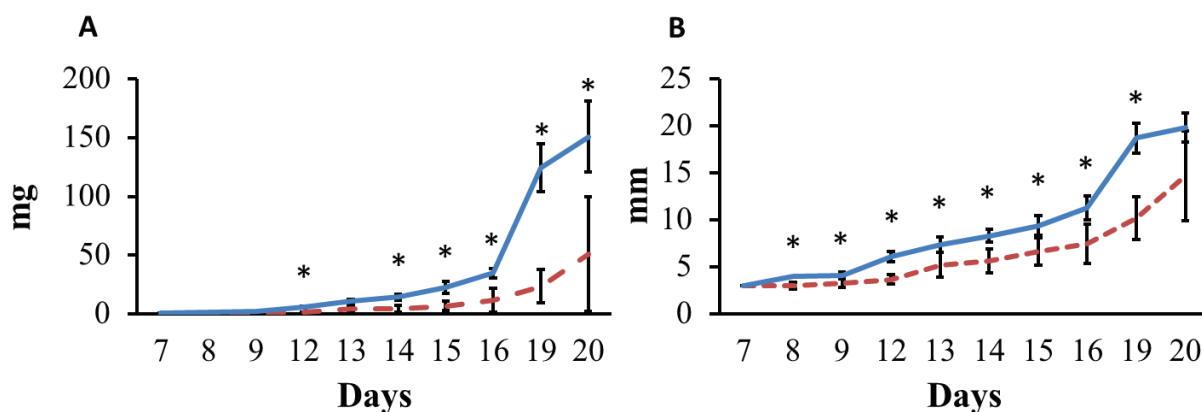
Figure 2. Effect of the plant secondary metabolite coumarin 6.84 µmol/g on the body weight (A) and length (B) of *S. littoralis* larvae over time (— –), compared to the control (—), one-way Anova, Dunnett's post test, *p < 0.05; ±1 SD, n = 20.
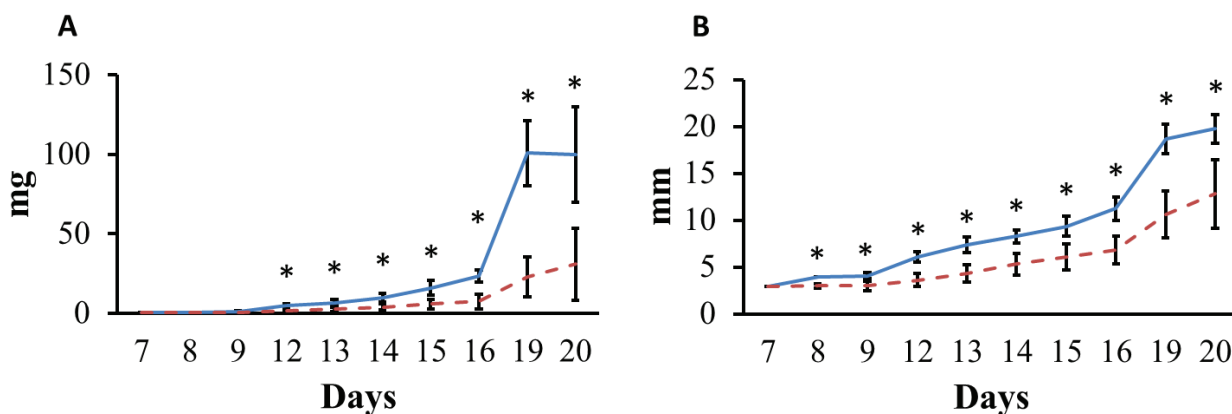
Figure 3. Effect of the plant secondary metabolite 8-MOP 0.46 µmol/g on the body weight (A) and length (B) of S. littoralis larvae over time (— –), compared to the control (—), one-way Anova, Dunnett's post test, *p < 0.05; ±1 SD, n = 20.

8-MOP was added to artificial diet to final concentration 0.46 µmol/g of diet. Larvae treated with 8-MOP had a significant decrease of body weight on 16 days of experiment (fig. 3 a). After 12 days of 8-MOP treatment significant difference in body length was observed (fig. 3 b). No dead larvae were detected in 8-MOP treated group. The pyrrolizidine alkaloid, crotaline significantly slow down growth of the larvae. Larvae treated with 6.14 µmol/g of diet of crotaline were significantly shorter after 12 days of treatment (fig. 4 b) compeer to the control group. Significant

decrease of body weight was detected after 14 days of feeding (fig. 4 a.). Now dead larvae were detected in the crotaline treated group.

Figure 4. Effect of the plant secondary metabolite crotaline 6.14 µmol/g on the body weight (A) and length (B) of *S. littoralis* larvae over time (— —), compared to the control (—),, one-way Anova, Dunnett's post test, *$p < 0.05$; ±1 SD, n = 20
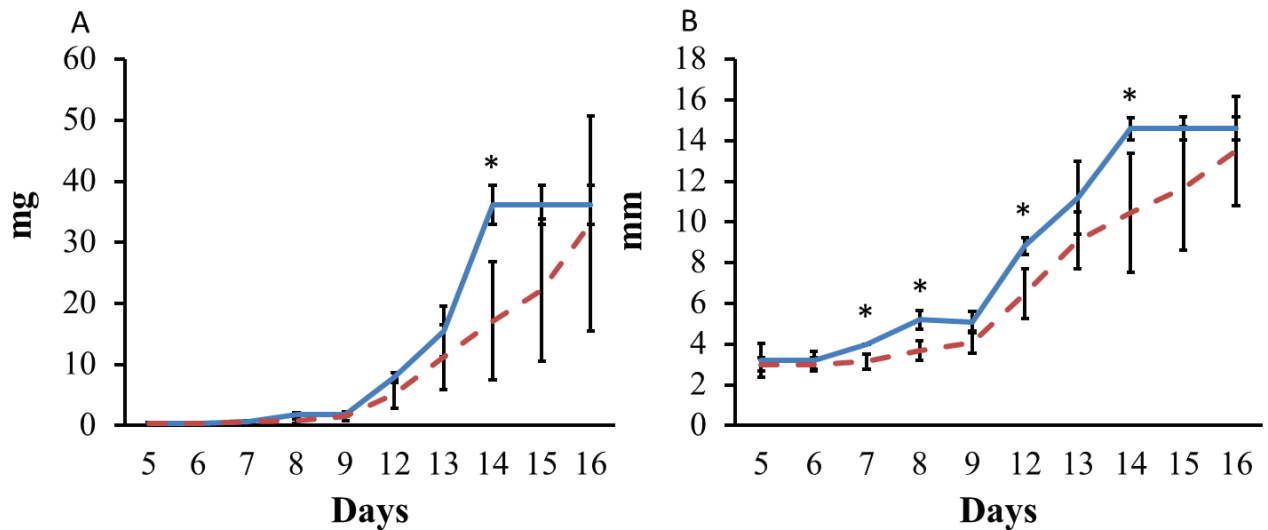
A toxic plant secondary metabolite could induce changes in the gut microbiome of the larvae. Effects of coumarin, amygdalin, 8-MOP and 3-NPA on the composition of the gut microbiome was studied. The larvae were fed on artificial diet with a mixture of toxins. The following concentrations were tested: coumarin 6.84 µmol/g, amygdalin 0.87 µmol/g, 8-MOP 0.46 µmol/g and 3-NPA 4.2µmol/g of diet. DNA was sampled from 4th and 6th instar larvae. Composition of gut microbiome was documented with 454 pyrosequencing. In the control group, the composition of gut microbial community changed and depended on larval instar. In 4th instar larvae in the gut microbial community the most abundant bacteria were Enterobacteriaceae and Enterococaceae, other classes of bacteria were presented in a low abundance group. Most abundant were Enterobacteriaceae 77% and Enterococaceae 17% (fig. 5). Also Erysipelotrichae could be found in 4th instar control larvae. Structure of gut microbiome is changed in 6th instar larvae. Most abundant class of bacteria is Enterococaceae 49% and Enterobacteriaceae 36%. Among others bacteria in untreated gut microbiome presented bacteria of Clostridia class. The abundance of Clostridia varies from 0.3% to 20% and the bacteria constantly present in untreated 6th instar *S. littoralis* gut. 3-NPA treatment had an effect on the composition of the gut microbiome. In 4th instar larvae after 3-NPA feeding, 90% of microbiome was presented by

50

Enterococaceae. In 6th instar larvae, Enterococaceae species dominated and represented 90% of the gut microbiome. No Clostridia species could be found in the 3-NPA treated larvae. Coumarin treatment had similar effects on the gut microbiome. In 4th instar larvae, Enterococcaceae species were the most abundant in the gut (72%). Enterobacteriaceae were the second most abundant species (16%).
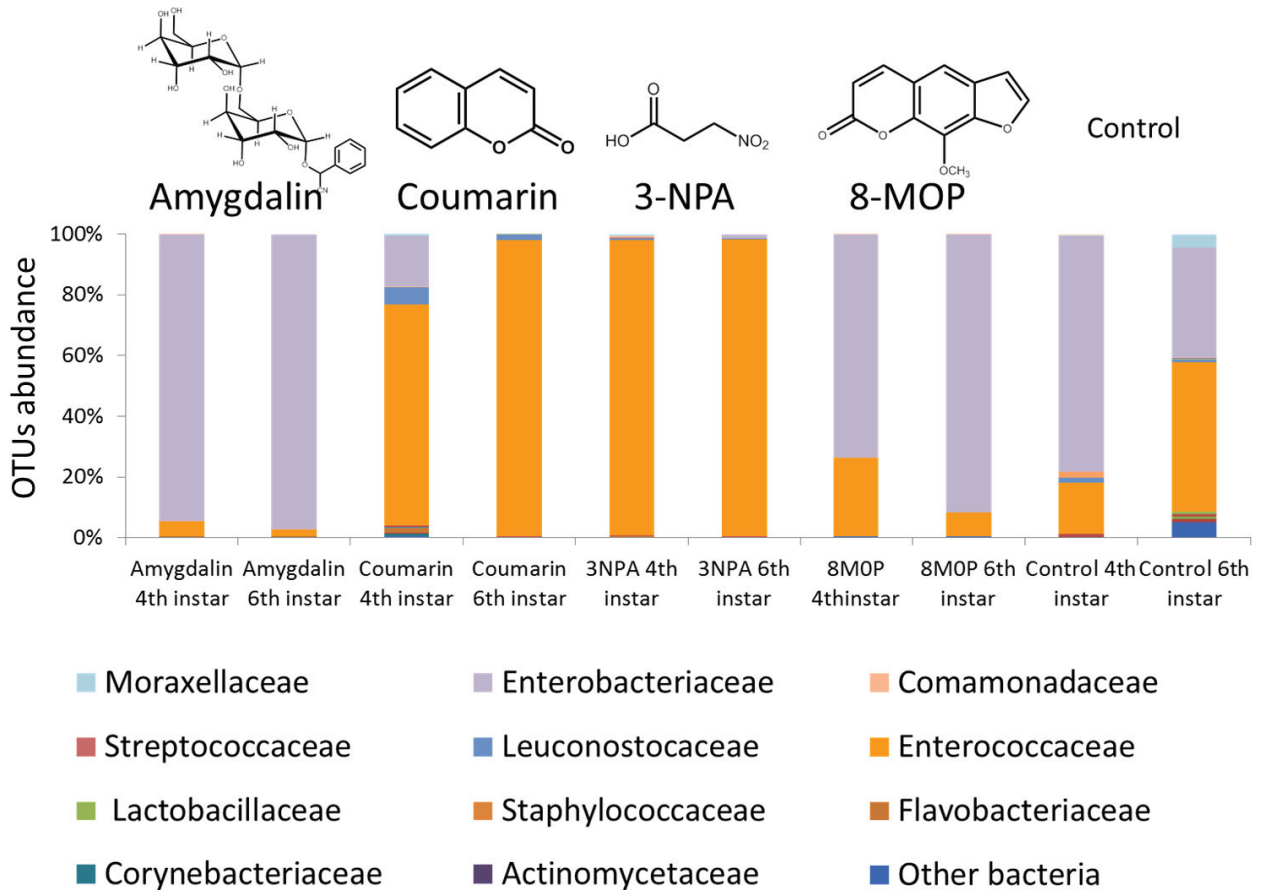
Figure 5. Relative abundance of OTUs in the samples. Larvae were fed on artificial diet with an admixture of toxins: coumarin 6.84 µmol/g, amygdalin 0.87 µmol/g, 8-MOP 0.46 µmol/g, 3-NPA 4.2µmol/g of diet. DNA was sampled from 4th and 6th instar larvae.

In 6th instar larvae Enterococcaceae achieved an 97% abundance in the gut microbiome. No Clostridia could be found after the coumarin treatment. In comparison to the coumarin and 3-NPA, amygdalin treatment inhibited the Enterococcaceae species. In 4th instar larvae, the abundance of Enterococcaceae decreased to 2% after amygdalin treatment. Enterobacteriaceae were highly resistant to the amygdalin treatment. The Abundance of Enterobacteriaceae in 4th instar larvae was 94%. In 6th instar larvae, the dominant genus of bacteria was

Enterobacteriaceae its abundance increased to 97% compared to the control. Enterococcaceae was a minor group in 6th instar larvae after the amygdalin treatment. No Clostridia or Erysipelotrichae could be detected in the amygdalin treated larvae. Methoxypsoralen also inhibited Enterococcaceae species. In 4th instar larvae, the Enterobacteriaceae abundance was 67%. In 4th instar larvae, the abundance of Enterococcaceae was 25.8% and decreased to 7.7% in 6th instar larvae. In 6th instar larvae the Enterobacteriaceae abundance reached to 91%. No Clostridia or Erysipelotrichae could be detected in the Methoxypsoralen treated larvae. Plant toxins inhibited Erysipelotrichae bacteria. Enterococcaceae species were presented in all treated samples. *Enterococcus mundtii* was highly resistant to plant toxins and probably transmitted throught the generation. The absolute abundance of *Enterococcus mundtii* in the gut of *S. littoralis* was measured. The titer of *Enterococcus mundtii* in the gut was measured with qPCR. Specific primers for *Enterococcus mundtii* were designed based on 454 amplicon library. The Gut microbial community was sampled from control larvae and from the ones treated with toxin. The toxins were added to artificial diet as an admixture.
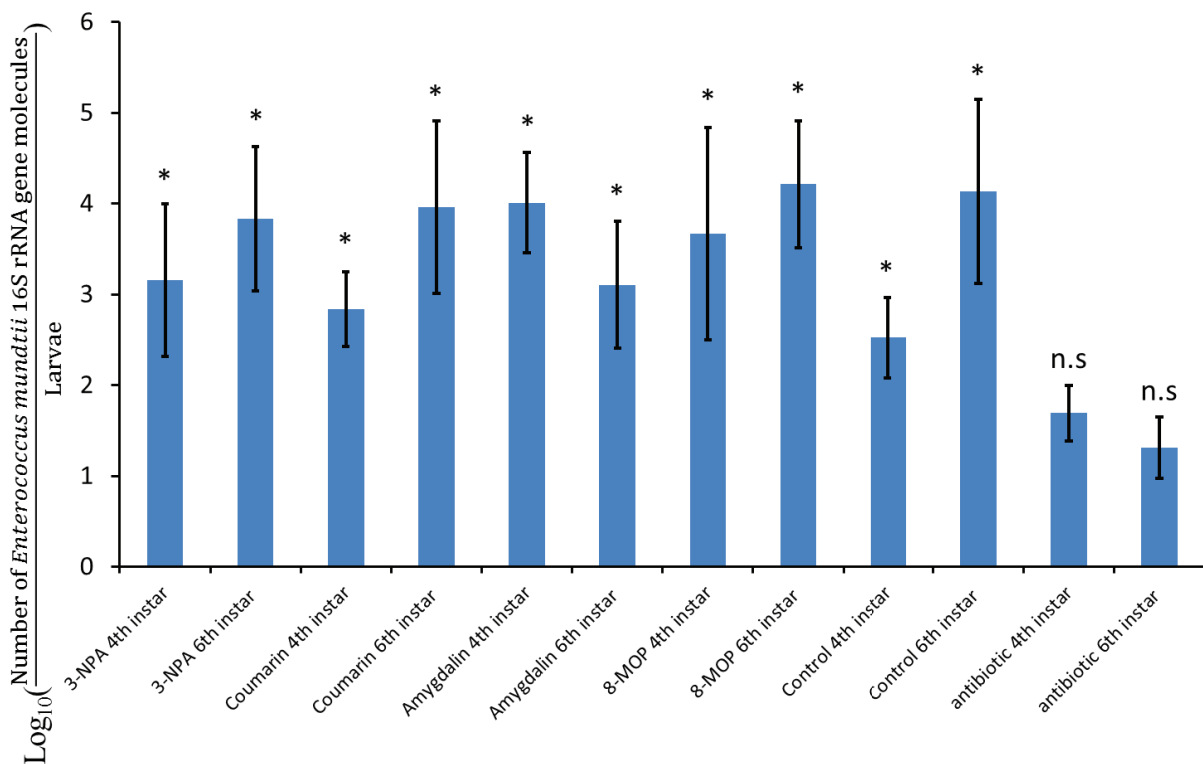

Figure 6. Number of *Enterococcus mundtii* 16S rRNA gene copies per larvae. DNA was sampled from the gut of 4th and 6th instar larvae after treatment of coumarin 6.84 µmol/g, amygdalin 0.87 µmol/g, 8-MOP 0.46 µmol/g, 3-NPA 4.2µmol/g of diet, one-way Anova, Dunnett's post test, , *p < 0,05; ± 1 SD, n.s - not significant, n =10.

3-NPA was added in a concentration of 4.2 µmol/g of diet, amygdalin was added in a concentration of 0.87 µmol/g of diet, coumarin was added in a concentration of 6.84 µmol/g of diet, 8-MOP was added to artificial diet in a nature relevant concentration of 0.46 µmol/g. Gut microbial communities were sampled from 4th and 6th instar larvae. Effects of antibiotics on the titer of *Enterococcus mundtii* in the gut also was studied (fig. 6). To develop a gnotobiotic model, the effect of antibiotic on the titre of bacterial cells in the gut was studied. The cffect of ampicillin and tetracycline mixture were tested. Mixture of antibiotics ampicillin and tetracycline was added to artificial diet to final concentrations of 5,75 µg/ml and 38 µg/ml accordingly. After treating with antibiotics, the gut microbial community was sampled from 4th and 6th instar larvae (fig. 6). Plant toxins' treatment did not have significant effect on the titer of *Enterococcus mundtii* in the gut. Only the mixture of ampicillin and tetracycline significantly inhibited *Enterococcus mundtii* (Dunnett's post test, $p < 0,05$. fig. 6). Antibiotic treatment significantly suppressed the gut microbiome. Consequently, the effect of antibiotic mixture on growth parameters of the larvae were studied. Effects of ampicillin, tetracycline mixture and ampicillin, tetracycline, 3-NPA mixture on the growth of *S. littoralis* larvae was measured (fig. 7). Feeding on the ampicillin and tetracycline mixture significantly decreased the body weight and length (Dunnett's post test, $p < 0,05$. fig. 7).

Figure 7 Effect of Antibiotic ampicillin 5,75 µg/ml and tetracycline 38 µg/ml mixture ——— , 3-NPA 4.2µmol/g of diet and mixture of ampicillin 5,75 µg/ml, tetracycline 38 µg/ml ——— , 3-NPA 4.2µmol/g of diet ——— and control group ——— , on fitness parameters of larvae, one-way Anova, Dunnett's post test, *$p < 0,05$; ± 1 SD, n = 20.

There were no dead larvae in the antibiotic treated group. Feeding on ampicillin, tetracycline and 3-NPA mixture significantly decreased body we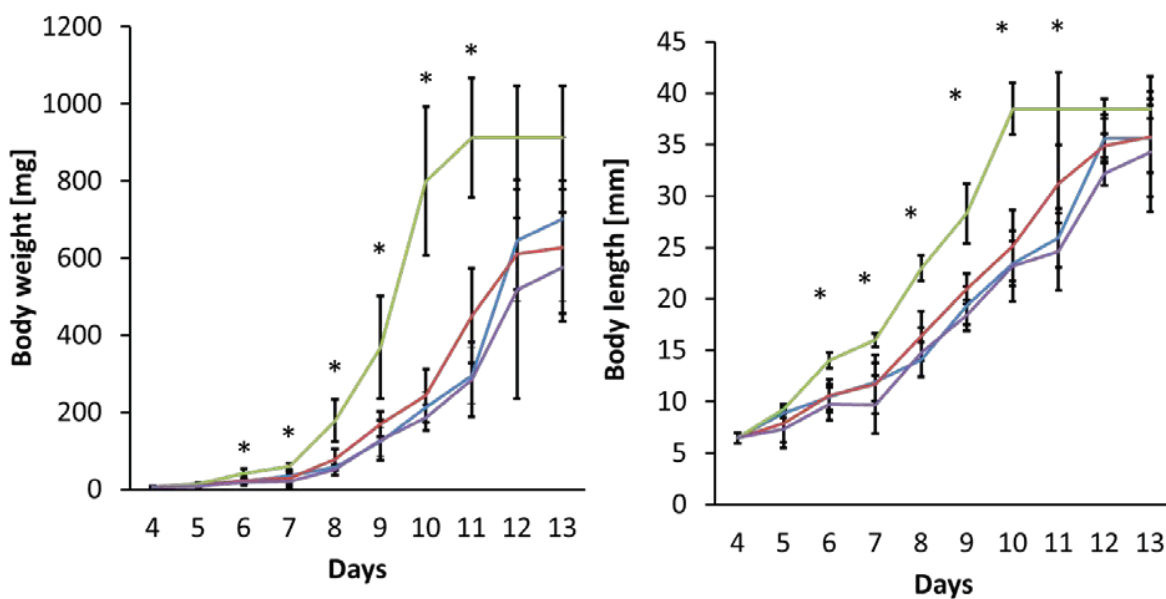ights and lengths (Dunnett's post test, $p < 0.05$. fig. 7). There were no dead larvae in the group treated with 3-NPA antibiotic mixture. There were also no statistically significant differences in body lengths and body weights of the larvae treated with the antibiotic and 3-NPA and the antibiotic mixture (fig. 7). The antibiotics' mixture had similar inhibition effects on the growth parameters as 3-NPA. There was no statistically significant difference between antibiotic treated group and 3-NPA treated group (fig. 7). The mixture of 3-NPA and antibiotics had similar effects on growth parameters as 3-NPA. Also antibiotic treatment decreased body weights and body lengths and significantly suppressed gut microbiome but did not increase in mortality. Treatments with antibiotics and 3-NPA mixture decrease body weights and lengths, but did not increase the mortality. These data indicate that the gut microbial community das not involved in 3-NPA detoxification. To clarify this conclusion, we evaluated effect of antibiotics on 3-NPA-glycine and 3-NPA-Serine amides production. The Control group of larvae was fed on 3-NPA containing artificial diet. The Experimental group was fed on 3-NPA and antibiotic mixture. The frass of 6th instar larvae was collected and the concentrations of 3-NPA, 3-NPA-glycine and 3-NPA-Serine were measured. There was no statistically significant difference of 3-NPA concentration in the control group and in the antibiotic- treated group (fig. 8). The Antibiotic did not have any effect on 3-NPA-glycine amides production. There was no statistically significant difference in 3-NPA-glycine concentration in the control group and in the antibiotic treated group (fig. 8). The concentration of 3-NPA-Serine was significantly lower in the antibiotic treated group as compared to the control group (Dunnett's post test, $p < 0.05$. fig. 8). In the next step, we studied the biochemical capacity of conjugation reaction in *S. littoralis*. Carboxylic acid fatty acid with chain length C4-C14 carbon atoms was tested. The toxic effect of carboxylic acid on *S. littoralis* larvae was estimated. Aliphatic fatty acid in a concentration of 34 µmol of fatty acid per g of diet was admixed to the diet. Also in this experiment 3 nitropropionic acid was tested. In case of the control diet, no dead larvae were detected. From our previous publication, we know that injection of 33.6 µmol of 3NPA per g of body weight is fatal to the larvae. In contrast, feeding on 34 µmol of 3NPA per g of diet is not toxic for the larvae. Pentanoic acid and isopentanoic acids were almost not toxic. There were no statistically significant difference in toxicity of this two isomers (one-way Anova, Dunnett's post test, $p < 0.05$. fig. 9). Hexanoic and Heptanoic acids were more toxic to the larvae. But toxicity significantly increased in 8, 9 and 11 carbon chain fatty acids. A toxicity of medium chain length fatty acids for *S. littoralis* larvae was described for the first time. Mechanism of the toxicity is unclear. Hydrophobic property increases with the increasing of the chain length, it makes medium chain length fatty acids more soluble in lipids, compared to short chain fatty acids. Most likely, because of high alkaline pH in the *S. littoralis* gut, the fatty acids are not soluble in the cell membrane. So, a possible mechanism of medium chain length fatty acids toxicity has not been yet proposed.

Long chain fatty acids are significantly less toxic than middle chain fatty acids. Decanoic acid represented outstanding exception in this range (fig. 9). Furthermore, the frass of the intoxicated larvae was studied with LC-MS. Previously, in the frass of 3-NPA intoxicated larvae, Glycine, Serine, Alanine and Threonine were detected. Similar set of deferential compounds were found in pentanoic acid, isopentanoic acid and hexanoic acid treated larvae (fig. 10). The chemical formula of the deferential compound was confirmed with HR-MS measurements. Glycine conjugates were the most abundant and, serine, alanine and threonine were less abundant. In 7 and 8 carbon acids only traces of threonine could be detected and no Alanine was found (fig. 11).
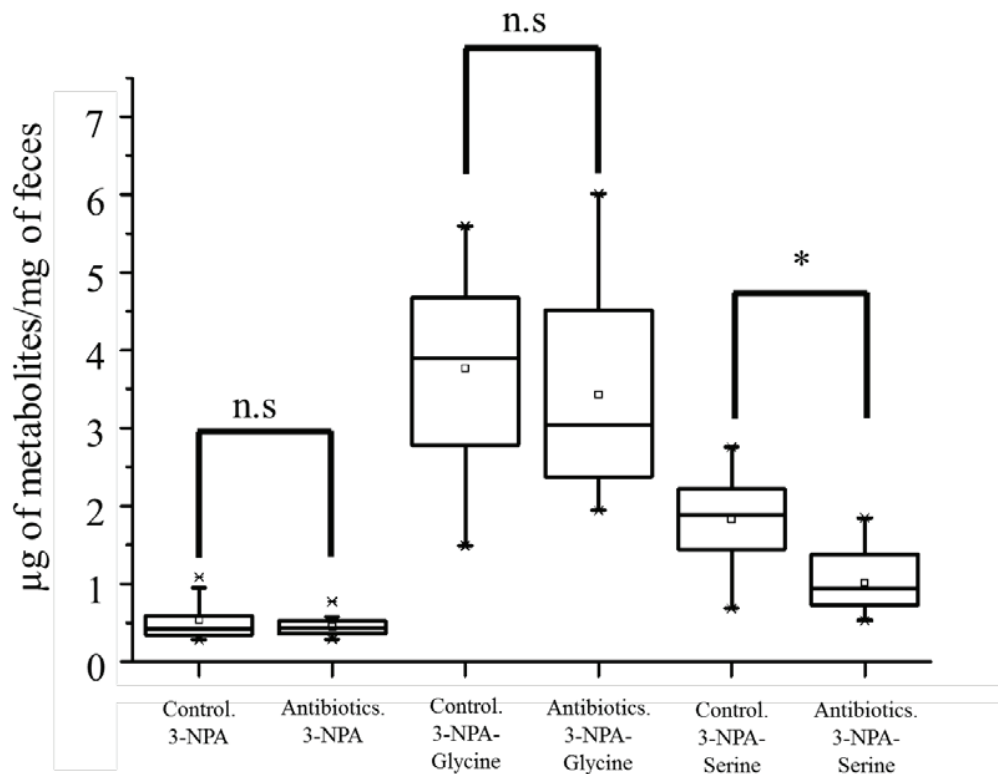
Figure 8. Effect of ampicillin 5,75 µg/ml and tetracycline 38 µg/ml mixture on production of 3-NPA-Glycine and 3-NPA-Serine in 6th instar larvae. The box plots show the smallest and largest values, 25% and 75% quartiles, the median, and outliers 1.5 (one-way Anova, Dunnett's post test, *$P<0.05$, n.s - not significant, n=20).

For medium chain acids conjugates with glycine and serine could be detected. A similar composition of the compounds in the frass of undecanoic acid treated larvae was detected. In the frass of the larvae treated with long chain fatty acids, glutamine conjugates were found. But the

most abundant compound were serine conjugate. Glycine conjugates were minor, whereas threonine and alanine conjugates were not detected at all (fig. 12). *S. littoralis* larvae demonstrated a similar spectrum of detoxification compounds across the whole range of aliphatic carboxylic acid. To clarify the outstanding resistant of larvae to decanoic acid, a contribution of the gut microbiome to metabolism of carboxylic acid was studied. From our unpublished data, it's known that a mixture of ampicillin and tetracycline significantly suppresses the core microbiome of the gut. But admixture of the antibiotics to diet did not have any effect on survival rates of the larvae. The Larvae were fed on the mixture of antibiotic and fatty acids. The toxic effect of the mixture of aliphatic fatty acids and antibiotic was compared with toxicity of the fatty acids. Fatty acids with carbon chain length from 5 to 10 carbon atoms were tested. An admixture of antibiotic did not increase mortality in the larvae treated with fatty acid up to 9 carbonatoms chain (fig. 13). Toxicity of decanoic acid was negligible as compared to C9 fatty acids. Treatment with the mixture of antibiotic and decanoic acid significantly increased the mortality (one-way Anova, Dunnett's post test, $p < 0,05$. fig. 12).
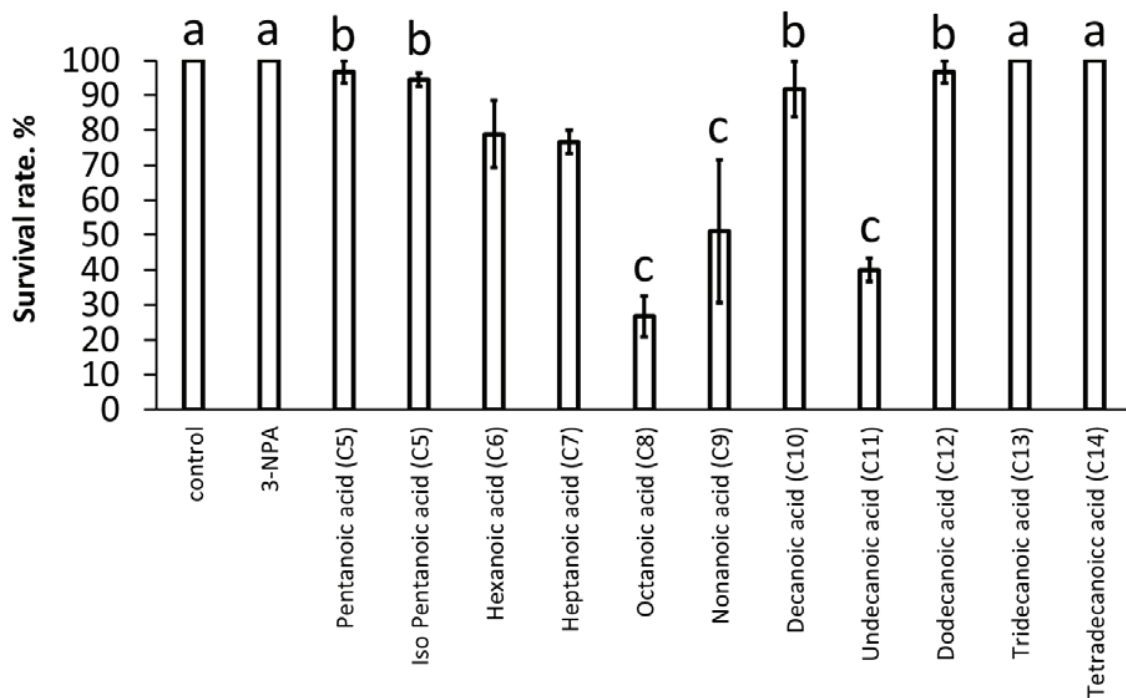
Figure 9. Toxicity of fatty acids after 3 days of feeding on diet containing 34 µmol fatty acids /g of diet . one-way Anova, Dunnett's post test, a,b,c; $p < 0,05$; ± 1 SD, n = 120

The data indicate that gut microbiome could significantly contribute to detoxification of decanoic fatty acid.
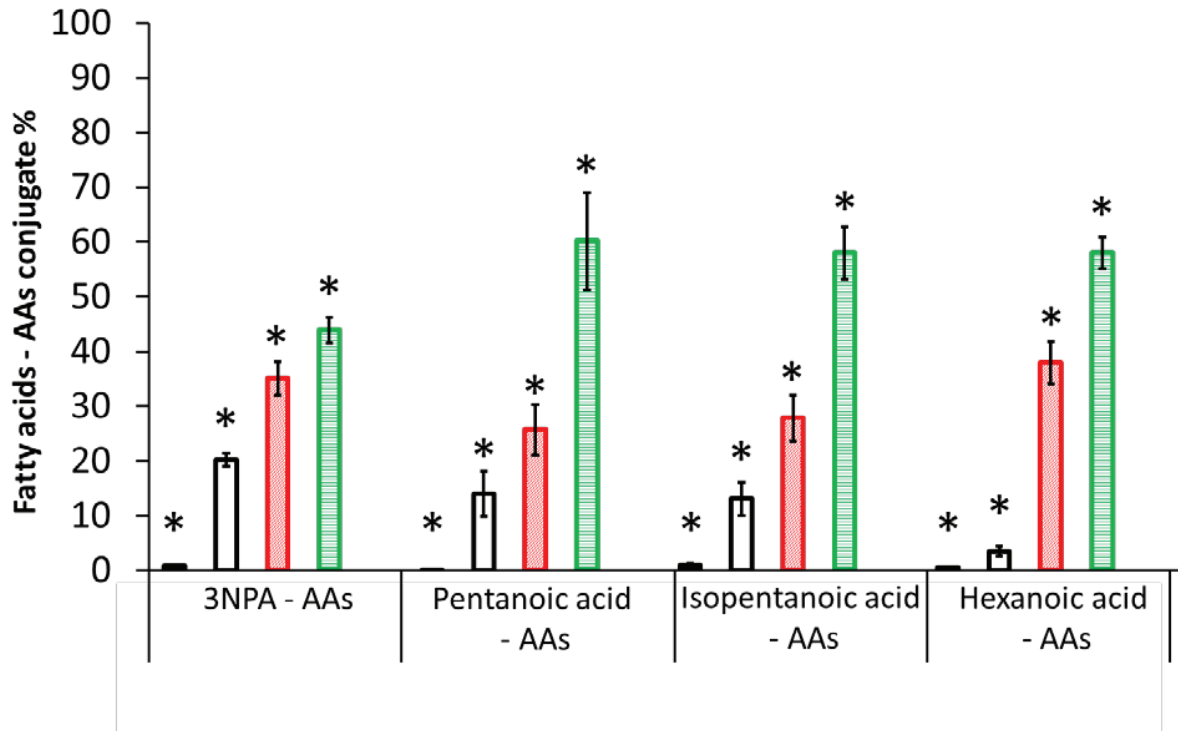
Figure 10. Amino acid amides of fatty acid in the frass of *S. littoralis* larvae after feeding on fatty acid containing diet. ▬▬ Fatty acid – Threonine, ▭ Fatty acid – Alanine, ▬ Fatty acid – Serine, ▤ Fatty acid – Glycine, one-way ANOVA, Dunnett's post test, *p < 0,05; ± 1 SD, n = 5.
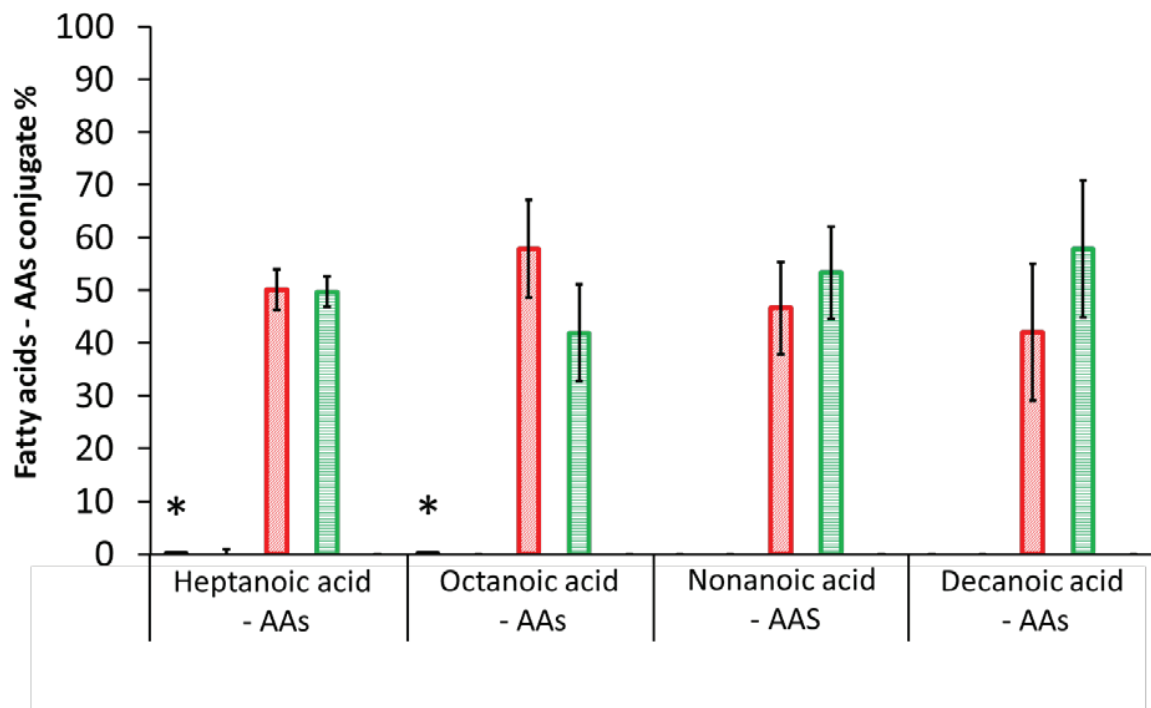
Figure 11. Amino acid amides of fatty acids in the frass of *S. littoralis* larvae after feeding on fatty acid containing diet. ▰▰▰ Fatty acid – Threonine, ▭ Fatty acid – Alanine, ▨ Fatty acid – Serine, ▤ Fatty acid – Glycine, ▦ Fatty acid – Glutamine. One-way ANOVA, Dunnett's post test, *p < 0,05; ± 1 SD, n = 5.
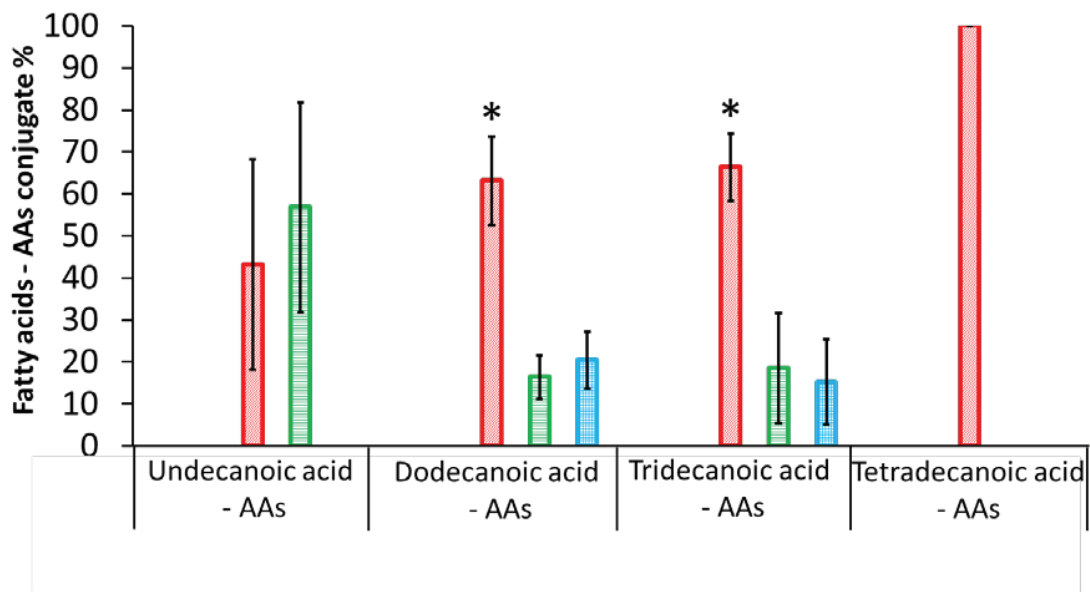
Figure 12. Amino acid amides of fatty acid in the frass of *S. littoralis* larvae after feeding on fatty acid containing diet. ▬▬ Fatty acid – Threonine, ▭ Fatty acid – Alanine, ▤ Fatty acid – Serine, ▤ Fatty acid – Glycine, ▦ Fatty acid – Glutamine. One-way ANOVA, Dunnett's post test, *p < 0,05; ± 1 SD, n = 5.

Figure 13. Antibiotic effect on survival rate of S. littoralis larvae after 3 days of feeding on fatty acid containing diet, 34 µmol/g diet. ▨ without antibiotic, ☐ with ampicillin 5,75 µg/ml and tetracycline 38 µg/ml. one-way ANOVA, Dunnett's post test, *p < 0,05; ± 1 SD, n = 120

7. Unpublished results Part II

7.1. Effect of salicin on structure and richness of the *S. littoralis* gut microbiome.
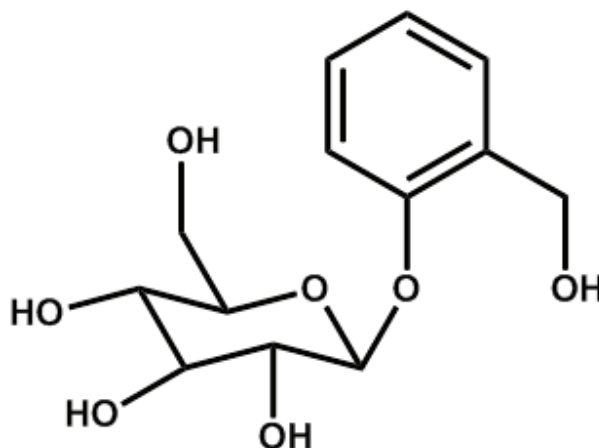
Figure 1. Phenolic glucoside, salicin.

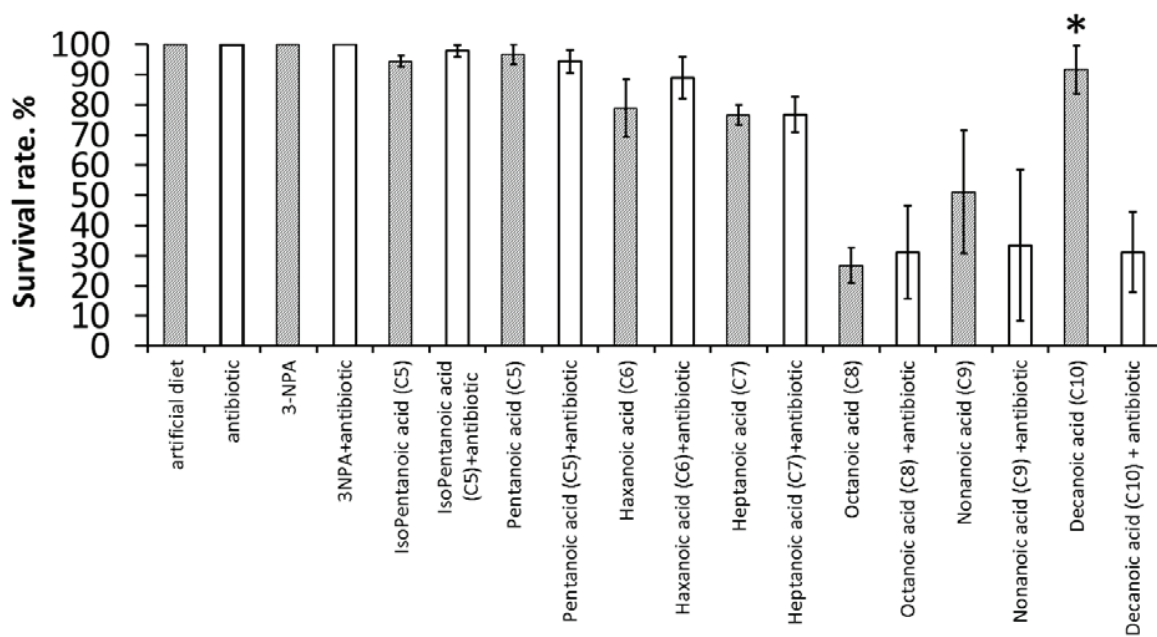The feeding experiment on artificial diet with a mixture of salicin (Fig. 1) was performed on *S. littoralis* larvae. Salicin was added to artificial diet in natural relevant concentration 1.03% (Boeckler et al., 2011). Total gut microbial community DNA was sampled from 6th instar larvae. Gut microbiome composition was documented with 454 pyrosequencing. The microbiome of experimental and control group was described rather fully, the rarefaction curve is close to saturation (Fig. 2). *S. littoralis* gut microbiome presents relatively small number of species, in average 29 and 34 in control and experimental group. Also, large number of observed OTUs present in control and experimental group, respectively. The observed range of variations is common for Lepidoptera (Hammer et al., 2014). Average number of OTUs in larvae of Lepidoptera species were estimated around 50 (Ji-Hyun et al., 2014). Laboratory reared Lepidoptera larvae had reduction of OTUs number (Staudacher H. et al., 2016). After feeding on standardized diet gut of *S. littoralis* inhabited by 23 OTUs (Bosheng et al., 2016). This previously published data are in good agreement with our data. The phylogenetic diversity per whole tree was not significantly different between control and experimental group (Monte Carlo permutations, p>0.05, supplementary materials fig. 1 a). This could be because of random composition of transient present species. The richness of experimental and control microbiome was almost equal (Monte Carlo permutations, p>0.05), chao 1 index in control group 20.3 and in experimental group 23.6(supplementary material fig. 1 b).
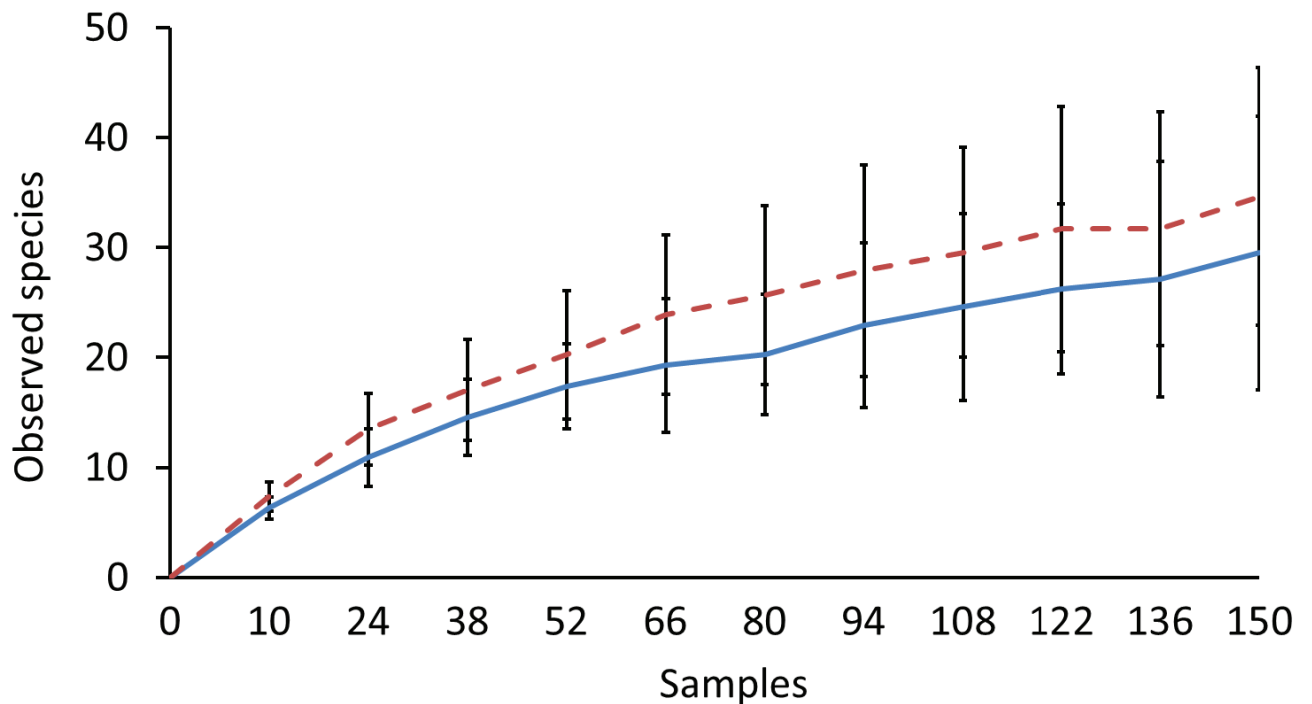
Figure 2. The observed species number in the samples was calculated after 150 random samplings with replacement, and the average was plotted as rarefaction curve ▬▬▬ control, ▬ ▬ salicin treatment (n=7, ± SE).

In untreated gut microbiome of *S. littoralis* 6th instar larvae are presented members of Actinobacteria, Flavobacteriia, Sphingobacteriia, Bacilli, Clostridia, Erysipelotrichia, Alphaproteobacteria, Betaproteobacteria, Gammaproteobacteria. Bacilli are dominant in the untreated gut microbiome. In the *S. littoralis* gut, the average relative abundance is 60%, but it has large amplitude between the samples (Fig. 3). In salicin treated microbiome the average relative abundance is 80%, but there is no statistically significant difference between control and experimental group (Wilcoxon rank sum test, p>0.05). Bacteria of Clostridia, Erysipelotrichia, Alphaproteobacteria, Gammaproteobacteria represent a lower abundance group. In untreated microbiome average relative abundance of Gammaproteobacteria is 18% and in salicine treated microbiome it relative abundance decries to 7%. Members of class Alphaproteobacteria are present in all samples but there relative abundance is low. In the untreated microbiome average relative abundance is 1.3% in salicin treated microbiome it slightly increases to 2.7%. Representatives of Clostridia class is facultative members of gut microbiome, there average relative abundance is 2.9% and 3.1% in treated and untreated gut microbiome. Salicin treatment has got no significant effect on Clostridia, Alphaproteobacteria, Gammaproteobacteria (Wilcoxon rank sum
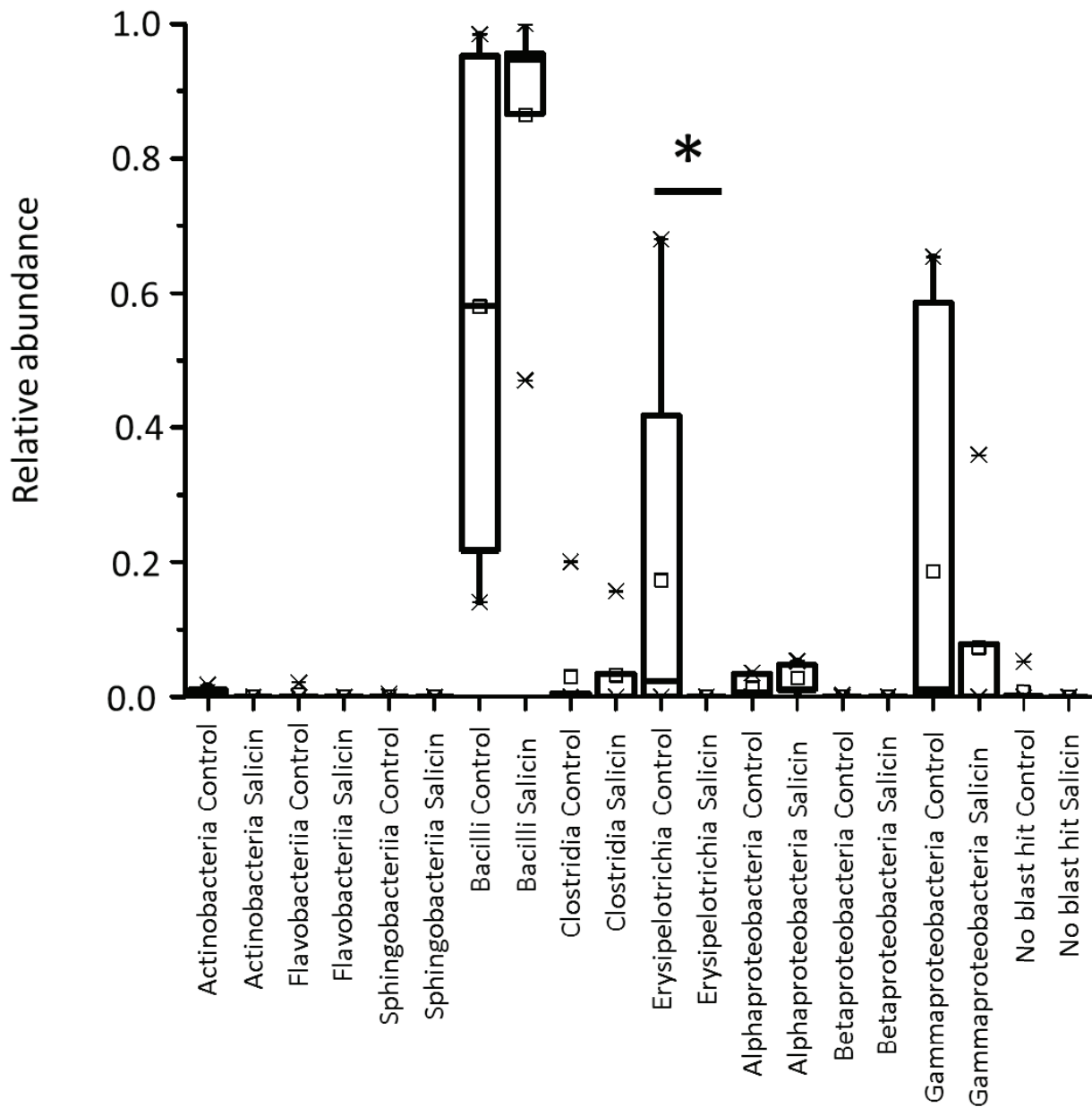
Figure 3. Effect of salicin treatment on relative abundance of major bacteria class in *S.littoralis* gut microbiome. The box plots show the smallest and largest values, 25% and 75% quartiles, the median, and outliers 1.5 (Wilcoxon rank sum test, * p<0.05, n = 7).

test, p>0.05). In contrast Erysipelotrichia are highly sensitive to salicin treatment. The average relative abundance in the untreated gut microbiome is 17.3%. After salicin treatment members of Erysipelotrichia are completely eliminated from gut microbiome (Wilcoxon rank sum test,

p<0.05. Fig. 3). The Actinobacteria, Flavobacteriia, Sphingobacteriia, Betaproteobacteria, represent a minor group and the OTUs could be found only in a few samples.

7.2 Deferential effect of salicin on the *S. littoralis* gut microbiome.

In *S. Littoralis* gut microbiome the highly abundant OTUs could be found in both the salicin treated and the untreated microbiome. In contrast, minor OTUs could by find only in a few samples. A third group of OTUs present almost at all control samples but could not be found in salicin treated samples (Supplementary materials. Fig. 2). Bacilli are members of the most abundant class of bacteria in *S. littoralis* gut, present in treated and untreated microbiome. Dominant OTUs such as *Enterococcus moraviensis*, *Enterococcus mundtii*, *Enterococcus gallinarum* are common at all samples and are highly resistant to salicin treatment. Several uncultured strains of *Weissella sp.* and uncultured *Planomicrobium sp.* are constantly present in the gut, and were not affected by salicin treatment (Fig. 4). Also alphaproteobacteria and gammaproteobacteria were widely distributed among the samples and resistant to salicin treatment. Several OTUs were abundant in untreated gut microbiome but were totally eliminated from the microbiome after salicin treatment. Two strains of gammaproteobacteria class were highly sensitive to salicin treatment. Uncultured *Pantoea sp.* and *Enterobacter* ASR 10 eliminated from the gut after salicin treatment (Wilcoxon rank sum test, p<0.05). Also, two strains of Firmicutes phylum significantly sensitive to salicin. Member of Lactobacillales order *Leuconstoc sp.* Is a minor component of the gut microbiome, after salicin treatment was completely removed from gut microbial community. Uncultured *Clostridium sp* member of Erysipelotrichales order was heighly sensitive to salicin treatment. Average relative abundance of the uncultured *Clostridium sp* in untreated microbiome is 17%, after salicin treatment no the *Clostridium sp* was not detected in the samples (Wilcoxon rank sum test, p<0.05. Fig. 4).
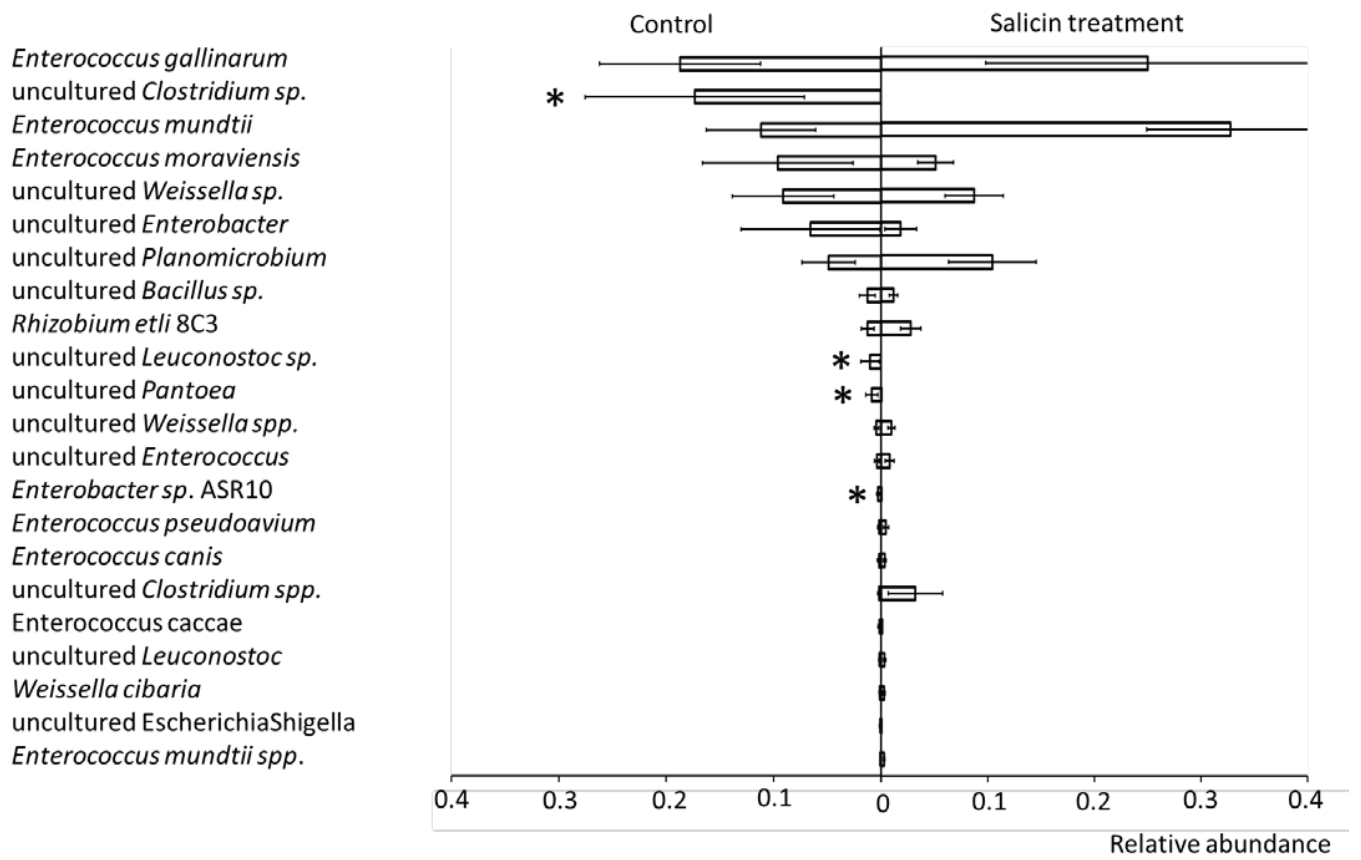
Figure 4. Effect of salicin treatment on relative abundance of 22 most common OTUs in *S.littoralis* gut microbiome (Wilcoxon rank sum test, * p<0.05, n = 7, ±SE).

NR 043550.1 Clostridium saccharogumia strain SDG-Mt85-3Db
Clostridium sp. SDG-Mt85-3Db (C. saccharogumia)
NR 119286.1 Clostridium cocleatum strain DSM 1551
NR 114393.1 Clostridium spiroforme strain JCM 1432
uncultured Clostridium sp (From Spodoptera)
NR 113243.1 Erysipelatoclostridium ramosum strain JCM 1298
Clostridium ramosum JCM 1298
NR 024733.1 Coprobacillus cateniformis strain JCM 10604
NR 027526.1 Catenibacterium mitsuokai strain DSM 15897
NR 041305.1 Kandleria vitulina strain JCM 1143
NR 044362.1 Haloplasma contractile strain SSD-17B
NR 028816.1 Turicibacter sanguinis strain MOL361
NR 113802.1 Brevibacillus reuszeri strain NBRC 15719
NR 042961.1 Acholeplasma parvum strain H23M
NR 028829.1 Acholeplasma axanthum strain S-743
NR 044648.2 Eubacterium tortuosum strain ATCC 25548
NR 113039.1 Solobacterium moorei strain JCM 10645
NR 025729.1 Streptococcus minor strain ON59
NR 040820.1 Streptococcus uberis strain JCM 5709
uncultured Clostridium spp (from S. LIttoralis)
Clostridium cellulolyticum H10
C.papyrosolvens
Clostridium clariflavum
Clostridium leptum DSM 753T
Clostridium difficile ATCC 9689
Clostridium subatlanticum
Clostridium isatidis DSM15098
Clostridium tertium DSM 2485
C tetani NCTC279
Clostridium oceanicum DSM 1290T
Clostridium acetobutylicum NCIMB 8052 (C. bei NCIMB 8052)
C.beijerinckii (DSM791) (C. bei DSM13821 (HKI0724))
C.puniceum

0.05

Figure 5. The tree was constructed from DNA sequence alignments using Clustal W, calculated algorithm maximum likelihood.

8. General discussion

S. littoralis is a widely spread generalist having a host plant range including 40 plant families. Due to their generalist feeding behavior larvae of *S. littoralis* are well adapted to the digestion of toxic plant material. In the following research presented here, the effect of plant toxins on *S. littoralis* larvae was evaluated. Toxic plant secondary metabolites were added to an artificial diet in naturally occurring and thus relevant concentrations. Amygdalin, coumarin, methoxypsoralen, crotaline, 3-NPA were added as an admixture in concentrations of 0.87; 6.84; 0.46; 6.14; 4.2 µmol/g of diet respectively. *S. littoralis* larvae were observed to grow slower on the diets containing amy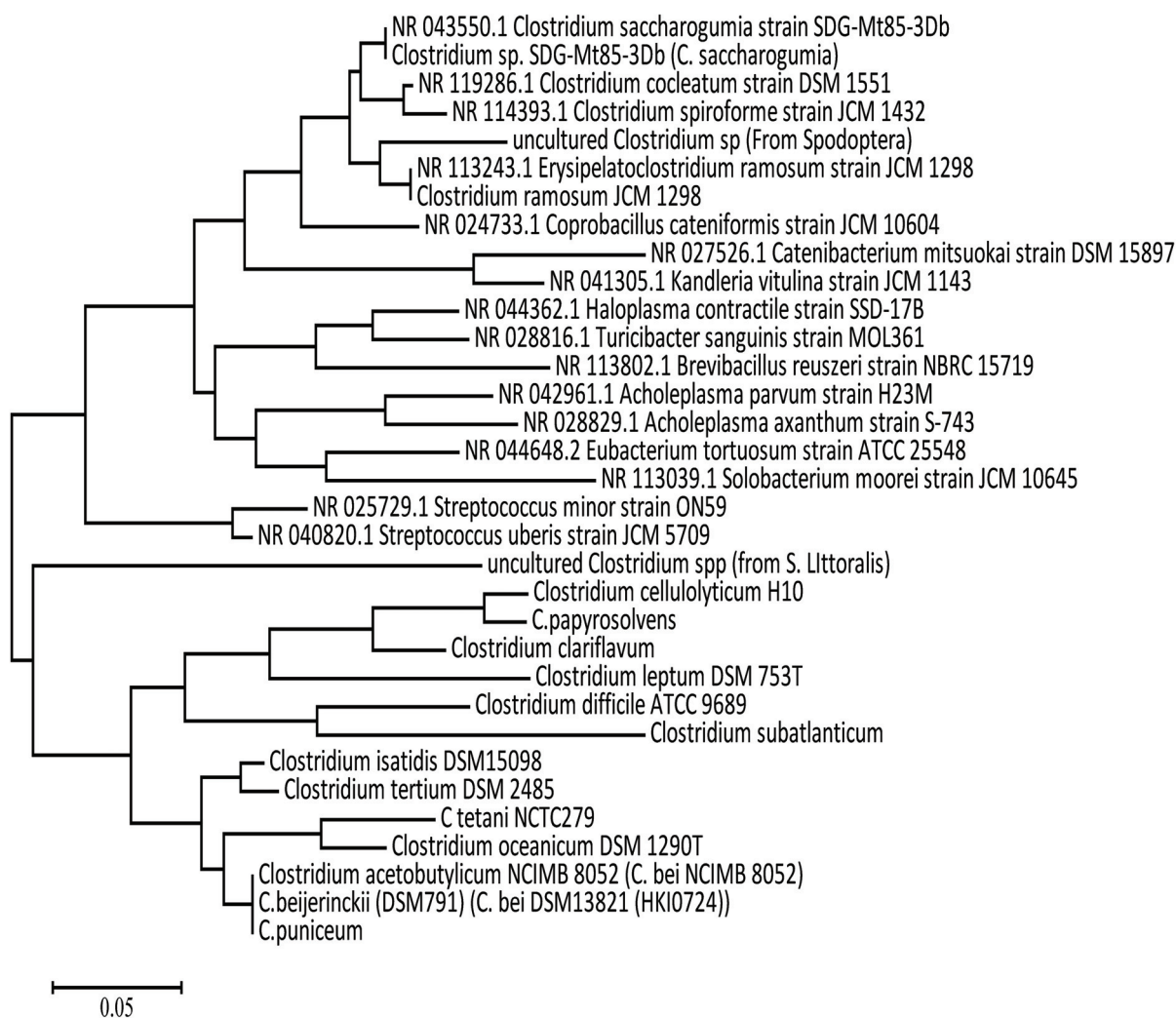gdalin, coumarin, methoxypsoralen, crotaline, 3-NPA (Novoselov et al., 2015. Unpublished materials part1, fig. 1, 2, 3, 4). It has been reported previously that insects observe the same delayed growth on imbalanced diets. Insects *Myzus persicae*, *Tribolium confusum* and *Apis mellifera* stop their development in the absence of arginine, histidine, leucine, isoleucine, lysine, methionine, phenylalanine, threonine, tryptophan, or valine. Lepidoptera *Pectinophora gossypiella*, *Helicoverpa zea* slow down their growth in the absence of one of these essential amino acids. In order to achieve optimal growth patterns, most insects need the optimum level of proteins in their diet. Insects cannot synthesize some vitamins, and thus acquire thiamine, riboflavin, nicotinic acid, pyridoxine, pantothenic acid, folic acid, and biotin, needed for growth from their diet (Dadd, 1985; Hanife, 2006). In response to imbalance diet most insects alter the total amount of ingested food (Dadd, 1985). Our experiments indicate that admixture of toxins did not have an effect on feeding rate. Observed decreases in body length and body weight could correspond to direct and indirect effect of plant toxins. Additionally, direct effect of toxins could alter gut epithelium.

Coumarins are highly toxic to generalist insect herbivores (Michael et al., 1992). In the digestive tract they are toxic to eukaryotic cells by means of the depletion of glutathione, through a tendency of the molecule to react with non-protein sulfhydryl groups. This reaction causes hepatotoxicity, oxidative stress and can lead to apoptosis (Lake et al., 1989) and a reduction of the size of larvae (Unpublished materials part1, fig. 2).

Larvae also showed reduced growth on the diet with admixture of 3-NPA (Novoselov et al., 2015); an irreversible non-competitive inhibitor of the enzyme succinate dehydrogenase (Burdock et al., 2001).

Amygdalin is a compound classified under cyanogenic glycosides. It exerts its toxicity by means of subsequent action of beta-glucosidases. First, the outer most sugar of amygdalin is cleaved into prunasin by the initial activating glucosidase, followed by the action of prunasin hydrolase, which cleaves prunasin into mandelonitrile; an unstable intermediate. Due to mandelonitrile's inherent instability, it is quickly converted to benzaldehyde and hydrogen cyanide by the action of mandelonitrile lyase or through spontaneous hydrolysis. The released hydrogen cyanide anion

primarily inhibits the action of the enzyme complex cytochrome C oxidase through irreversible binding to the heme moeity. Inactivation of cytochrome C oxidase leads to insufficent production of ATP by disruption of the electron transport chain, which can lead to delayed growth of larvae. (Unpublished materials part1, fig. 1).

Feeding on methoxypsoralen significantly reduced body lengths and body weights of the larvae (Unpublished materials part1, fig. 3). Methoxypsoralen nonspecifically affects different cellular prosthesis. It covalently binds to DNA, fatty acids and proteins.

Crotalin is one of the most common pyrrolizidine alkaloids. In the gut N-oxides of crotalin are reduced to crotalin form by the microsomal cytochrome P450 enzyme. The Active form of crotalin reacts with DNA and damages the gut tissue. Consequently, the intoxicated larvae demonstrated reduced body size (Unpublished materials part1, fig. 4).

Plant toxins could have indirect effect on the larvae. The toxic compound could alter the composition, molecular state and functions of gut microbiota. It is known that gut microbiota could provide nutrient supplementation to the host, like essential amino acids and vitamin biosynthesis. For example the synthesis of vitamins and essential amino acids has been shown for strict gut symbionts (Eichler, Schaub, 2002; Hongoh et al., 2008; Nikoh et al., 2011). Changes in microbiome could have an effect on the nutrient supplementation functions. In the present work, it has been shown that plant toxins had an effect on composition of gut microbiome (Unpublished materials part1, fig. 5). 3-NPA and Coumarin treatment had similar effect on the gut microbiome. In 4th instar larvae, the abundance of Enterococaceae in the gut was 90% - 72%. In 6th instar larvae abundance of Enterococaceae increased to 90 – 97%. Enterobacteriaceae were minor component of microbiome after coumarin treatment the abundance decreased to 16% (Unpublished materials part1, fig. 5). Despite the fact that 3-NPA and Coumarin have similar effects on the gut microbiota composition, these compounds have different molecular mechanisms of action. Coumarins have an antibiotic activity against Gram-positive bacteria, and are able to inhibit growth of *Pseudomonas* spp. (de Souzaa et al., 2005). In *S.littoralis,* coumarin inhibited Gram-negative bacteria in the gut. Coumarin inhibited DNA replication, by targeting the enzyme DNA gyrase an ATP-dependent bacterial type II topoisomerase. Gyrase is responsible for the introducing of negative supercoils into DNA (Andreza et al., 2004). Enterococaceae could have a mechanism to overcome the toxic coumarin's effect.

3-NPA is the irreversible non-competitive inhibitor of the enzyme succinate dehydrogenase and it toxic to aerobic bacteria (Burdock et al., 2001). In the gut of *S. littoralis,* Enterococaceae could survive in anaerobic zone and utilize glycolysis as energy metabolism. *Enterococcus mundtii* have been shown as the dominant gut microbe in *S. littoralis* larvae (Tang et al., 2012). Bacteria of the Enterococcus family are ubiquitous members of the normal gut microbiota in diverse species, including vertebrates and insects (Mason et al., 2011). Under anaerobic conditions *Enterococcus faecalis* undergoess homolactic fermentation (Snoep et al., 1992). Similar ability could provide the resistance of Enterococaceae to 3-NPA.

In comparison to the coumarin and 3-NPA, amygdalin and 8-MOP treatment inhibited the Enterococcaceae species. After coumarin and amygdalin treatment abundance of Enterococcaceae species decreased to 2 – 7% in 6th instar larvae. The abundance of Enterobacteriaceae increased to 91%. No Clostridia or Erysipelotrichae could be detected after plant toxins treatment. Amygdalin and 8-MOP inhibited Enterococcaceae species, Clostridia and Erysipelotrichae, but these compounds have different mechanisms of toxicity. Amygdalin is a cyanogenic glycoside. The released hydrogen cyanide anion from amygdalin hydrolysis primarily inhibits cytochrome C oxidase. 8-MOP covalently binds to DNA. Most likely Enterobacteriaceae have mechanisms to overcome the toxic effects of amygdalin and 8-MOP.

It is important to mention that Clostridia and Erysipelotrichae are constantly present in the untreated microbiome (Unpublished materials part1, fig. 5). Clostridia and Erysipelotrichae are highly sensitive to plant toxins.

The observed changes in the gut microbiome are not fatal to the larvae. There were no dead larvae detected after the rearing them on the intoxicated diet.

General function of gut microbial community like nutrient supplementation could be undertaken by different members of microbial community if the composition of microbial community is changed after the toxins' treatment. Contributions of gut microbiome to growth of the larvae have been estimated using the addition of antibiotic to the diet. Ampicillin is highly active against Gram-positive bacteria, which are highly abundant in *S. littoralis* larval gut. Tetracycline has bacteriostatic activity against wide range of aerobic and anaerobic bacterial genera, both Gram-positive and Gram-negative. Eukaryotic cells are not susceptible to these antibiotics. The Larvae, after feeding on artificial diet with admixture of ampicillin and tetracycline, slowed down the growth (Unpublished materials part1, fig. 7). Mixture of ampicillin and tetracycline suppressed the main component of gut microbial community (Unpublished materials part1, fig. 6). Feeding of *S. littoralis* larvae on the artificial medium mixed with 4.2 µmol 3-NPA /g of diet and antibiotics did not lead to death of larvae, but slowed down the growth. The same happened after admixture of 3-NPA alone (Unpublished materials part1, fig. 7). Ampicillin and tetracycline did not increase toxicity of 3-NPA to *S. littoralis* larvae. It's possible that gut microbiota accelerates the growth of larvae, or produces important components of nutrition.

The application of biologically relevant concentrations of toxic 3-NPA was shown to significantly reduce the growth rate of *S. littoralis* larvae (Novoselov et al., 2015; Nishino et al., 2010; Diawara et al., 1993). Observed growth rate reduction by 3-NPA in *S. littoralis* suggests that 3-NPA, in fact, inhibits the growth of Lepidoptera (Cipollini et al., 2008; Wang et al., 2010). Although the larval growth decreased after the feeding of *S. littoralis* on 3-NPA, their ingestion was not lethal; concentrations of 3-NPA up to 33.6 µmol/g did not result in higher mortality compared to insects in the control group, demonstrating that *S. littoralis* is highly resistant to oral uptake of 3-NPA. In contrast, injecting the same amounts of 3-NPA into the insect's hemolymph resulted in mortality and death, suggesting that the total detoxification capacity of *S. littoralis* is based by conjugation of 3-NPA in the gut epithelium and the fat body.

Comparative analysis of the frass of *S. littoralis* larvae fed on a diet with or without 3-NPA, revealed the presence of new components, shown to originate from 3-NPA by feeding stable isotope labelled precursors. Molecular structures of these 3-NPA conjugation products were deduced from HR-MS/MS data and confirmed by total synthesis (see supporting information). Other conjugates, e.g. with glutathione were not detected. 3-Nitropropanoyl glycine and 3-nitropropanoyl serine had previously been described as metabolites in the grasshopper *Melanoplus bivittatus*. The grasshopper also produces a glutamine derivative which is absent in *S. littoralis* (Majak et al., 1998). Homologous 3-nitropropanoyl alanine and (3-nitropropanoyl) threonine were exclusively detected in *S. littoralis* and represent novel compounds. Although 3-NPA amino acid conjugates have previously been identified as putative detoxification products from *M. bivittatus*, no data concerning the toxicity of these compounds have been reported (Majak et al., 1998). We found that, in *S. littoralis* the injection of the amino acid amides of 3-NPA into the hemolymph was not toxic. However, the injection of the same amount of free 3-NPA caused mortality in 92% of the larvae (Novoselov et al., 2015), demonstrating that conjugation with amino acids represents an efficient way to cope with 3-NPA. Amino acid conjugation represents a common detoxification mechanism in insects and, as such, is similar to glycosylation or reaction with glutathione (Schramm et al., 2012) which force excretion.

Conjugation to amino acids is well known from Lepidoptera. Glycine conjugates have been described as products of glucosinolate metabolism (Stauber et al., 2012).

Conjugation of long chain fatty acids to glutamine is mainly facilitated by gut tissue or membrane-associated enzymes (Alborn et al., 1997; Lait et al., 2003; Yoshinaga et al., 2005). However, occasionally the insect gut microbial community exhibited conjugation activity, as in the case of N-linolenoyl glutamine biosynthesis by *Microbacterium arborescens* in *Spodoptera exigua* (Ping et al., 2007). In *S. littoralis*, however, no 3-NPA conjugation activity of the gut microbes under aerobic or anaerobic conditions has been detected. Also antibiotic treatment did not affect the amino acid amides production (Unpublished materials part1, fig. 8).

In contrast, cytosolic proteins, isolated against the *S. littoralis* gut tissue, were shown to catalyze the formation of 3-NPA amino acid amides in the presence of ATP and CoA (Novoselov et al 2015). Dedicated enzymes, catalyzing the conjugation of 3-NPA to amino acids from this or other organisms have not been described previously. Taken together, these results indicated that amino acid conjugation via amide formation represents an important detoxification pathway in *S. littoralis*. Although the exact mechanisms of 3-NPA conjugation remains to be elucidated our results allow us to propose a functional model.

The epithelial cells protect the larval hemolymph from the free toxin taken up with the food, as was previously shown for tannins (Appel and Michael, 1990; Engel and Moran, 2013; Giordana et al., 1989). Due to the high consumption rate of *S. littoralis* (consumed diet passes the gut within 2 hours), larvae may accumulate a large amount of 3-NPA in the gut that can pass the membrane barriers via different membrane carriers (Lamp et al., 2011). Once taken up by the epithelium, as-yet unidentified cytosolic proteins detoxify 3-NPA by converting it to non-toxic amino acid conjugates. From the cytosol, the detoxification products can be transported back into

the gut lumen via apocrine secretion, or passed onto the hemolymph (Cristofoletti et al., 2001; Ratzka et al., 2002; Terra and Ferreira, 1994; Wittstock et al., 2004;). Amino acid conjugates were detected in the hemolymph after the feeding of insects on a high concentration of 3-NPA (12.6 μmol/g of artificial diet weight). In addition, amino acid conjugates were detected in the frass of the larvae after sublethal doses of 3-NPA (8.4 μmol 3-NPA per g body weight) were injected into the hemolymph. When the toxin reaches the hemolymph after larvae have consumed high amounts of plant material, the fat body is also able to produce amino acid amides. Once amino acid amides are produced, they can be transported from the hemolymph to the hind gut via the malpighian tubules and finally excreted from the system.

In conclusion, we demonstrated that the formation of 3-NPA amides of glycine, serine, threonine and alanine by cytosolic enzymes of the insect epithelium represents an important detoxification pathway in *S. littoralis*. Details of 3-NPA metabolism and the responsible enzymes in *S. littoralis* remain to be identified.

Consequently we have studied the ability of the larvae to conjugate short, medium, and long chain fatty acids. In the first step the toxicity of short, medium, and long chain fatty acids for *S.littoralis* larvae have been evaluated. We have tested the toxic effect of 34 μmol of fatty acid per g of diet with chain length from 5 to 14 carbon atoms. Pentanoic acid and isopentanoic acid were not toxic to the larvae. Fatty acids with chain length from 6 to 11 carbon atoms were highly toxic to the larvae. Long chain fatty acids were not toxic to larvae (one-way Anova, Dunnett's post test, $p < 0,05$. Unpublished materials part1, fig. 9).

Furthermore, frass of the intoxicated larvae was studied with LC-MS. Conjugates of Glycine, Serine, Alanine and Threonine were detected in pentanoic acid, isopentanoic acid and hexanoic acid treated larvae (one-way Anova, Dunnett's post test, $p < 0,05$. Unpublished materials part1, fig. 10). It has been shown that conjugation of fatty acids happen in two steps and two enzymes are involved, acetyl CoA synthetase and acyl-Coa: glycine N-acyltransferses (Kinghts and Miners. 2012). Middle chain CoA synthetase, activates fatty acid with chain length from 4-12 carbon atoms have not been yet annotated in *Bombyx Mori* genome according to Kyoto University Database. Also, acyl-Coa: glycine N-acyltransferses have not been found in *Bombyx Mori* genome. Nevertheless, Glycine and Serine conjugates of fatty acids could be detected in 7 – 14 carbon atoms fatty acids treated larvae (one-way Anova, Dunnett's post test, $p < 0,05$. Unpublished materials part1, fig. 11, 12). In the frass of long chain fatty acid- treated larvae, glutamine conjugates were found. The most abundant compound was the serine conjugate. Glycine conjugate was minor, whereas threonine and Alanine conjugates were not detected at all (one-way Anova, Dunnett's post test, $p < 0,05$. Unpublished materials part1, fig. 12). In *Bombyx Mori* genome, 3 long-chain fatty acids CoA synthetase has been annotated. This enzyme is located in the endoplasmic reticulum. But unlikely, CoA esters of long chain fatty acids target for amino acid conjugation. Some others reported that membrane-associated enzymes could provide long chain fatty acid conjugation to glutamine (Alborn et al., 1997; Lait et al., 2003; Yoshinaga et al., 2005). These data indicate that the amino acid conjugation system of *S. littoralis* has different organization compared to other animals.

Gut microbial community could be involved in the utilization of middle chain fatty acids. Larvae treated with antibiotic and decanoic acid showed significantly increased mortality compared to decanoic acid treatment without antibiotic admixture (one-way Anova, Dunnett's post test, p < 0,05. Unpublished materials part1, fig. 13).

In the next step, we were interested to test the effect of salicin on *S.littoralis* larvae. Salicin is a phenolic glycoside widely distributed among Salicaceae and Populus species (Boeckler et al., 2011). It has been shown that phenolic glycosides serve plants as a defensive tool. Rearing of lepidopteran species *Lymantria dispar* on phenolic glycoside rich foliage of *Populus tremuloides* significantly increased the development time and affected the fitness parameters (Osier. T.L. et al, 2000). The plant derived phenolic glycoside salicin significantly slowed down the growth of *S. littoralis* larvae (Supplementary materials, unpublished results part 2, fig. 4). After feeding on artificial diet containing 1.03% salicin, the 6th instar larvae were significantly smaller than the control larvae (data from bachelor work of Christian Seiffert). Compared to the other tested plant toxins, which have got direct toxic effect on the insect cells, salicin did not have a toxic effect. Antinflammation activity of salicin is known since centuries (Boeckler et al, 2011). It was shown, that D(-)-Salicin suppressed the activation of mitogen-activated protein kinase (MAPKs) and NF-κB signaling pathways (Li Y et al., 2015). MAPK signal transduction pathways are evolutionarily conserved, nevertheless, it is difficult to predict the effect of salicin on the insect cells. Salicin could indirectly affect the performance of larvae through the moderation of the gut microbiome. Gut represents a niche, which can be colonized by different microbial communities (Lee et al, 2013). Numerous bacteria populated insects' guts are involved in different interactions (Ruokolainen et al, 2016). Recently, it was shown that the insect gut microbial community is involved in nutrient supplementation and intestinal cell renewal (Engel and Moran, 2013). Commensal gut bacteria can promote systematic growth. Germ-free larvae of *D. melanogaster* exhibited reduced growth and developed more slowly than conventionally reared individuals (Ridley et al., 2012). *S. littoralis* gut microbiome treated with salicin significantly differed from the untreated microbiome. In untreated microbiome of 6th instar larvae, Bacilli, Clostridia, Erysipelotrichia and Alpha-, Beta-, and Gammaproteobacteria were present(Unpublished materials part 2, fig. 2). Among the *S. littoralis* microbiome, the average abundance of Erysipelotrichia was 17% (Unpublished materials part 2, fig. 3). After the salicin treatment, the bacteria of Erysipelotrichia class was completely eliminated from the gut (Wilcoxon rank sum test, p<0.05, fig. 3). A lot of Erysipelotrichia species utilize broad spectrum of glycoside including salicin, and fermented glucose to lactic acid. Common products of Erysipelotrichia species metabolism are short chain fatty acids acetic, butyric and iso-butyric acids (Kageyama A, Benno Y. 2000). It has been shown that short chain fatty acids promote epithelial cell turnover and increase intestinal stem cell pool. *Acetobacter pomorum* commonly present in the gut of *D. melanogaster*, are able to produce acetic acid. The *A. pomorum* mutant strain with knocked out periplasmic pyrroloquinoline quinone–dependent alcohol dehydrogenase (PQQ-ADH) is not able to produce acetic acid. The larvae of *D. melanogaster* monoassociated with the *A. pomorum* mutant strain had smaller bodies and intestine sizes (Shin et al., 2011).

Bacteria carry out different biochemical functions. Same biochemical functions can be shared between different bacteria (Huttenhower C. et al., 2012). The biochemical functions of eliminated bacteria can be taken over by other members of microbial community. Phylogenetic based prediction of metagenome functional content (PICRUSt) indicated that salicin treatment did not have any effect on the large portion of biochemical functions. Only 33 of 6909 functions were down regulated by salicin treatment, among them was hyaluronoglucosaminidase gene (Supplementary materials Fig. 3). Studies on different insect orders showed that bacteria within the phylum Proteobacteria and Firmicutes are dominant in almost all examined insects (Jones RT et al., 2013). In *S. littoralis* gut microbiome, members of two phyla, Firmicutes and Proteobacteria dominate (Tang at all 2012). In *S. littoralis* 6th instar larvae, Firmicutes and Proteobacteria were highly abundant and were not affected by salicin treatment (Unpublished materials part 2, fig. 3). It was shown that Enterococcus species dominated in microbiome of different Lepidopteran (Vilanova C. et al., 2016, Tang X. et al., 2012, Staudacher H. et al., 2016). In *S. littoralis* larvae *Enterococcus moraviensis, Enterococcus mundtii, Enterococcus gallinarum* dominated (Unpublished materials part 2, fig. 4). Relative abundance of OTUs in the gut microbiome had several orders magnitude of variations (Qin et al., 2010). In *S. littoralis* gut microbiome *Enterococcus mundtii* was rather stable, closely associated with the host and transmitted through generations (Teh et al., 2016). Salicin did not have any effect on the abundance of Enterococcus species in *S. littoralis* (Unpublished materials part 2, fig. 4). *Enterococcus mundtii* is high resistant to environmental stress factors. They were present in the gut of Lepidoptera after feeding on plant enriched with toxins (Vilanova et al., 2016). In contrast to Enterococcus species, uncultured *Clostridium sp*. was highly sensitive to salicin and were completely eliminated after feeding on the intoxicated diet (Wilcoxon rank sum test, $p < 0.05$, Unpublished materials part 2, fig. 3). The uncultured *Clostridium sp* from *S. littoralis* gut belongs to Erysipelotrichia class. Erysipelotrichia is commonly present in gut microbiome of mammals, and is associated in high abundance with a high fat diet (Conterno et al., 2011, Ruan et al., 2016). Gut microbial communities of vertebrates and invertebrates have similar composition, and members of Erysipelotrichia class also were found in the gut of wood feeding insects (Waite et al., 2012, Ley et al., 2008). Comparative analysis of predicted metagenome functions (PICRUSt) of treated and untreated microbiome revealed several biochemical functions, which were not present in the salicin treated microbiome. Genomes of bacteria are closely related to uncultured *Clostridium sp.,* and carried hyaluronoglucosaminidase gene. This function is completely eliminated in the salicin treated microbiome. Hyaluronan contributes significantly to cell proliferation and migration. Oligosaccharides of hyaluronan promote the survival of basal stem cells (Termeer et al., 2002; Choi HR et al., 2012). The uncultured *Clostridium sp*. from *S. littoralis* were closely related to *Clostridium ramosum* (Unpublished materials part 2, fig. 5), the main agent promoting obesity in mice (Woting et al., 2014). Uncultured Clostridium sp. from *S. littoralis* gut was high sensitive to salicin treatment. No *Clostridium sp* were detected in the samples of larvae rearing on salicin containing diet (Wilcoxon rank sum test, $p < 0.05$. Unpublished materials part 2, fig. 4). Larvae of *S. littoralis*

gained weight significantly slower on intoxicated diet, as compared to the normal food (data not shown). Uncultured *Clostridium sp.* can affect the fatty acid and sugar uptake, as it was described for *Clostridium ramosum* in mice (Woting et al., 2014). Several OTUs were minor components of microbiome and were sensitive to the salicin treatment. Uncultured Leuconostoc from *S. littoralis* presented 1% of microbiome (Unpublished materials part 2, fig. 4). This *Leuconostoc sp.* is closely related to *Leuconostoc mesenteroides* and could contribute to the carbohydrate metabolism. Salicin treatment completely eliminated the uncultured *Leuconostoc sp.* from the gut microbiome (Wilcoxon rank sum test, $p < 0.05$. Unpublished materials part 2, fig. 4). Proteobacteria are the common members of the insect gut microbiome (Morrow et al., 2015). Alphaproteobacteria and Gammaproteobacteria are constantly present in the *S. littoralis* gut and their abundance is 2% and 18% respectively (Unpublished materials part 2, fig. 3). A Minor OTU of Gammaproteobacteria was sensitive to salicin. In untreated gut microbiome, the abundance of *Enterobacter sp.* ASR10 was 2%, and it was completely removed from salicin treated microbiome (Wilcoxon rank sum test, $p < 0.05$. Unpublished materials part 2, fig. 4). Strain *Enterobacter sp.* ASR10 was isolated from the soil, and common in environment (Suvendu et al., 2014). It has been shown that diet derived factors like lignocellulosic materials could affect the composition of *Periplaneta americana* gut microbiome (Bertino-Grimaldi et al., 2013, Hammer, Bowers. 2015). Our data indicated that the food derived factors like plant secondary metabolites could shape the gut microbial community. Salicin treatment changed the ratio between the main components of microbiome Firmicutes/Proteobacteria and increased proportion of Firmicutes. Enterococcus species were closely associated with *S. littoralis* and was resistant to salicin treatment. Salicin specifically eliminate certain OTUs from the gut microbiome. *Erysipelotrichia* species were high sensitive to salicin treatment. The uncultured *Clostridium sp.*, the member of Erysipelotrichia class were completely removed from the *S. littoralis* gut after the salicin treatment.

9. Summary

In the last decade, the amount of publications on microbiome research has increased enormously. In 2012, the number of publications was around 800, while last year this number surpassed 2000. Research on the microbiome has a significant effect on different fields of life sciences, health care, agriculture, and food industry (Arnold et al., 2016).

Microbiome-wide association studies (MWAS) can link whole microbiomes to a variety of disorders like obesity, cardiovascular disease and colon cancer, among others. However, causal and network-based interactions remain unclear in many cases (Gilbert et al., 2016).

Microbes carry out numerous biochemical functions and contribute to numerous processes. Several functions of bacteria in the insect guts are well known. It has been shown that, the gut microbiome provides colonization resistance against pathogens or parasites, facilitate degradation of cellulose and nutrient supplementation, such as the synthesis of vitamins and essential amino acids, or contribute to the fixation of nitrogen (Engel, Moran, 2013). Gut bacteria have also been shown to degrade toxins, ingested with the diet. Gut microbiome in some cases could carry out specific functions like a production of molecules involved in intraspecific and interspecific communication, such as pheromones and kairomones. The commensal gut microbiota has been shown to be involved in basic cellular processes of the host. Most important of them are intestinal cell renewal, stem cell pull maintain and promotion of systemic growth. Disruption in the gut microbiome composition could lead to malfunction of vital processes and consequently is harmful to the host. Insects with suppressed gut microbiome have abnormal intestine sizes, repressed oogenesis, and their offsprings are more sensitive to stress. Composition of the gut microbiome depends on numerous environmental factors like food derived plant secondary metabolites (Elgart et al., 2016).

The present project established a useful model to study the effect of plant secondary metabolites on the gut microbial community of *Spodoptera littoralis*. The model is easy to handle, concentrations and amounts of applied toxins can be clearly defined, and the effect on the composition of the gut microbiome could be evaluated. The experiments could be conducted under controlled laboratory conditions and allowed to make measurements of a broad spectrum of parameters.

The gut microbiome with its myriad of interactions between the bacteria plays an essential role in the host development and performance. We have made an attempt to evaluate the effect of plant secondary metabolites on the gut microbiome of *S. littoralis*.

Part 1. Effect of plant toxins on the growth parameters of *S. littoralis* larvae.

In the present research, effects of plant secondary metabolites on *S. littoralis* larvae was evaluated. In the first step, the effect of plant secondary metabolites on the growth parameters of *S. littoralis* was measured. Body lengths and body weights were measured in a time dependent manner. Six different plant secondary metabolites, belonging to different classes of chemical compounds, were selected. The compounds have different toxic mechanisms of action and are widely distributed among host plants of *S. littoralis*. Effects of coumarin, methoxypsoralen, 3-NPA, amygdalin, crotalin and salicin were studied.

Coumarin is a common plant secondary metabolite from the benzopyrone *class of chemical compounds*. Coumarins are highly toxic to generalist insect herbivores. In the digestive tract they

75

are toxic to eukaryotic cell. In eukaryotic cells, coumarin binds to the non-protein sulfhydryl groups and deplete glutathione. They cause hepatotoxicity, oxidative stress and lead to apoptosis (Andreza et al., 2004). Methoxypsoralen is a typical furanocoumarin. Methoxypsoralen nonspecifically affects different cellular components. It covalently binds to DNA, fatty acids and proteins (Studzian et al., 1999).

We have tested the effect of nitrocompounds on *S. littoralis* larvae. We have select 3-nitro propionic acid from this class. 3-NPA has a specific target, it irreversibly and non-competitively inhibits the enzyme succinate dehydrogenase (Olsen et al., 1999; Tarazona, Sanz, 1987; Hipkin et al., 2004).

Amygdalin is the member of the class of cyanogenic glycosides. Amygdalin undergoes certain metabolic reactions and finally releases hydrogen cyanide. The released hydrogen cyanide anion primarily inhibits cytochrome C oxidase. Inactivation of cytochrome C oxidase leads to the suppression of the respiratory chain (Atta-Ur-Rahman, 2002).

We have tested a common pyrrolizidine alkaloid crotalin. In the gut crotalin is reduced from the N-oxide to its active form. The active form of crotalin reacts with DNA and damages the gut tissue (Bernays, 2004).

We also have tested the effects of phenolic glycosides on the growth rate of *S. littoralis*. For our experiments we have selected salicin. Compared to the other tested plant toxins, which have direct toxic effect on the insect cell, salicin was not previously described to have a toxic effect on insect cells. It was shown that, D-(-)-Salicin suppressed the activation of mitogen-activated protein kinase (MAPKs) and NF-κB signaling pathways, and have antiinflammatory activity (Li Y et al., 2015).

To estimate the effects of plant secondary metabolites on the growth of the larvae the feeding assay was conducted. Toxic plant secondary metabolites were added to the artificial diet in natural relevant concentrations. The amygdalin, coumarin, methoxypsoralen, crotaline, 3-NPA, salicin were added as admixture in concentrations 0.87; 6.84; 0.46; 6.14; 4.2; 5,55 µmol/g of diet respectively. *Spodoptera littoralis* larvae slowed down the growth on the diet with an admixture of the toxins. But no dead larvae were observed during the experiments (Unpublished materials part 1, fig. 1 – 4).

Some insects demonstrate similar symptoms after rearing on imbalanced diet. Some apidae, tenebrionidae and aphididae end their development in the absence of arginine, histidine, leucine, isoleucine, lysine, methionine, phenylalanine, threonine, tryptophan, or valine. Also lepidoptera slow down their growth in the absence of one of these essential amino acids. Insects cannot synthesize vitamins, and they require thiamine, riboflavin, nicotinic acid, pyridoxine, pantothenic acid, folic acid, and biotin, in small amounts for growth (Dadd, 1985; Hanife, 2006).

Decrease in body lengths and body weights also could correspond to the direct effect of plant toxins on epithelial cells of the host. We checked the susceptibility of the larvae to high concentrations of the toxins. We have fed larvae on 3-NPA containing diet with concentrations of 3-NPA at 4.2; 8.4; 16.8; 33.6 µmol/g. Feeding on the high concentrations of 3-NPA did not increase mortality compared to the control. *Spodoptera littoralis* larvae are able to survive on 3-NPA concentrations which 3 times exceed the LD50 for rats (Novoselov et al., 2015). The observed decrease in body lengths and body weights could correspond to the direct effect of the plant toxins on the gut microbiome. General function of the gut microbial community like nutrient supplementation could be suppressed by plant toxins.

In the next step we have checked the contribution of the gut microbiome to the nutrient supplementation. Contribution of the gut microbiome to growth of the larvae has been estimated using the adding of antibiotics to the diet. Mixtures of tetracycline and ampicillin significantly suppressed the gut microbiome. Larvae after feeding on artificial diet with admixture of ampicillin and tetracycline slowed down the growth (Unpublished materials part 1, fig. 7). This data shows, as suggested, that the gut microbiome could contribute to systemic growth of the larvae.

The gut microbiome also could contribute to the detoxification of 3-NPA. To evaluate the contribution of the gut microbiome to 3-NPA metabolism, we fed gnotobiotic *S. littoralis* larvae with 3-NPA. Feeding of gnotobiotic *S. littoralis* larvae on the artificial medium mixed with 4.2 μmol 3-NPA /g of diet and antibiotics did not lead to their death, but slowed down the growth (Unpublished materials part 1, fig. 7). These results could indicate that the gut microbiome did not contribute to 3-NPA detoxification, which affecs the development of the larvae.

Part 2 Detoxification processes in *S. littoralis* larvae.

Comparative analysis of the frass of *S. littoralis* larvae fed on the diet with or without 3-NPA, revealed the presence of new components, shown to originate from 3-NPA by feeding stable isotope labelled precursors. The new compounds were identified as 3-MPA glycine, serine, threonine and alanine. Molecular structures of these 3-NPA conjugation products were deduced from HR-MS/MS data and confirmed by total synthesis. Other conjugates, e.g. with glutathione were not detected. 3-Nitropropanoyl glycine and 3-nitropropanoyl serine had previously been described as metabolites in the grasshopper *Melanoplus bivittatus* (Majak et al., 1998). The grasshopper also produces a glutamine derivative which is absent in *S. littoralis*. Homologous 3-nitropropanoyl alanine and (3-nitropropanoyl) threonine were exclusively detected in *S. littoralis* and represent novel compounds. Although 3-NPA amino acid conjugates have previously been identified as putative detoxification products from *M. bivittatus,* no data concerning the toxicity of these compounds have been reported. We found that, in *S. littoralis* the injection of the amino acid amides of 3-NPA into the hemolymph was not toxic. However, the injection of the same amount of free 3-NPA caused mortality in 92% of the larvae, demonstrating that conjugation with amino acids represents an efficient way to cope with 3-NPA. Amino acid conjugation represents a common detoxification mechanism in insects and, as such, is similar to glycosylation or reaction with glutathione which force excretion.

Cytosolic proteins, isolated from the *S. littoralis* gut tissue, were shown to catalyze the formation of 3-NPA amino acid amides in the presence of ATP and CoA. Dedicated enzymes, catalyzing the conjugation of 3-NPA to amino acids from this or other organisms have not been described previously (Novoselov et al., 2015).

Consequently, we studied the biochemical capacity of the conjugation processes. We have tested the ability of the larvae to conjugate short, medium, and long chain fatty acids. In the first step the toxicity of short, medium, and long chain fatty acids in *S.littoralis* larvae were evaluated. Fatty acids with chain length from 5 to 14 carbon atoms was added to the artificial diet in concentration 34 μmol per g of diet. Pentanoic acid and isopentanoic acid were not toxic to the larvae. Middle chain fatty acids (chain length 6 - 11 carbon atoms) were high toxic to the larvae. Long chain fatty acids showed no toxicity (Unpublished materials part 1, fig. 9).

Furthermore, the frass of intoxicated larvae was studied with LC-MS. Conjugates of Glycine, Serine, Alanine, Threonine and Glutamine were detected (Unpublished materials part 1, fig.

10,11). Glycin and serine conjugates of fatty acid were detected over the whole range of studied compounds. Glutamine conjugates were found only in the frass of long chain fatty acid treated larvae (Unpublished materials part 1, fig. 12). Enzymes responsible for metabolism of carboxylic acid with chain length from 4-12 carbon atoms, have not been yet annotated in *Bombix Mori* genome according to Kyoto University Database. In contrast, three genes responsible for metabolism of long-chain fatty acids were annotated in *Bombix Mori* genome. The enzyme is located in the endoplasmic reticulum. But it is unlikely that the activated long chain fatty acids are a target for amino acid conjugation.

Some others have reported that the membrane-associated enzymes facilitate conjugation of long chain fatty acids to glutamine (Alborn et al., 1997; Lait et al., 2003; Yoshinaga et al., 2005). However, occasionally the insect gut microbial community exhibited conjugation activity, as in the case of *N*-linolenoyl glutamine biosynthesis by *Microbacterium arborescens* in *Spodoptera exigua* (Ping et al., 2007).

Our data indicate that, *S. littoralis* has an efficient way to metabolize a broad spectrum of chemical compounds via amino acid conjugation. The detoxification system involves a cytosolic enzyme, and has a rather distinct organization compared to other known amino acid conjugation systems.

Part 3 Effect of plant toxins on the gut microbiome and its functions.

Gut microbial community has several important functions like intestinal cell renewal, immune response modulation and nutrient supplementation of the host. Plant toxins could have an indirect effect on the larvae (Engel, Moran, 2013). The toxic compound could alter composition, molecular state and functions of gut microbiota. Application of toxins could lead to malfunction of essential amino acid production and vitamin biosynthesis.

We have studied an effect of amygdalin, coumarin, methoxypsoralen, 3-NPA and salicin on the gut microbiome composition. Amygdalin, coumarin, methoxypsoralen, 3-NPA and salicin were added as admixture to artificial diet in following concentrations 0.87; 6.84; 6.14; 4.2; 5,55 µmol/g, respectively.

3-NPA and Coumarin treatment had similar effects on the gut microbiome. In 4th and 6th instar treated larvae, only *Enterococaceae* survived. The relative abundance of *Enterococaceae* in the treated microbiome was 72% - 97%. *Enterobacteriaceae* were strongly inhibited by 3-NPA and coumarin treatment. In the treated microbiome, the relative abundance of *Enterobacteriaceae* decreased to 16%

Treatment with amygdalin and 8-MOP had an opposite effect on the composition of the gut microbiome, as compared to the coumarin and 3-NPA treatment. Amygdalin and 8-MOP treatment inhibited *Enterococcaceae* species. After 8-MOP and amygdalin treatment, the abundance of *Enterococcaceae* species decreased to 2 – 7% in 6th instar larvae. The abundance of Enterobacteriaceae increased up to 91%. No Clostridia or Erysipelotrichae could be detected after the plant toxins treatment. Clostridia and Erysipelotrichae were constantly present in the untreated microbiome (Unpublished materials part 1, fig. 5). Studied plant toxins had distinct effects on the gut microbiome, but the host had similar response to the treatment. On treatment with plant toxins, the host larvae slowed down their growth. The cause of this observed decrease in body weights could be the lack of essential amino acids or vitamins synthesized by the gut microbiota. But it was shown that, same biochemical functions can be shared between different bacteria. The biochemical functions of eliminated bacteria can be taken up by other members of

the microbial community. Function of amino acid production and vitamin biosynthesis could be taken up by the whole community and were not affected with the toxins. Genes corresponding to amino acid production and vitamin biosynthesis are present in the gut metagenome after the toxin treatment (supplementary materials, part 2, fig. 3).

The plant secondary metabolites 3-NPA, coumarin, amygdalin and 8-MOP could have a toxic effect on *S. littoralis,* and also the compounds have antimicrobial activity. In contrast to the studied compounds (3-NPA, coumarin, amygdalin and 8-MOP), only salicin had an antimicrobial activity. The effect of salicin on the gut composition was studied in detail.

Salicin significantly slowed down the growth of *S. littoralis* larvae. After feeding on the artificial diet containing 5,55 µmol/g salicin the 6th instar larvae were significantly smaller than control larvae (supplementary materials, part 2, fig. 4).

It has been shown that salicin suppressed the MAPKs pathways, but the effect of salicin on insects cell has not been described yet (Li Y et al., 2015). The gut microbiome of *S. littoralis* treated with salicin was significantly different from the untreated microbiome. In the untreated microbiome of 6th instar larvae, Bacilli, *Clostridia*, *Erysipelotrichia* and Alpha-, Beta-, and Gammaproteobacteria were present. After salicin treatment, bacteria of *Erysipelotrichia* class were completely eliminated from the gut (Unpublished materials part 2, fig. 3). A common product of *Erysipelotrichia* metabolism are short chain fatty acids (Kageyama A, Benno Y. 2000). It has been shown that, short chain fatty acids promote epithelial cell turnover and increase intestinal stem cell pool. In the same time malfunction of short chain fatty acid production leads to smaller body lengths and intestine sizes of the host (Shin et al., 2011). *Erysipelotrichia* in *S. littoralis* gut are mainly presented by uncultured *Clostridium sp*. The uncultured *Clostridium sp.* from *S. littoralis* gut were highly sensitive to the salicin treatment. There was no uncultured *Clostridium sp.* detected in the samples of the larvae rearing on the salicin containing diet (Unpublished materials part 2, fig. 4). Uncultured *Clostridium sp.* could have an effect on the gene expression of the host and indirectly stimulate nutrient uptake. Similar mode of action was described for *Clostridium ramosum*. The uncultured *Clostridium sp.* from *S. littoralis* is closely related to *Clostridium ramosum* and could stimulate fatty acid and sugar uptake (Woting et al., 2014). Alternative pathway of promoting of systemic growth is a proliferation of intestinal cells. Comparative analysis of predicted metagenome functions (PICRUSt) of the treated and untreated microbiome revealed several biochemical functions, which were not present in the salicin treated microbiome. Genomes of bacteria were closely related to the uncultured *Clostridium sp.* carrying an hyaluronoglucosaminidase gene. This function was completely missing in the salicin treated microbiome (supplementary materials, part 2, fig. 4). Hyaluronan contributes significantly to cell proliferation and migration. Oligosaccharides of hyaluronan promote the survival of basal stem cells (Termeer et al., 2002; Choi HR et al., 2012). In contrast to the uncultured *Clostridium sp*, the *Enterococcus mundtii* from *S. littoralis* gut microbiome was rather stably, closely associated with the host and transmitted through generation. Salicin did not affect the abundance of *Enterococcus* species in *S.littoralis*.

In this case, *Enterococcus* is suggested to share the biochemical functions, as amino acid production or vitamin biosynthesis of uncultured Clostridium sp. and other eliminated bacteria species.

Phylogenetic based prediction of metagenome functional content (PICRUSt) indicated that salicin treatment did not affect a large portion of biochemical functions. Only 33 of 6909

functions down regulated by salicin treatment. Genes responsible for amino acid and vitamin biosynthesis or carbohydrate metabolism were still presented in the treated microbiome (supplementary materials, part 2, fig. 4).

Our data indicated that the food derived factors like plant secondary metabolite could shape gut microbial community. Salicin treatment changed the ratio between main components of microbiome *Firmicutes*/*Proteobacteria* and increased the proportion of *Firmicutes*. *Enterococcus* species were closely associated with *S.littoralis* and were resistant to salicin treatment. Salicin specifically eliminated certain OTUs from gut microbiome. The uncultured *Clostridium sp* and the member of *Erysipelotrichia* class were highly sensitive to salicin treatment, and were completely removed from the *S.littoralis* gut. Thus, the gut microbiome significantly contributes to the growth rate of larvae.

10. Zusammenfassung

In den letzten zehn Jahren ist die Zahl der Publikationen innerhalb der Mikrobiomforschung enorm gestiegen. Im Jahr 2012 lag die Zahl der Publikationen bei 800, während im letzten Jahr die Zahl von 2000 überschritten wurde. Die Mikrobiomforschung hat einen signifikanten Einfluss auf verschiedene Gebiete der Lebenswissenschaften, Gesundheitsvorsorge, Agrikultur und der Lebensmittelindustrie (Arnold et al., 2016).

Mikrobiom-weite Assoziationsstudien (microbiome-wide association studies; MWAS) konnten Verbindungen zwischen dem Gesamtmikrobiom und einer Vielzahl an Erkrankungen wie Fettleibigkeit, Gefäßerkrankungen und Darmkrebs aufzeigen (Gilbert et al., 2016).

Mikroben besitzen zahlreiche biochemische Funktionen und tragen zu einigen Prozessen bei. Verschiedene Funktionen von Bakterien in den Verdauungstrakten von Insekten sind gut untersucht. Es wurde gezeigt, dass das Darm-Mikrobiom Resistenz gegen die Kolonisierung von Pathogenen oder Parasiten vermittelt, den Zelluloseabbau und die Nährstoffzufuhr erleichtert, durch Synthese von Vitaminen und essentiellen Aminosäuren, oder tragen zur Stickstofffixierung bei (Engel, Moran, 2013). Es wurde außerdem gezeigt, dass Darmbakterien Giftstoffe abbauen, die mit der Nahrung aufgenommen werden. Das Darmmikrobiom erfüllt in manchen Fällen spezifische Funktionen, wie die Produktion von Molekülen, die in intra- und interspezifische Kommunikation involviert sind, wie beispielsweise Pheromone und Kairomone. Es wurde gezeigt, dass die Gesamtdarmmikroben in grundlegende zelluläre Prozesse des Wirts involviert sind. Am wichtigsten unter diesen sind die Darmzellerneuerung, Stammzellenerneuerung und die Förderung des systemischen Wachstums. Die Störung der Zusammensetzung des Darmmikrobioms führt zum Ausfall vitaler Prozesse und ist dementsprechend schädlich für den Wirt. Insekten mit unterdrücktem Darmmikrobiom weisen abnorme Darmgrößen und unterdrückte Eibildung auf und Ihre Nachkommen sind verstärkt stressanfällig. Die Zusammensetzung des Darmmikrobioms hängt von einer Vielzahl an Umweltfaktoren ab, wie zum Beispiel pflanzliche Sekundärmetabolite aus der Nahrung (Elgart et al., 2016).

In dem hier beschriebenen Projekt wurde eine Methode zur Untersuchung der Effekte von pflanzlichen Sekundärmetaboliten auf das Darmmikrobiom in *Spodoptera littoralis* entwickelt. Der Modelorganismus ist einfach zu handhaben, die Konzentrationen und Mengen der verwendeten Toxine können klar definiert werden und der Effekt auf die Zusammensetzung des Darmmikrobioms konnte untersucht werden. Die Experimente konnten unter kontrollierten Laborbedingungen durchgeführt werden und erlaubten die Untersuchung eines breiten Spektrums von Parametern.

Das Darmmikrobiom mit seiner Myriade an Wechselwirkungen zwischen den Bakterien spielt eine essentielle Rolle in der Entwicklung und der Gesundheit des Wirts. Wir haben einen Versuch unternommen den Effekt von sekundären Pflanzenmetaboliten auf das Darmmikrobiom von *S. littoralis* zu evaluieren.

Teil 1. Der Effekt von Pflanzentoxinen auf die Wachstumsparameter von *S. littoralis* Larven

In der vorliegenden Arbeit wurden die Effekte von sekundären Pflanzenmetaboliten auf *S. littoralis* Larven evaluiert. Im ersten Schritt wurde der Effekt von pflanzlichen Sekundärmetaboliten auf die Wachstumsparameter von *S. littoralis* bestimmt. Körperlängen und –Massen wurden zeitabhängig gemessen. Sechs verschiedene pflanzliche Sekundärmetabolite, die zu unterschiedlichen Stoffklassen gehören, wurden ausgewählt. Die Verbindungen weisen verschiedene Wirkmechanismen auf und sind weit verbreitet innerhalb der Nahrungspflanzen von *S. littoralis*. Die Effekte von Coumarin, Methoxypsoralen, 3-NPA, Amygdalin, Crotalin und Salicin wurden untersucht.

Coumarin ist ein weit verbreiteter pflanzlicher Sekundärmetabolit aus der Klasse der Benzopyrone. Coumarine sind hochgiftig für generalistische herbivore Insekten. Im Verdauungstrakt sind sie giftig für eukaryotische Zellen. In eukaryotischen Zellen bindet Coumarin an nicht-proteinogene Sulfhydrylgruppen und verbraucht Glutathion. Sie verursachen Hepatotoxizität und oxidativen Stress und führen zur Apoptose (Andreza et al., 2004). Methoxypsoralen ist ein typisches Furanocoumarin. Methoxypsoralen beeinflusst unspezifisch verschiedene zelluläre Komponenten. Es bindet kovalent an DNA, Fettsäuren und Proteine (Studzian et al., 1999).

Wir haben den Einfluss von Nitroverbindungen auf *S. littoralis* Larven getestet. Wir haben aus dieser Verbindungsklasse 3-Nitropropionsäure ausgewählt. 3-NPA hat ein spezifisches Ziel, es inhibiert das Enzym Succinatdehydrogenase irreversibel (Olsen et al., 1999; Tarazona, Sanz, 1987; Hipkin et al., 2004).

Amygdalin ist das Mitglied aus der Verbindungsklasse der cyanogenen Glykoside. Amygdalin unterliegt bestimmten metabolischen Reaktionen und setzt schließlich Cyanwasserstoff frei. Das freigesetzte Cyanidanion inhibiert primär die Cytochrom C Oxidase. Die Inaktivierung von Cytochrom C Oxidase führt zur Inhibition der Atmungskette (Atta-Ur-Rahman, 2002).

Wir haben das typische Pyrrolizidinalkaloid Crotalin getestet. Im Darm wird Crotalin vom N-Oxid zur aktiven Form reduziert. Die aktive Form von Crotalin reagiert mit DNA und schädigt das Darmgewebe (Bernays, 2004).

Wir haben außerdem die Wirkung von phenolischen Glykosiden auf die Wachstumsrate von *S. littoralis* getestet. Für unsere Experimente haben wir Salicin ausgewählt. Verglichen mit den anderen untersuchten Pflanzentoxinen, die einen direkten giftigen Effekt auf die Insektenzellen aufweisen, ist zuvor keine direkte giftige Wirkung von Salicin auf Insektenzellen beschrieben worden. Es wurde gezeigt, dass D-(-)-Salicin die Aktivierung von Mitogen-Aktivierter Proteinkinase (MAPKs) und NF-κB Signalwege unterdrückt, und entzündungshemmende Aktivität besitzt (Li Y et al., 2015).

Um die Effekte von pflanzlichen Sekundärmetaboliten auf das Wachstum der Larven zu untersuchen wurde ein Fütterungsversuch durchgeführt. Die giftigen pflanzlichen Sekundärmetabolite wurde der artifiziellen Diät in natürlichen Konzentrationen zugesetzt. Amygdalin, Coumarin, Methoxypsoralen, Crotalin, 3-NPA, Salicin wurden in folgenden Konzentrationen zugesetzt: 0.87; 6.84; 0.46; 6.14; 4.2; 5,55 µmol/g d. Diät. *Spodoptera littoralis* Larven zeigten verlangsamtes Wachstum auf Diäten, welche die Toxine enthielten. Tote Larven wurden jedoch nicht beobachtet (Unpubliziertes Material Teil 1, Abb. 1 – 4).

Manche Insekten zeigen ähnliche Symptome bei Züchtung mithilfe einer unausgewogenen Diät. Manche Apidae, Tenebrionidae und Aphididae beenden Ihre Entwicklung unter Abwesenheit von Arginin, Histidin, Leucin, Isoleucin, Lysin, Methionin, Phenylalanin, Threonin, Tryptophan, oder Valin. Lepidoptera verlangsamen ebenfalls Ihr Wachstum bei Abwesenheit einer dieser essentiellen Aminosäuren. Insekten können keine Vitamine synthetisieren und benötigen Thiamin, Riboflavin, Nicotinsäure, Pyridoxin, Pantothensäure, Folsäure, und Biotin in kleinen Mengen für Ihr Wachstum (Dadd, 1985; Hanife, 2006).

Eine Verringerung von Körperlänge und –Gewicht könnte ebenso mit der direkten Wirkung von Pflanzentoxinen auf Epithelzellen des Wirts korrespondieren. Wir untersuchten die Empfindlichkeit der Larven gegenüber hohen Konzentrationen der Toxine. Wir haben die Larven mit künstlicher Diät gefüttert, welche die folgenden Konzentrationen an 3-NPA enthielt: 4.2; 8.4; 16.8; 33.6 µmol/g. Die Fütterung hoher 3-NPA-Konzentrationen führte nicht zu einer Erhöhung der Sterblichkeit im Vergleich zur Kontrolle. *Spodoptera littoralis* Lavren können 3-NPA Konzentrationen überleben, die 3-fach den LD50-Wert für ratten übersteigt (Novoselov et al., 2015). Die beobachtete Verringerung von Körperlängen und –Gewichten könnte mit dem direkten Effekt der Pflanzentoxine auf das Darmmikrobiom korrespondieren. Generelle Funktionen des Darmmikrobioms wie die Nährstoffversorgung könnten durch die Pflanzentoxine unterdrückt werden.

Im nächsten Schritt haben Wir den Beitrag des Darmmikrobioms auf die Nährstoffversorgung untersucht. Der Beitrag des Darmmikrobioms auf das Wachstum der Larven wurde durch Zugabe von Antibiotika zur künstlichen Diät abgeschätzt. Mischungen von Tetracyclin und Ampicillin unterdrückten signifikant das Darmmikrobiom. Larven, welche mit artifizieller Diät gefüttert wurden, die Tetracyclin und Ampicillin enthielt, wiesen verlangsamtes Wachstum auf (Unpubliziertes Material Teil 1, Abb. 7). Diese Daten zeigen, wie vermutet, dass das Darmmikrobiom zum systemischen Wachstum der Larven beitragen kann.

Das Darmmikrobiom könnte ebenso zur Entgiftung von 3-NPA beitragen. Um den Beitrag des Darmmikrobioms auf den 3-NPA Metabolismus zu untersuchen, fütterten wir gnotobiotische *S. littoralis* Larven mit 3-NPA. Die Fütterung gnotobiotischer *S. littoralis* Larven mit artifiziellem Medium, das mit 4.2 µmol 3-NPA /g Diät und mit Antibiotika gemischt wurde, führte nicht zu ihrem Tod, aber verringerte das Wachstum (Unpubliziertes Material Teil 1, Abb. 7). Diese Ergebnisse könnten darauf hindeuten, dass das Darmmikrobiom nicht an der Entgiftung von 3-NPA beteiligt ist, was die Entwicklung der Larven beeinflusst.

Teil 2 Entgiftungsprozesse in *S. littoralis* Larven.

Vergleichende Analyse der Exkremente von *S. littoralis* Larven, die mit oder ohne Zugabe von 3-NPA gefüttert wurden, zeigte die Anwesenheit neuer Verbindungen auf, welche von 3-NPA abgeleitet sind, was durch Fütterung von isotopenmarkierten Vorstufen gezeigt wurde. Die neuen Verbindungen wurden identifiziert als 3-NPA Glycin, -Serin, -Threonin und –Alanin. Die Molkeülstrukturen dieser 3-NPA Konjugate wurde mittels HR-MS/MS sowie durch Totalsynthese bestätigt. Andere Konjugate, zum Beispiel mit Glutathion, wurden nicht detektiert. 3-Nitropropanoylglycin und 3-Nitropropanoylserine wurden bereits zuvor als Metabolite in der

Graßhüpferspezies *Melanoplus bivittatus* beschrieben (Majak et al., 1998). Der Graßhüpfer produziert außerdem ein Glutaminderivat, welches in *S. littoralis* abwesend ist. Die homologen Verbindungen 3-Nitropropanoylalanin und (3-Nitropropanoyl-)Threonin wurden ausschließlich in S. littoralis gefunden und stellen neue Naturstoffe dar. Obwohl 3-NPA-Aminosäurekonjugate zuvor als putative Entgiftungsprodukte in *M. bivittatus* beschrieben wurden, wurden keine Daten zur Giftigkeit dieser Verbindungen erhoben. Wir haben gefunden, dass in *S. littoralis* die Injektion der Aminosäureamide von 3-NPA in die Hämolymphe nicht toxisch ist. Die Injektion derselben Menge freier 3-NPA führte zu einer Sterblichkeit der Larven von 92%, was aufzeigt, dass die Konjugation mit Aminosäuren einen effizienten Entgiftungsweg von 3-NPA darstellt. Aminosäurekonjugation ist ein allgemeiner Entgiftungsweg in Insekten, und ist als solcher ähnlich zur Glykosylierung oder der Reaktion mit Glutathion, welches die Exkretion forciert.

Cytosolische Proteine, welche die aus dem Darmgewebe von *S. littoralis* isoliert wurden, katalysieren die Darstellung von 3-NPA-Aminosäureamiden in der Anwesenheit von ATP und CoA. Dedizierte Enzyme, die die Konjugation von 3-NPA mit Aminosäuren in diesem oder anderen Organismen katalysieren, wurden zuvor nicht beschrieben (Novoselov et al., 2015).

Folglich haben wir die biochemische Kapazität der Konjugationsprozesse untersucht. Wir untersuchten die Fähigkeit der larven zur Konjugation von kurz-, mittel- und langkettigen Fettsäuren. Im ersten Schritt wurde die Toxizität von kurz-, mittel- und langkettigen Fettsäuren auf *S. littoralis* untersucht. Fettsäuren mit Kettenlängen von 5 bis 14 Kohlenstoffatomen wurden in Konzentrationen von 34 µmol pro Gramm der artifiziellen Diät zugesetzt. Pentansäure und Isopentansäure waren nicht giftig für die Larven. Mittelkettige Fettsäuren (Kettenlängen von 6 bis 11 Kohlenstoffatomen) waren hochgiftig für die Larven. Langkettige Fettsäuren zeigten keine Giftigkeit (Unpubliziertes Material Teil 1, Abb. 9).

Außerdem wurden die Exkremente vergifteter Larven mit LC-MS untersucht. Konjugate von Glycin, Serin, Alanin, Threonin und Glutamin wurden detektiert (Unpubliziertes Material Teil 1, Abb. 10,11). Glycin- und Serinkonjugate der Fettsäuren wurden über das gesamte Substratspektrum detektiert. Glutaminkonjugate wurden nur in den Exkrementen von Larven gefunden, die mit langkettigen Fettsäuren behandelt wurden (Unpubliziertes Material Teil 1, Abb. 12). Enzyme, die für den Metabolismus von Carbonsäuren mit Kettenlängen von 4 bis 12 Kohlenstoffatomen verantwortlich sind, wurden bisher noch nicht im Genom von *Bombyx Mori*, in Bezug auf die Kyoto Universitätsdatenbank, annotiert. Im Gegensatz dazu wurden drei Gene, die für den Metabolismus von langkettigen Fettsäuren verantwortlich sind, im Genom von *Bombyx Mori* annotiert. Das Enzym ist im endoplasmatischen Retikulum lokalisiert. Es ist jedoch unwahrscheinlich, dass die aktivierten langkettigen Fettsäuren Substrate für die Aminosäurekonjugation sind.

Andere haben berichtet, dass die membran-assoziierten Enzyme die Konjugation von langkettigen Fettsäuren mit Glutamin katalysieren (Alborn et al., 1997; Lait et al., 2003; Yoshinaga et al., 2005).

Mitunter vermittelte das Darmmikrobiom Konjugationsaktivität, wie im Fall der Biosynthese von *N*-linolenoylglutamin in *Microbacterium arborescens* aus *Spodoptera exigua* (Ping et al., 2007).

Unsere Daten zeigen, dass S. littoralis einen effizienten Weg besitzt, um ein breites Spektrum chemischer Verbindungen durch Aminosäurekonjugation zu metabolisieren. Das Entgiftungssystem beinhaltet ein zytosolisches Enzym, und besitzt eine eher distinkte Organisation im Vergleich zu anderen bekannten Aminosäurekonjugationssystemen.

Teil 3 Effekt von Pflanzentoxinen auf das Darmmikrobiom und seine Funktionen.

Das Darmmikrobiom hat mehrere wichtige Funktionen, wie die Darmzellerneuerung, Modulation der Immunantwort und Nährstoffversorgung des Wirts. Pflanzentoxine könnten einen indirekten Einfluss auf die Larven ausüben (Engel, Moran, 2013). Die toxische Verbindung könnte die Zusammensetzung, den molekularen Status und die Funktionen des Darmmikrobioms verändern. Die Zuführung von Toxinen könnte die Produktion essentieller Aminosäuren und die Vitaminbiosynthese stören.

Wir haben einen Effekt von Amygdalin, Coumarin, Methoxypsoralen, 3-NPA und Salicin auf die Zusammensetzung des Darmmikrobioms untersucht. Amygdalin, Coumarin, Methoxypsoralen, 3-NPA und Salicin wurden der artifiziellen Diät in folgenden Konzentrationen zugesetzt: 0.87; 6.84; 6.14; 4.2; 5,55 µmol/g.

Die Zugabe von 3-NPA und Coumarin hatte ähnliche Wirkung auf das Darmmikrobiom. In entsprechend behandelten Larven des Stadiums vier und sechs überlebten lediglich *Enterococaceae*. Die relative Häufigkeit von *Enterococaceae* im behandelten Mikrobiom betrug zwischen 72 und 97%. *Enterobacteriaceae* wurden stark durch 3-NPA- und Coumarinbehandlung inhibiert. Im behandelten Mikrobiom wurde die relative Häufigkeit von *Enterobacteriaceae* auf 16% reduziert.

Die Behandlung mit Amygdalin und 8-MOP hatte einen gegenteiligen Effekt auf die Mikrobiomzusammensetzung, im Vergleich zur Coumarin- und 3-NPA-Behandlung. Amygdalin- und 8-MOP-Behandlung inhibierte *Enterococaceae* Spezies. Nach der Behandlung mit 8-MOP and Amygdalin wurde die Häufigkeit von *Enterococaceae* Spezies des larvalen Stadiums sechs auf 2 bis 7% verringert. Die Häufigkeit von *Enterobacteriaceae* erhöhte sich auf bis zu 91%. Keine Clostridien oder Erysipelotrichae konnten nach Behandlung mit Pflanzentoxinen detektiert werden. Clostridien und Erysipelotrichae waren stets im unbehandelten Mikrobiom vorhanden (Unpubliziertes Material Teil 1, Abb. 5). Die untersuchten Pflanzentoxine zeigten distinkte Effekte auf das Darmmikrobiom, aber der Wirt zeigte ähnliche Reaktionen auf die Behandlung. Nach Behandlung mit Pflanzentoxinen zeigten Larven des Wirts verringertes Wachstum. Die Ursache dieser verringerten Körpermassen könnte im Mangel an essentiellen Aminosäuren und Vitaminen, welche durch das Darmmikrobiom synthetisiert werden, begründet sein. Es wurde jedoch gezeigt, dass dieselben biochemischen Funktionen von mehreren verschiedenen Bakterien übernommen werden können. Die biochemischen Funktionen eliminierter Bakterien können durch andere Mitglieder des Mikrobioms übernommen werden. Die Funktion der Aminosäure- und Vitaminbiosynthese könnte durch die gesamte bakterielle Gemeinschaft übernommen werden und wäre dadurch nicht von den Toxinen beeinflusst. Gene, welche mit der Aminosäureproduktion und Vitaminbiosynthese korrespondieren sind nach der Behandlung mit Toxinen im Darmmetagenom vorhanden (Zusatzmaterial, Teil 2, Abb. 3). Die pflanzlichen Sekundärmetabolite 3-NPA, Coumarin, Amygdalin und 8-MOP könnten einen toxischen Effekt auf *S. littoralis* haben und die Verbindungen zeigen außerdem antimikrobielle Aktivität. Im Gegensatz zu den untersuchten Verbindungen (3-NPA, Coumarin, Amygdalin und 8-MOP) hatte nur Salicin antimikrobielle Aktivität. Der Einfluss von Salicin auf die Darmzusammensetzung wurde im Detail untersucht. Salicin verlangsamte signifikant das Wachstum von *S. littoralis* Larven. Nach Fütterung mit artifizieller Diät, welche 5,55 µmol/g

Salicin enthielt, waren Larven des Larvenstadiums sechs significant kleiner als Kontrolllarven (Zusatzmaterial, Teil 2, Abb. 4).

Es wurde gezeigt, dass Salicin die MAPKs Wege unterdrückt, jedoch wurde der Effekt von Salicin auf Insektenzellen noch nicht beschrieben (Li Y et al., 2015). Das Darmmikrobiom von *S. littoralis*, welches mit Salicin behandelt wurde, war signifikant von dem unbehandelten Mikrobiom verschieden. Im unbehandelten Mikrobiom des Larvenstadiums sechs waren Bacilli, *Clostridia*, *Erysipelotrichia* und Alpha-, Beta-, und Gammaproteobacteria vorhanden. Nach Salicinbehandlung wurden Bakterien der *Erysipelotrichia*-Klasse komplett aus dem Darm entfernt (Unpubliziertes Material Teil 2, Abb. 3). Ein häufiges Produkt des *Erysipelotrichia* Metabolismus sind kurzkettige Fettsäuren (Kageyama A, Benno Y. 2000). Es wurde gezeigt, dass kurzkettige Fettsäuren die Teilungsrate der Epithelzellen und den intestinalen Stammzellpool erhöhen. Gleichzeitig führt eine Störung des Metabolismus kurzkettiger Fettsäuren zu verringerten Körperlängen und Darmgrößen des Wirts (Shin et al., 2011). *Erysipelotrichia* sind im Darm von *S. littoralis* hauptsächlich durch unkultivierbare Clostridiumspezies repräsentiert. Die unkultivierten Clostridiumspezies aus dem Darm von *S. littoralis* waren höchstempfindlich gegenüber einer Salicinbehandlung. Es wurde keine unkultivierte Clostridiumspezies in Proben von larven auf Salicindiät detektiert (Unpubliziertes Material Teil 2, Abb. 4). Unkultivierte Clostridiumspezies könnten einen Effekt auf die Genexpression des Wirts haben und damit indirekt die Nährstoffaufnahme beeinflussen. Eine ähnliche Funktion wurde im Fall von *Clostridium ramosum* beschrieben. Die unkultivierte Clostridiumspezies ist eng verwandt mit *Clostridium ramosum* und könnte die Fettsäure- und Zuckeraufnahme beeinflussen (Woting et al., 2014). Ein alternativer Weg das systemische Wachstum zu fördern ist die Vermehrung von intestinalen Zellen. Vergleichende Analyse von vorhergesagten Metagenomfunktionen (PICRUSt) des behandelten und unbehandelten Mikrobioms offenbarte mehrere biochemische Funktionen, die nicht im salicinbehandelten Mikrobiom vorhanden waren. Die Genome der Bakterien waren eng verwandt mit der unkultivierten Clostridiumspezies und trugen ein Hyaluronoglucosaminidasegen. Diese Funktion war gänzlich absent in dem salicinbehandelten Mikrobiom (Zusatzmaterial, Teil 2, Abb. 4). Hyaluronan trägt signifikant zum Zellwachstum und zur Zellmigration bei. Oligosaccharide von Hyaluronan fördern das Überleben von basalen Stammzellen (Termeer et al., 2002; Choi HR et al., 2012). Im Gegensatz zu der unkultivierten Clostridiumspezies war *Enterococcus mundtii* aus dem Darmmikrobiom von *S. littoralis* eher stabil, eng assoziiert mit dem Wirt und von Generation zu Generation übertragbar. Salicin hatte keinen Einfluss auf die Häufigkeit von *Enterococcus mundtii* Spezies in *S. littoralis*.

In diesem Fall wird angenommen, dass *Enterococcus* die biochemischen Funktionen, wie Aminosäureproduktion oder Vitaminbiosynthese, mit der unkultivierten Clostridiumspezies und anderen eliminierten Bakterienspezies teilt. Phylogeniebasierte Vorhersage des funktionalen Metagenoms (PICRUSt) zeigte an, dass Salicinbehandlung keine großen Anteile an biochemischen Funktionen beeinflusst. Lediglich 33 von 6909 Funktionen wurden durch Salicinbehandlung herunterreguliert. Gene, die Für die Aminosäure- und Vitaminbiosynthese oder den Zuckermetabolismus verantwortlich sind, waren weiterhin im behandelten Mikrobiom vorhanden (Zusatzmaterial, Teil 2, Abb. 4).Unsere daten zeigen, dass nahrungsabhängige Faktoren, wie pflanzliche Sekundärmetabolite, das Darmmikrobiom beeinflussen können. Die Salicinbehandlung veränderte das Verhältnis zwischen Hauptkomponenten des Darmmikrobioms *Firmicutes*/*Proteobacteria* und erhöhte den Anteil an *Firmicutes*. *Enterococcus* Spezies waren

eng verbunden mit *S. littoralis* und resistent gegenüber Salicinbehandlung. Salicin eliminiert spezifisch bestimmte OTUs aus dem Darmmikrobiom. Die unkultivierte Clostridiumspezies und das Mitglied der *Erysipelotrichia*-Klasse waren hochsensitiv gegenüber der Salicinbehandlung und wurden komplett aus dem Darm von *S. littoralis* entfernt. Folglich trägt das Darmmikrobiom signifikant zur Wachstumsrate der Larven bei.

11. References

1. Akopian, G., Crawford, C., Petzinger, G., Jakowec, M.W., Walsh, J.P., 2012. Brief mitochondrial inhibition causes lasting changes in motor behavior and corticostriatal synaptic physiology in the Fischer 344 rat. Neuroscience 215, 149–159.

2. Alborn, H.T., Turlings, T.C. J., Jones, T.H., Stenhagen, G., Loughrin, J.H., Tumlinson, J.H., 1997. An elicitor of plant volatiles from beet armyworm oral secretion. Science 276, 945-949.

3. Appel, H.M., Michael, M.M., 1990. Gut redox conditions in herbivorous lepidopteran larvae. J. Chem. Ecol. 16, 3277-3290.

4. Arnold, J.W., Roach, M.J., Azcarate-Peril, A., 2016. Emerging Technologies for Gut Microbiome Research. Trends in Microbiology. Volume 24, Issue 11, p887–901

5. Atta-Ur-Rahman, 2002. Studies in Natural Products Chemistry. Bioactive Natural Products (Part G). Volume 26. Amsterdam: 698.

6. Beck, E., Müller-Hohenstein, K., Schulze, E. D., 2005. Plant Ecology. Heidelberg: 235-237.

7. Berenbaum, M., 1980. Adaptive significance of midgut pH in larval Lepidoptera. Am Nat 115*:* 138–146.

8. Bernays, E.A., Hartmann, T., Chapman, R.F., 2004. Gustatory responsiveness to pyrrolizidine alkaloids in the Senecio specialist, Tyria jacobaeae (Lepidoptera, Arctiidae). Physiological Entomology. Volume 29: 67–72.

9. Bertino-Grimaldi, D., Medeiros M.N., Vieira, R.P., Cardoso, A.M., Turque, A.S., Silveira, C.B., Albano, R.M., Bressan-Nascimento S., Garcia, E.S., de'Souza W., Martins, O.B., Machado E.A., 2013. Bacterial community composition shifts in the gut of *Periplaneta americana* fed on different lignocellulosic materials. Springerplus. 2: 609.

10. Bertolucci, S.K., Pereira, A.B., Pinto, J.E., Oliveira, A.B., Braga, F.C., 2013. Seasonal variation on the contents of coumarin and kaurane-type diterpenes in Mikania laevigata and M. glomerata leaves under different shade levels. Chem Biodivers. 10(2),288-95.

11. Blahová, J., Svobodová, Z., 2012. Assessment of Coumarin Levels in Ground Cinnamon Available in the Czech Retail Market. ScientificWorldJournal.263851.

12. Boeckler, G. A., Gershenzon, J., Unsicker, B. S., 2011 Phenolic glycosides of the Salicaceae and their role as anti-herbivore defenses. Phytochemistry. Volume 72, Issue 13, 1497–1509.

13. Bosheng, C., The, B. S., Sun, C., Hu, S., Lu, X., Boland, W., Shao, Y., 2016. Biodiversity and Activity of the Gut Microbiota across the Life History of the Insect Herbivore *Spodoptera littoralis*. Scientific Reports. 6.

14. Broderick, N.A., Raffa, K.F., Goodman, R.M., Handelsman J., 2004. Census of the bacterial community of the gypsy moth larval midgut by using culturing and culture-independent methods. Appl Environ Microbiol 70: 293–300.

15. Bryson, P.D., 1996. Comprehensive Reviews in Toxicology for Emergency Clinicians. 3rd edition. Washington: 354-357.

16. Burdock, G.A., Carbin, I.G., Soni, M.G., 2001. Safety assessment of β-nitropropionic acid: a monograph in support of an acceptable daily intake in humans. Food Chemistry. Volume 75(1): 1-27.

17. Choi H.R., Kang Y.A., Na J., Huh S.Y., Huh C.H., Kim K. H., Park K.C., 2012. Oligosaccharides of hyaluronic acid increased epidermal cell stemness by modulation of integrin expression. J Cosmet Dermatol. 11(4):290-6.

18. Cipollini, D., Stevenson, R., Enright, S., Eyles, A., Bonello, P., 2008. Phenolic metabolites in leaves of the invasive shrub, *Lonicera maackii*, and their potential phytotoxic and anti-herbivore effects. J. Chem. Ecol. 34, 144–152.

19. Cohen, M. B., Schuler, M. A., Berenbaum, M. R., 1992. A host-inducible cytochrome P-450 from a host-specific caterpillar: Molecular cloning and evolution. Biochemistry Vol. 89, pp. 10920-10924.

20. Colegate, S.M., Coulombe, R.A., Edgar, J.A., Gardner, D.R., Molyneux, R.J., Schoch, T.K., Stegelmeier, B.L., 1999. Pyrrolizidine alkaloid plants, metabolism and toxicity. Journal of Natural Toxins. Volume 8. Number 1. USA: 95-99

21. Conterno, L., Fava, F., Viola, R., Tuohy, K.M., 2011. Obesity and the gut microbiota: does up-regulating colonic fermentation protect against obesity and metabolic disease? *Genes Nutr.* **6**, 241–260.

22. Cristofoletti, P.T., Ribeiro, A.F., Terra, W.R., 2001. Apocrine secretion of amylase and exocytosis of trypsin along the midgut of *Tenebrio molitor* larvae. J. Insect Physiol. 47, 143–155.

23. Dadd R.H., 1985. Nutrition: organisms. In: Kerkut GA, Gilbert LI (eds) Comparative insect physiology, biochemistry and pharmacology, vol 4. Pergamon Press, New York, pp 313–390.

24. Davis, E.E., Heisler, H. Larson, M., Venette, R.C., Zaspel, J., 2003. Mini Risk Assessment. Egyptian cotton leafworm, *Spodoptera littoralis* Boisduval. Department of Entomology. University of Minnesota: 1-4.

25. de Souzaa, S. M., Monacheb, F. D., Jr, A. S., 2005. Antibacterial Activity of Coumarins Z. Naturforsch. 60c, 693 D 700.

26. Diawara M.M., Trumble J.T., White K.K., Carson W.G., Martinez L.A. 1993. Toxicity of linear furanocoumarins to *Spodoptera exigua:* evidence for antagonistic interactions. Journal of Chemical Ecology, Vol. 19, No. 11.

27. Dillon, R.J., Dillon, V.M., 2004. The gut bacteria of insects: Nonpathogenic Interactions. Annu. Rev. Entomol.. 49:71–92

28. Dolan, L.C., Matulka, R.A., Burdock G.A.., 2010. Naturally Occurring Food Toxins. Toxins (Basel). 2(9): 2289–2332.

29. Dugrand-Judek, A., Olry, A., Hehn, A., Costantino, G., Ollitrault, P., Froelicher, Y., Bourgaud, F., 2015. The Distribution of Coumarins and Furanocoumarins in Citrus Species Closely Matches Citrus Phylogeny and Reflects the Organization of Biosynthetic Pathways. PLoS One. 10(11): e0142757.

30. Eichler S, Schaub G.A., 2002. Development of symbionts in triatomine bugs and the effects of infections with trypanosomatids. Exp Parasitol 100: 17–27.

31. El Aidy S, Dinan TG, Cryan JF (2015) Gut microbiota: the conductor in the orchestra of immune-neuroendocrine communication. Clin Ther 37: 954-967

32. Elgart M., Stern, S., Salton, O., Gnainsky, Y., Heifetz, Y., Soen, Y., 2016. Impact of gut microbiota on the fly's germ line. Nature Communications 7, Article number: 11280.

33. Engel P., Moran N.A., 2013.The gut microbiota of insects - diversity in structure and function. FEMS Microbiol Rev. 37(5): 699-735.

34. Firstenberg, D.E., Silhacek, D.L., 1973. Juvenile hormone regulation of oxidative metabolism in isolated insect mitochondria. Experientia. 29, 1420-1422.

35. Francis, K., Smitherman, C., Nishino, S.F., Spain, J.C., Gadda, G., 2013. The biochemistry of the metabolic poison propionate 3-nitronate and its conjugate acid, 3-nitropropionate. Int. Union Biochem. Mol. Biol. Life. 65, 759–768.

36. Frasera C. M., Clint C., 2011. The Phenylpropanoid Pathway in Arabidopsis Arabidopsis Book. 9, e0152.

37. Futuyma D.J., Agrawal A.A., 2009. Macroevolution and the biological diversity of plants and herbivores. Proc Natl Acad Sci U S A. Oct 27;106 (43):18054-61.

38. Gilbert, J.A., Quinn, R.A., Debelius, J., Xu, Z.Z., Morton, J., Garg, N., Jansson, J.K., Dorrestein, P.C, Knight, R., 2016. Microbiome-wide association studies link dynamic microbial consortia to disease. Nature 535, 94–103.

39. Giordana, B., Sacchi, V.F., Parenti, P., Hanozet, G.M., 1989. Amino acid transport systems in intestinal brush-border membranes from lepidopteran larvae. Amer. J. Physiol. 257, 494-500

40. Gomes, F. M., Carvalho D. B., Machado E. A., Miranda K., 2013. Ultrastructural and functional analysis of secretory goblet cells in the midgut of the lepidopteran *Anticarsia gemmatalis* Cell and Tissue Research Springer-Verlag Berlin Heidelberg 10.1007/s00441-013-1563-4).

41. Hammer, T. J., McMillan, W. O., Fierer, N., 2014. Metamorphosis of a Butterfly-Associated Bacterial Community. PLoS ONE 9(1): e86995. doi:10.1371/journal.pone.0086995

42. Hanife G. 2006. General principles of insect nutritional ecology. Trakya Univ J Sci, 7(1): 53-57.

43. Harrison, J.F., 2001. Insect acid/base homeostasis. Annu. Rev. Entomol. 46,221 -250

44. Hehmann, M., Lukacin, R., Ekiert, H., Matern, U., 2004. Furanocoumarin biosynthesis in Ammi majus L. Cloning of bergaptol O-methyltransferase. Eur J Biochem. 271(5):932-40.

45. Hipkin, C.R., Simpson, D.J., Wainwright, S.J., Salem, M.A., 2004. Nitrification by plants that also fix nitrogen. Nature. 430, 98–101.

46. Hongoh, Y., Sharma, V.K, Prakash T, Noda S, Toh H, Taylor T.D, Kudo, T., Sakaki, Y., Toyoda. A., Hattori, M., Ohkuma, M., 2008. Genome of an endosymbiont coupling N2 fixation to cellulolysis within protist cells in termite gut. Science 322: 1108–1109.

47. Huttenhower, C., The Human Microbiome Project Consortium., 2012. Structure, function and diversity of the healthy human microbiome. Nature. 486, 207–214.

48. Iriti, M., Faoro F., 2009. Chemical Diversity and Defence Metabolism: How Plants Cope with Pathogens and Ozone Pollution. Int J Mol Sci. 10(8): 3371–3399.

49. Ji-Hyun, Y., Roh, S. W., Whon, T. W., Jung, M. J., Kim, M. S., Park, D. S., Yoon, C., Nam, Y. D., Kim, Y.J., Choi, J. H., Kim, J. Y., Shin, N. R., Kim, S. H., Lee, W. J., Bae, J. W., 2014.Insect Gut Bacterial Diversity Determined by Environmental Habitat, Diet, Developmental Stage, and Phylogeny of Host. *Appl. Environ. Microbiol.* vol. 80 no. 17 5254-5264.

50. Jones, R.T, Sanchez, L.G, Fierer, N., 2013. A Cross-Taxon Analysis of Insect-Associated Bacterial Diversity. PLoS ONE 8(4): e61218. doi:10.1371/journal.pone.0061218.

51. Kageyama, A., Benno, Y., 2000.Catenibacterium mitsuokai gen. nov., sp. nov., a gram-positive anaerobic bacterium isolated from human faeces. Int J Syst Evol Microbiol. ; 50 Pt 4:1595-9.

52. Kinghts, M.K., Miners, J.O., 2012. Amino acid conjugation: a novel route of xenobiotic carboxylic acid metabolism in man. Encyclopedia of drug metabolism and interactions. Vol 6. 595-610.

53. Köhler, T., 2011. Physicochemical gradients and deep sequencing of the bacterial microbiota indicate functional compartmentation in the gut of the higher termite Nasutitermes corniger. Diversity and evolutionary patterns in the bacterial gut microbiota of termites and cockroaches. PhD Thesis, Philipps-Universität Marburg, Marburg, Germany, pp. 11–42.

54. Lait, C.G., Alborn, H.T., Teal, E.A., Tumlinson J. H., 2003. Rapid biosynthesis of *N*-linolenoyl-L-glutamine, an elicitor of plant volatiles, by membrane-associated enzyme(s) in *Manduca sexta*. Proc. Natl. Acad. Sci, USA 100, 7027–7032.

55. Lak, B., Gray, T. j. B., Evans, j. g., Lewis, D. V., Beamand, J. A., Hue K. L., 1989. Studies on the Mechanism of Coumarin-induced Toxicity in Rat Hepatocytes: Comparison with Dihydrocoumarin and Other Coumarin Metabolites'. Toxicology and applied pharmacology. 97.3 1 l-323.

56. Lamp, J., Keyser, B., Koeller, D.M., Kurt, U., Braulke, T.,. Mühlhausen, C., 2011. Glutaric aciduria type 1 metabolites impair the succinate transport from astrocytic to neuronal cells. *J. Biol. Chem.* 286, 17777-17784

57. Lee M.S., Donaldson, G.P., Zbigniew, M., Boyajian, S., Ley, K., Mazmanian, S. K., 2013. Bacterial colonization factors control specificity and stability of the gut microbiota. Nature 501, 426–429.

58. Ley, E.R., Lozupone, A.C., Hamady, M., Knight, R., Gordon, I.J., 2008. Worlds within worlds: evolution of the vertebrate gut microbiota. Nature Reviews Microbiology. 6, 776-788.

59. Li, Y., Wu, Q., Deng, Y., Lv, H., Qiu, J.C., Feng. H., 2015. D(-)-Salicin inhibits the LPS-induced inflammation in RAW264.7 cells and mouse models. Int Immunopharmacol. ;26(2):286-94.

60. Lyte M (2015) Microbial endocrinology in the pathogenesis of infectious disease. Microbiol Spectrum 4(2): VMBF-0021-2015. doi: 10.1128/microbiolspec.VMBF-0021-2015

61. Lyte M (2016) Microbial endocrinology: an ongoing personal journey. In: Lyte M (ed) Microbial Endocrinology: Interkingdom Signaling in Infectious Disease and Health. Springer, New York, pp.1-24. doi: 10.1007/978-3-319-20215-0_1

62. Majak, W., Johnson, D.l., Benn, M.H., 1998. Detoxification of 3-nitropropionic acid and karakin by Melanopline grasshoppers. *Phytochemistry*. 49, 419-422

63. Manimozhiyan, A., Raes, J., Pelletier, E., Paslier, D.L., Yamada, T., Mende, D.R., Fernandes, G.R., Tap, J., Bruls, T., Batto, J.M., Bertalan, M., Borruel, N., Casellas, F., Fernandez, L., Gautier, L., Hansen, T., Hattori, M., Hayashi, T., Kleerebezem, M., Kurokawa, K., Leclerc, M., Levenez, F., Manichanh, C., Nielsen, H.B, Nielsen, T., Pons, N., Poulain, J., Qin, J., Sicheritz-Ponten, T., Tims, S., Torrents, D., Ugarte, E., Zoetendal,

E.G., Wang, J., Guarner, F., Pedersen, O., de Vos, W.M., Brunak, S., Doré, J., Weissenbach, J., Ehrlich, S.D., Bork, P.S., 2011. Enterotypes of the human gut microbiome. Nature 473, 174–180.

64. Mason K.L, Stepien TA, Blum JE, Holt JF, Labbe NH, et al. 2011. From commensal to pathogen: translocation of *Enterococcus faecalis* from the midgut to the hemocoel of *Manduca sexta.* mBio 2(3):e00065-11. doi:10.1128/mBio.00065-11.

65. Matern, U., 1991. Coumarins and other phenylpropanoid compounds in the defense response of plant cells. Planta Med. 57, 15-20.

66. Meldrum, B.S., 2000. Glutamate as a Neurotransmitter in the Brain: Review of Physiology and Pathology. J. Nutr. 130, 1007-1015.

67. Mithöfer, A., Boland, W., 2012. Plant defense against herbivores: chemical aspects. Annu. Rev. Plant Biol. 63, 431-450.

68. Morrow J.L., Frommer M., Shearman D.C.A., Riegler. M., 2015.The Microbiome of Field-Caught and Laboratory-Adapted Australian Tephritid Fruit Fly Species with Different Host Plant Use and Specialisation. Microbial Ecology. Volume 70, Issue 2, pp 498–508.

69. Murphy, K., Teakle, D., Macrae, I., 1994. Kinetics of colonization of adult queensland fruit flies(bactrocera tryoni) by dinitrogen-fixing alimentary tract bacteria applied and environmental microbiology., vol. 60, no. 7p. 2508-2517

70. Nikoh, N., Hosokawa, T., Oshima, K., Hattori, M., Fukatsu, T., 2011. Reductive evolution of bacterial genome in insect gut environment. Genome Biol Evol 3: 702–714.

71. Nishino S.F., Shin K.A., Payne, R.B., Spain, J.C., 2010. Growth of Bacteria on 3-Nitropropionic Acid as a Sole Source of Carbon, Nitrogen, and Energy. Applied and environmental microbiology. Vol. 76, No. 11p. 3590–3598

72. Novoselov, A., Becker, T., Pauls, G., von Reuß, S. H., Boland, W., 2015. *Spodoptera littoralis* detoxifies neurotoxic 3-nitropropanoic acid by conjugation with amino acids. Insect Biochemistry and Molecular Biology, 63, 97-103. doi:10.1016/j.ibmb.2015.05.013.

73. Oleskin AV, El'-Registan GI, Shenderov BA (2016) Role of neuromediators in the functioning of the human microbiota: "business talks" among microorganisms and the microbiota-host dialogue. Microbiology+ 85(1): 1-22

74. Oleskin AV, Shenderov BA, Rogovsky VS (2017) Role of neurochemicals in the interaction between the microbiota and the immune and the nervous system of the host organism. Probiotics Antimicrob Proteins. doi: 10.1007/s12602-017-9262-1

75. Olsen, C., Rustad, A., Fonnum, F., Paulsen, R.E., Hassel, B., 1999. 3-Nitropropionic acid: an astrocyte-sparing neurotoxin in vitro. Brain Res. 850, 144–149.

76. Ortego F., 2012. Physiological adaptations of the insect gut to herbivory, in Arthropod-Plant Interactions, Novel Insights and Approaches for IPM, Progress in Biological Control, Vol. 14, eds Smagghe G., Diaz I., editors. (Dordrecht: Springer-Verlag;), 75–88.

77. Osier, T.L., Hwang, S.Y., Lindroth, R.L., 2000. Effects of phytochemical variation in quaking aspen *Populus tremuloides* clones on gypsy moth Lymantria dispar perfomence in the field and laboratory. Ecol. Entomol. 25, 197-207.

78. Ott, S.J., Musfeldt, M., Ullmann, U., Hampe, J., Schreiber S.J., 2004. Quantification of Intestinal Bacterial Populations by Real-Time PCR with a Universal Primer Set and Minor Groove Binder Probes: a Global Approach to the Enteric Flora. Clin Microbiol. June; 42(6): 2566–2572

79. Parry, R., Nishino, S., Spain, J., 2011. Naturally-occurring nitro compounds. Nat. Prod. Rep. 28, 152–167.

80. Ping, L., Büchler, R., Mithöfer, A., Svatoš, A., Spiteller, D., Dettner, K., Gmeiner, S., Piel, J., Schlott, B., Boland, W., 2007. A novel Dps-type protein from insect gut bacteria catalyses hydrolysis and synthesis of *N*-acyl amino acids. Environm. Microbiol. 9, 1572–1583.

81. Priya, N.G., Ojha, A., Kajla, M.K, Raj, A., Rajagopal, R., 2012. Host plant induced variation in gut bacteria of *Helicoverpa armigera*. PLoS ONE 7: e30768.

82. Qin, J., Li R., Raes, J., Arumugam, M., Solvsten, K. B., Manichanh, C., Nielsen, T., Pon,s N., Levenez, F., Yamada, T.M., Daniel, R., Li, J., Xu, J., Li, S., Li D., Cao J., Wang, B., Liang, H., Zheng, H., Xie, Y., Tap, J., Lepage, P., Bertalan, M., Batto, J.M., Hansen, T., Paslier, D.L., Linneberg, A., Nielsen, H.B., Pelletier, E., Renault, P., Sicheritz-Ponten, T., Turner, K., Zhu, H., Yu, C., Li, S., Jian, M., Zhou, Y., Li, Y., Zhang, X., Li, S., Qin, N., Yang, H., Wang, J., Brunak, S., Doré, J., Guarner, F., Kristiansen, K., Pedersen, O., Parkhill, J., Weissenbach, J., 2010. A human gut microbial gene catalogue established by metagenomic sequencing. *Nature* 464, 59-65.

83. Ratzka, A., Vogel, H., Kliebenstein, D.J., Mitchell-Olds, T., Kroymann, J., 2002. Disarming the mustard oil bomb. Proc. Natl. Acad. Sci. USA. 99, 11223–11228.

84. Ridley, E.V., Wong. A. C.N., Westmiller, S., Douglas, A.E., 2012 Impact of the resident microbiota on the nutritional phenotype of Drosophila melanogaster. PLoS ONE 7: e36765

85. Robinson, C.J., Schloss, P., Ramos, Y., Raffa, K., Handelsman, J., 2010. Robustness of the bacterial community in the cabbage white butterfly larval midgut. Microb Ecol 59: 199–211.

86. Rösemann, M., 2006. Analysis of pyrrolizidine alkaloids in Crotalaria species by HPLC-MS/MS in order to evaluate related food health risks. Thesis for the degree of Philosophiae Doctor. University of Pretoria: 1-4.

87. Ruan J.W., Statt S., Huang C.T., Tsai Y.T., Kuo C.C., Chan H.L., Liao Y.C., Tan T.H., Kao C.Y., 2016. Dual-specificity phosphatase 6 deficiency regulates gut microbiome and transcriptome response against diet-induced obesity in mice. *Nature Microbiology*. 2.

88. Ruokolainen, L., Ikonen, S., Makkonen H., Hanski, I., 2016. Larval growth rate is associated with the composition of the gut microbiota in the Glanville fritillary butterfly. Oecologia, Volume 181, Issue 3, pp 895–903.

89. Scatigno A. C., Garrido S. S., Marchetto R., 2004. A 4.2 kDa Synthetic Peptide as a Potential Probe to Evaluate the Antibacterial Activity of Coumarin Drugs *J. Peptide Sci.* 10: 566–577.

90. Schramm, K., Vassão, D.G., Reichelt, M., Gershenzon, J., Wittstock, U., 2012. Metabolism of glucosinolate-derived isothiocyanates to glutathione conjugates in generalist lepidopteran herbivores. Insect Biochem. Mol. Biol.42, 174-182

91. Shin, S.C., Kim S.H., You, H., Kim, B., Kim, A.C., Lee, K.A., Yoon, J.H., Ryu, J.H., Lee, W.J., 2011. Drosophila microbiome modulates host developmental and metabolic homeostasis via insulin signaling. Science 334: 670–674.

92. Snoep, J.L., de Graef M.R ., Joost. M., de Mattos T., Neijssel, O.M., 1992. Pyruvate catabolism during transient state conditions in chemostat cultures of *Erzterococcus faecalis* NCTC 775: importance of internal pyruvate concentrations and NADH/NAD + ratios. Journal of General Microbiology. 138, 201 5-2020.

93. Stauber, E.J., Kuczka, P., van Ohlen M., Vogt, B., Janowitz, T, Piotrowski, M., Beuerle, T., Wittstock, U., 2012. Turning the 'Mustard Oil Bomb' into a 'Cyanide Bomb': aromatic glucosinolate metabolism in a specialist insect herbivore. PLoS ONE 7, e35545.

94. Staudacher, H., Kaltenpoth, M., Breeuwer J.A., Steph B.J., Menken J., Heckel, D.G., Groot, A.T., 2016. Variability of Bacterial Communities in the Moth *Heliothis virescens* Indicates Transient Association with the Host. PLoS One.; 11(5): e0154514.

95. Studzian, K., Tołwińska-Stańczyk, Z., Wilmańska, D., Palumbo, M., Gniazdowski, M., 1999. Crosslinking of cellular DNA by nitracrine and furocoumarin derivatives. Neoplasma. 46(1):50-3.

96. Suvendu, D., Jiin-Shuh, J., Kar S., Chou, M.L., Chen, C.Y., 2014. Screening of plant growth-promoting traits in arsenic-resistant bacteria isolated from agricultural soil and their potential implication for arsenic bioremediation. Journal of Hazardous Materials. 272, 112–120.

97. Tang X, Freitak D, Vogel H, Ping L, Shao Y, et al., 2012. Complexity and Variability of Gut Commensal Microbiota in Polyphagous Lepidopteran Larvae. PLoS ONE 7(7): e36978. doi:10.1371/journal.pone.0036978.

98. Tarazona, J.V., Sanz, F., 1987 Aliphatic nitro compounds in *Astragalus lusitanicus* Lam. Vet. Hum. Toxicol. 29, 437–439.

99. Termeer, C., Frauke, B., Sleeman, J., Fieber, C., Voith, U., Ahrens T., Freudenberg M. K., Galanos C. M., Simon J. C., 2002. Oligosaccharides of Hyaluronan Activate Dendritic Cells via Toll-like Receptor 4. J Exp Med. 7; 195(1): 99–111.

100. Terra, W.R., Ferreira, C., 1994. Insect digestive enzymes: properties, compartmentalization and function. Comp. Biochem. Physiol. 109, 1–62.

101. The, B.S., Apel J., Shao Y., Boland W., 2016. Colonization of the Intestinal Tract of the Polyphagous Pest *Spodoptera littoralis* with the GFP-Tagged Indigenous Gut Bacterium *Enterococcus mundtii.* Front Microbiol. 7: 928.

102. Venugopala, K. N., Rashmi, V., Odhav, B., 2013. Review on Natural Coumarin Lead Compounds for Their Pharmacological Activity. Biomed Res Int. 963248.

103. Vilanova, C., Baixeras J., Latorre A., Porcar M., 2016. The Generalist Inside the Specialist: Gut Bacterial Communities of Two Insect Species Feeding on Toxic Plants Are Dominated by *Enterococcus* sp. Front Microbiol. 7: 1005.

104. Waite, W., David, D.M., Biswas, K., Ward, F.D., Deines, P., Taylor W.M., 2015. Microbial community structure in the gut of the New Zealand insect Auckland tree weta (*Hemideina thoracica*). Archives of Microbiology., Volume 197, Issue 4, pp 603–612.

105. Wang, S.D., Liu, W., Xue, C.B., Luo, W.C., 2010. The effects of luteolin on phenoloxidase and the growth of *Spodoptera exigua* (Hubner) larvae (Lepidoptera: Noctuidae) J. Pestic. Sci. 35, 483–487.

106. Williams, M.C., 1994. Impact of poisonous weeds on livestock and humans in north America. Rew. Weed Sci. 6, 1-27.

107. Wittstock, U., Agerbirk, N., Stauber, E.J., Olsen, C.E., Hippler, M., Mitchell-Olds, T., Gershenson, J., Vogel, H., 2004. Successful herbivore attack due to metabolic diversion of a plant chemical defense. Proc Natl Acad Sci USA. 101, 4859–4864.

108. Woting, A., Pfeiffer, N., Loh, G., Klaus S., Blaut, M., 2014. *Clostridium ramosum* Promotes High-Fat Diet-Induced Obesity in Gnotobiotic Mouse Models. *mBio* vol. 5, no. 5.

109. Yoshinaga, N., Morigaki, N., Matsuda, F., Nishida, R., Mori, N., 2005. In vitro biosynthesis of volicitin in *Spodoptera litura*. Insect Biochem. Mol. Biol. 35, 175–184.

110. Yuna, J.H., Roha, S.W, Whona, T.W., Junga, M.J., Kima, M.S., Parkc, D.S., Yoonb, C., Nama, Y.D., Kima, Y.J., Choia, J.H., Kima, J.Y., Shina, N.R., Kimd, S.H., Leed, W.J., Baea, J.W., 2014. Insect Gut Bacterial Diversity Determined by Environmental Habitat, Diet, Developmental Stage, and Phylogeny of Host. Appl. Environ. Microbiol. vol. 80 no. 17, 5254-5264.

12. Selbständigkeitserklärung

Hiermit erkläre ich, entsprechend § 5 Absatz 3 der Promotionsordnung der Biologisch-Pharmazeutischen Fakultät der Friedrich Schiller Universität Jena, das mir die geltende Promotionsordnung bekannt ist. Die vorliegende Dissertation habe ich eigenständig und nur unter Verwendung angegebener Quellen und Hilfsmittel angefertigt, wobei von Dritten übernommene Textabschnitte entsprechend gekennzeichnet wurden. Alle Personen, die einen entscheidenden Beitrag zu den Manuskripten geleistet haben, sind in Kapitel 2 aufgeführt beziehungsweise in der Danksagung erwähnt. Die Hilfe eines Promotionsberaters wurde nicht in Anspruch genommen noch haben Dritte geldwerte Leistungen für Arbeiten im Zusammenhang mit der vorliegenden Dissertation erhalten. Gemäß Anlage 5 zum § 8 Absatz3 der Promotionsordnung wurde die Beschreibung des von mir geleisteten Eigenanteils von dem Betreuer der Dissertation, Prof. Dr. Wilhelm Boland, mit Unterschrift bestätigt und der Fakultät vorgelegt. Zu keinem früheren Zeitpunkt wurde diese Dissertation, eine in wesentlichen Teilen ähnliche Arbeit oder eine andere Abhandlung bei einer Hochschule als Dissertation eingereicht.

Alexey Novoselov

Jena, den 15. 2.2017

13. Acknowledgements

14 Curriculum vitae

Alexey Novoselov

Curriculum Vitae

Personal
Birth date: 14.06.1984
Birth place: Moscow, Russia

Address: Oberlauengasse 5, 07743, Jena, Germany
Phone: +49 1638985645
E-Mail: anovoselov@ice.mpg.de, alexenematov@mail.ru

Current position

Group leader "Insect gut microbiota"
Department of Bioorganic Chemistry
Max Planck Institute for Chemical Ecology
Hans-Knöll-Straße 8
07745 Jena, Germany

Experience
10/2012 – present
Max Planck Institute for Chemical Ecology, Jena, Germany, Grantee

The main goal of the current project is the reconstruction of metabolic network for the turnover of plant toxins in the gut of insects. Products of plant toxins metabolism were detected with HPLC-MS, HR-MS (TOF). Changes in gut microbial community was documented with NGS technology, sequencing of 16S rRNA (454), metagenome sequencing (Illumina, HiSeq 2500) . Using omics approach (metagenomic, metabolomic) the metabolic network in the gut is reconstructed.

03/2012 – 06/2012
Moscow Institute of Medical Chemistry, Moscow, Russia, Scientific Researcher

Our group studied the LOH (loss of heterozygosity) associated with colorectal cancer. We investigated LOH in 18th human chromosome. I was responsible for PCR and electrophoresis techniques. I prepared PCR with micro satellite markers and then separate PCR product in the PAG. After that I carried out the analysis of PAG for the presence of LOH.

07/2010 – 09/2012
Cell Movement Lab, Dep. of Cell Biology, Biological Faculty, Moscow State University, Moscow, Russia, Scientific Researcher

Lab studies the mechanisms of cell movement, in particular observe the interactions between different components of cytoskeleton during cell movement using luminescent microscopy. I used transient transfection to develop cell lines with recombinant two-domain proteins' (fluorescent domain taqBlueFP/taqGFP2/EGFP/mKate2 and functional domain tubulin/EB1/paxillin/zyxin) expression to observe cell movement. Analysis and sorting of developed cell lines were carried out on BD FACSAria III cell sorter.

Grants

10/2011 – 11/2011
Was granted with Erasmus Mundus scholarship for Academic Staff and took the training course in the University of Udine within the Erasmus Mundus Iamonet-Ru Cooperation Project (Udine, and Tarvisio pre-Alpine region, Italy)

Education
Diplom in Soil Biology, Dep. of Soil Biology, Faculty of Soil Science, Moscow State University, Moscow, Russia
Diploma thesis "Biological Activity of Soil Colonized by *Lasius niger* Ants"

Candidate of Science in Ecology (Biology), Dep. of Ecology, Biological Faculty, Moscow State University, Moscow, Russia
Candidate's thesis "Biological Activity of Soil Colonized by *Lasius niger* Ants"

Awards

04/2006

Was awarded with the diploma for the best report on the Undergraduate and Postgraduate Student International Conference on Fundamental Sciences "Lomonosov" (Moscow State University, Moscow, Russia)

Publications

Pol Alonso-Pernas, Erika Arias-Cordero, **Alexey Novoselov**, Christina Große, Jürgen Rybak, Martin Kaltenpoth, Martin Westermann, Ute Neugebauer, Wilhelm Boland, (2017). Bacterial community and PHB-accumulating bacteria associated with the wall and specialized niches of the hindgut of the forest cockchafer (*Melolontha hippocastani*). Frontiers in Microbiology 8, 291. doi: 10.3389/fmicb.2017.00291.

Chen B., Sun C., Liang X., Lu X., Gao Q., Alonso-Pernas P., Teh B., **Novoselov A. L**., Boland W., Shao Y. (2016) Draft Genome Sequence of *Enterococcus mundtii* SL 16, an Indigenous Gut Bacterium of the Polyphagous Pest *Spodoptera littoralis*. Front Microbiol, 7, 1676. doi: 10.3389/fmicb.2016.01676.

Novoselov, A., Becker, T., Pauls, G., von Reuß, S. H., Boland, W. (2015) *Spodoptera littoralis* detoxifies neurotoxic 3-nitropropanoic acid by conjugation with amino acids. Insect Biochemistry and Molecular Biology, 63, 97-103. doi:10.1016/j.ibmb.2015.05.013.

Golichenkov M.V., **A.L. Novoselov**, O.E. Marfenina, T.G. Dobrovol'skaya, Yu.V. Zakalyukina, E.V. Lapygina, and D.G. Zamolodchikv (2011) Microbiological Characteristic of Anthills of *Lasius niger*. Biology Bulletin 38 (3): 277–282.

Golichenkov M.V., **A.L. Neymatov***, and A.V. Kiryushin (2009) Microbiological Activity of Soils Populated by *Lasius niger* Ants. Eurasian Soil Science 42 (7): 788–792.

Golod N.A., N.G. Loiko, A.L. Mulyukin, **A.L. Neymatov***, L.I. Vorobjeva, N.E. Suzina, E.F. Shanenko, V.F. Gal'chenko, and G.I. El-Registan (2009) Adaptation of Lactic Acid Bacteria to Unfavorable Growth Conditions. Microbiology 78 (3): 280–289

* Changed surname from Neymatov to Novoselov in 2009.

15 Supplementary material

15.1. Article I

Appendix I

**Characterization of the synthetic standards.**

High-resolution MS (HRMS) measurements of the synthetic standards were acquired by direct injection (Orbitrap XL, Thermo-Fisher, San Jose, CA, USA). Infrared spectra were measured with an IR spectrometer over a range of $700-4000$ cm^{-1} in transmission mode with a spectral resolution of 2 cm^{-1}. Optical rotations were measured at 589 nm in water (temperatures are given). NMR spectra were measured using a Bruker AV400 spectrometer operating at 400 MHz (^{1}H) and 100 MHz (^{13}C). Chemical shifts (δ) are quoted in parts per million (ppm) and are referenced to the signal of residual protonated solvent (CD_3OD at 3.31 ppm in ^{1}H and 49.0 ppm in ^{13}C). MeOH was added as a reference for ^{13}C NMR spectra in D_2O (δ 49.5 ppm). Assignment of peaks was carried out using 1D (^{1}H, ^{13}C $\{^{1}H\}$, APT, DEPT) and 2D NMR experiments (COSY and HSQC). The multiplicities are given as follows: d, doublet; t, triplet; dd, doublet of doublets; q, quartet; m, multiplet.

Synthesis of stable isotope labelled 3-[1-^{13}C,3-^{15}N]-3-NPA (98% ^{13}C, 95% ^{15}N)

The synthesis of 3-[1-^{13}C, 3-^{15}N]-nitropropanoic acid was achieved using the protocol of Baxter et al (**1985**) with Na$^{15}NO_2$ to introduce a second stable isotope label. The analytical data were in excellent agreement with the literature results.

Synthesis of amino acid amides of 3-NPA

Due to the low solubility of free amino acids in non-aqueous solvents the synthesis of the described 3-NPA amino acid amides **1-4** was performed counterintuitively in an aqueous solution at rt using dicyclohexyl carbodiimide (DCC) as a coupling reagent (Scheme 1) (Neises, and Steglich, 1978; Becker et al, 2015). 3-NPA was dissolved in small amounts of water. To the aqueous solution DCC in acetonitrile and the free amino acid in water were added over 2h simultaneously. The mixtures were purified by extraction and column chromatography (Et$_2$O/AcOH). This procedure provides significant amounts of the natural products in one synthetic step without the need of protecting groups.

1 R = H
2 R = Me^3
3 R = H$_2$C^{3}OH
4 R = HC^{3}OHC^{4}H$_3$
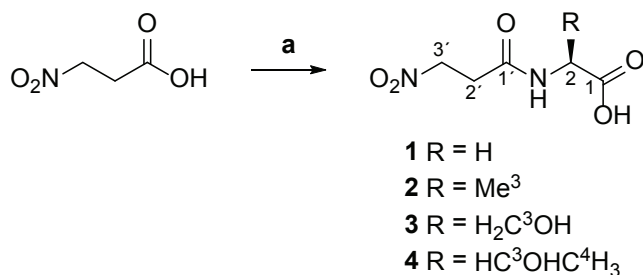
Scheme 1: Synthetic protocol for the amino acid amides of 3-NPA; a) DCC/MeCN 0.4 M, amino acid/H$_2$O 0.4 M, rt, 2h, H$_2$O.

General synthesis of the 3-Nitropropanoic acid (3-NPA) amides of amino acids 1 to 4.

To a solution of 750 mg (6.3 mmol, 1.05 equ.) 3-NPA in water (0.4 ml) a solution of 1.3 g (6.3 mmol, 1.05 equ.) DCC in 20 ml MeCN and 1 equ. of the amino acid in 20 ml water were added drop wise and simultaneously over 2 h at rt. After the addition was completed 400 ml of MeCN

were added so that the solvents were removed completely at 75 mbar and 25°C. To the dry crude mixture 15 ml of water were added to extract the amino acid derivatives from the water insoluble DCU and the suspension was shaken for 30 min at rt. After the mixture was filtrated and washed with 10 ml of water 300 ml MeCN and 3g dry Silica were added to the filtrate. The solvents were removed under reduced pressure and rt. The silica adsorbed crude mixture was applied to a column and eluted with ethyl ether/acetic acid (ratios are given as follows). The product fractions were combined, the same volume of cyclohexane was added and the solvents were removed under reduced pressure at rt. To the oily residue 3 ml of cyclohexane and 3 ml of diethyl ether were added and the solvents were removed again at rt under reduced pressure. This procedure was repeated until a colorless solid was obtained.

The columns for preparative chromatography were packed by pouring a suspension of silica gel (0.03-0.063 mm) and the eluent into the column containing 10 ml of the eluent. The separations were carried out at 1.1 bar additional pressure.

Thin-layer chromatography was performed on TLC silica gel 60 F254 aluminum sheets. Compounds were visualized using anisaldehyde reagent. All chemicals were purchased in the highest purity that was commercially available and used without further purification. All solvents were purchased in HPLC grade and used without further purification. Diethyl ether was distilled prior to use.

Analytical data for (3-nitropropanoyl)glycine **1**: (135 mg, 0.77 mmol, 12.8 %); R_f(Et$_2$O/AcOH 7:1)=0.21; **^{1}H NMR** (400 MHz, CD$_3$OD): 4.71 (t, J = 6.1 Hz, 2H, H-3´), 3.92 (s, 2H, H-2), 2.95 (t, J = 6.1 Hz, 2H; H-2´); **^{13}C NMR** (100 MHz, CD$_3$OD): 173.0 (C-1 or C-1´), 172.0 (C-1 or C-1´),

71.1 (C-3′), 41.9 (C-2), 32.9 (C-2′); **MS** (ESI-TOF, neg. mode) m/z (in %) 373.06 (100) $[M_2-2H+Na]^-$, 175.04 (27) $[M-H]^-$, 128.04 (88) $[M-H-HNO_2]^-$; **HRMS** (ESI-TOF, neg. mode) m/z calcd for $C_5H_7N_2O_5^-$ 175.03604 $[M-H]^-$, found 175.03546; **IR** (thin film, cm^{-1}) 3314 (br, s), 3078 (m), 2980 (m), 2927 (m), 1702 (s), 1652 (s), 1555 (s), 1427 (s), 1408 (s), 1377 (s), 1235 (s), 1208 (m).

These data are in excellent agreement with the literature results (Majak, W., et al 1998).

Analytical data for (3-nitropropanoyl)alanine **2**: (93 mg, 0.49 mmol, 8.2 %); $[\alpha]_D^{21}$ -17.6 (c 0.75, CD_3OD); R_f(Et_2O/AcOH 14:1)=0.24; **^{1}H NMR** (400 MHz, CD_3OD): 4.70 (m, 2H, H-3′), 4.39 (q, J = 7.3 Hz, 1H, H-2), 2.92 (m, 2H; H-2′), 1.40 (d, J = 7.3 Hz, 3H, H-3); **^{13}C NMR** (100 MHz, D_2O): 177.3 (C-1 or C-1′), 172.4 (C-1 or C-1′), 70.9 (C-3′), 49.5 (C-2), 32.2 (C-2′), 16.7 (C-3); **MS** (ESI-TOF, neg. mode) m/z (in %) 379.11 (40) $[M_2-H]^-$, 189.05 (60) $[M-H]^-$, 142.05 (100) $[M-H-HNO_2]^-$; **HRMS** (ESI-TOF, neg. mode) m/z calcd for $C_6H_9N_2O_5^-$ 189.05169 $[M-H]^-$, found 189.05253; IR (thin film, cm^{-1}) 3320 (br, s), 2987 (m), 2941 (m), 1731 (s), 1659 (s), 1556 (s), 1457 (m), 1419 (m), 1378 (m), 1224 (m), 1157 (m).

Analytical data for (3-nitropropanoyl)serine **3**: (117 mg, 0.57 mmol, 9.4 %); $[\alpha]_D^{22}$ 15.2 (c 1.12, CD_3OD); R_f(Et_2O/AcOH 7:2)=0.21; **^{1}H NMR** (400 MHz, CD_3OD): 4.71 (m, 2H, H-3′), 4.46 (br, t, J = 4.4 Hz, 1H, H-2), 3.89 (dd, J_1 = 11.2 Hz, J_2 = 4.9, 1H; H_A-3), 3.81 (dd, J_1 = 11.2 Hz, J_2 = 4.1, 1H; H_B-3), 2.98 (m, 2H, H-2′); **^{13}C NMR** (100 MHz, D_2O): 174.5 (C-1 or C-1′), 172.6 (C-1 or C-1′), 70.9 (C-3′), 61.9 (C-3), 56.1 (C-2), 32.4 (C-2′); **MS** (ESI-TOF, neg. mode) m/z (in %) 433.08 (50) $[M_2-2H+Na]^-$, 205.05 (100) $[M-H]^-$, 158.05 (70) $[M-H-HNO_2]^-$; **HRMS** (ESI-TOF, neg. mode) m/z calcd for $C_6H_9N_2O_6^-$ 205.04661 $[M-H]^-$, found 205.04615; IR (thin film, cm^{-1}) 3324 (br, s),

2927 (m), 1718 (s), 1660 (s), 1555 (s), 1419 (s), 1379 (s), 1235 (s), 1137 (m), 1072 (s). These data are in excellent agreement with the literature results (Majak, W., et al 1998).

Analytical data for (3-nitropropanoyl)threonine **4**: (68 mg, 0.31 mmol, 5 %); $[\alpha]_D^{22}$ 25.6 (c 0.63, CD_3OD); $R_f(Et_2O/AcOH$ 6:1)=0.18; **^{1}H NMR** (400 MHz, CD_3OD): 4.72 (m, 2H, H-3′), 4.41 (d, J = 2.4 Hz, 1H, H-2), 4.3 (m, 1H; H-3), 3.0 (m, 2H, H-2′), 1.18 (d, J = 6.3 Hz, 3H, H-4); **^{13}C NMR** (100 MHz, D_2O): 175.0 (C-1 or C-1′), 172.9 (C-1 or C-1′), 71.0 (C-3′), 67.9 (C-3), 59.3 (C-2), 32.4 (C-2′), 19.4 (C-4); **MS** (ESI-TOF, neg. mode) m/z (in %) 461.11 (24) $[M_2-2H+Na]^-$, 219.06 (100) $[M-H]^-$; **HRMS** (ESI-TOF, neg. mode) m/z calcd for $C_7H_{11}N_2O_6^-$ 219.06226 $[M-H]^-$, found 219.06136; IR (thin film, cm^{-1}) 3326 (br, s), 2980 (m), 2937 (m), 1731 (s), 1662 (s), 1557 (s), 1418 (s), 1379 (s), 1223 (m), 1150 (m), 1089 (m).
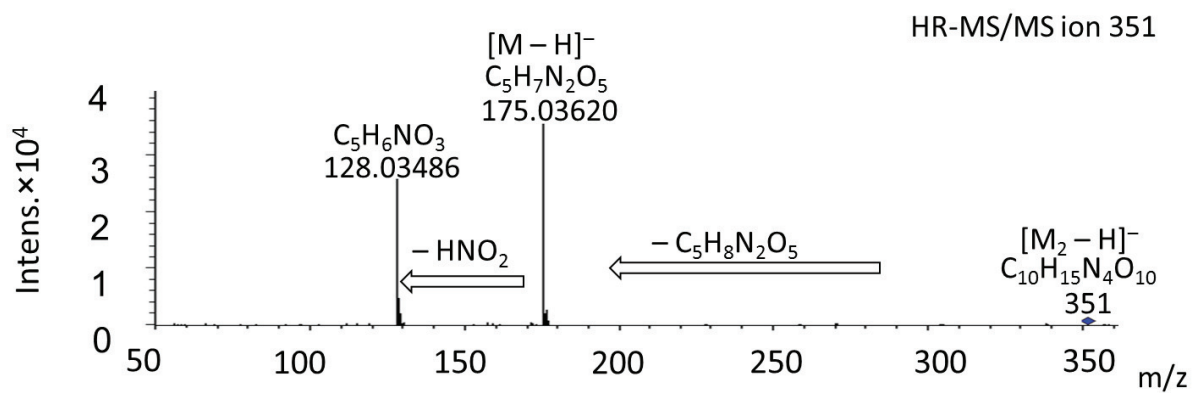
Fig. S1. HR-MS/MS of ion 351.
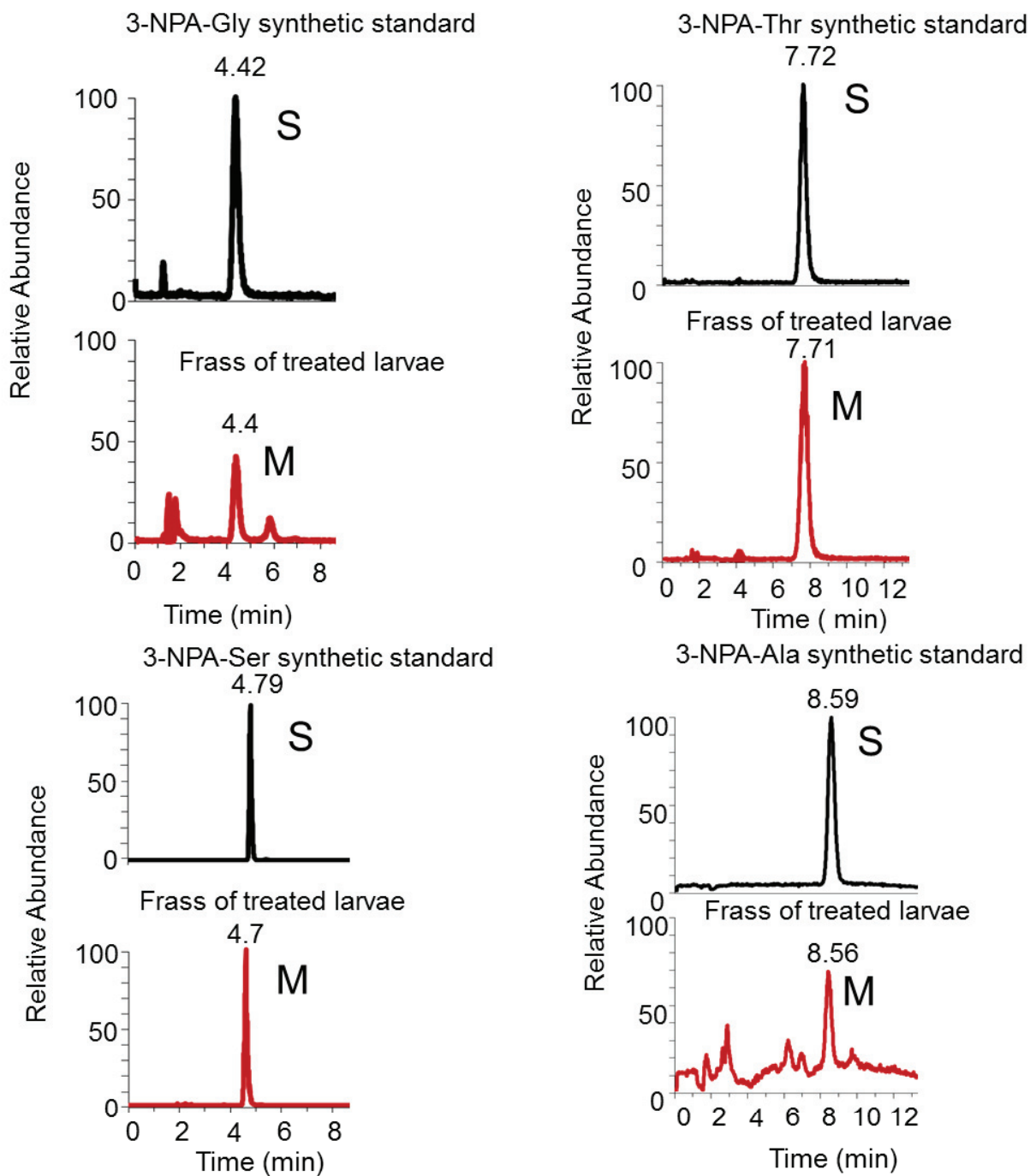
Fig. S2. Comparison of feces of 6th instar larvae treated with 3-NPA and synthetic amino acid amides.

(S- synthetic standard, M- metabolite).

Appendix II

^{1}H-,^{13}C NMR- and IR-spectra of compounds 1-4

Fig. S3. ¹H NMR compound 1.

¹³C NMR of compound **1** at 100 MHz in D₂O + MeOH

174.01
173.15

70.89

41.87

32.29
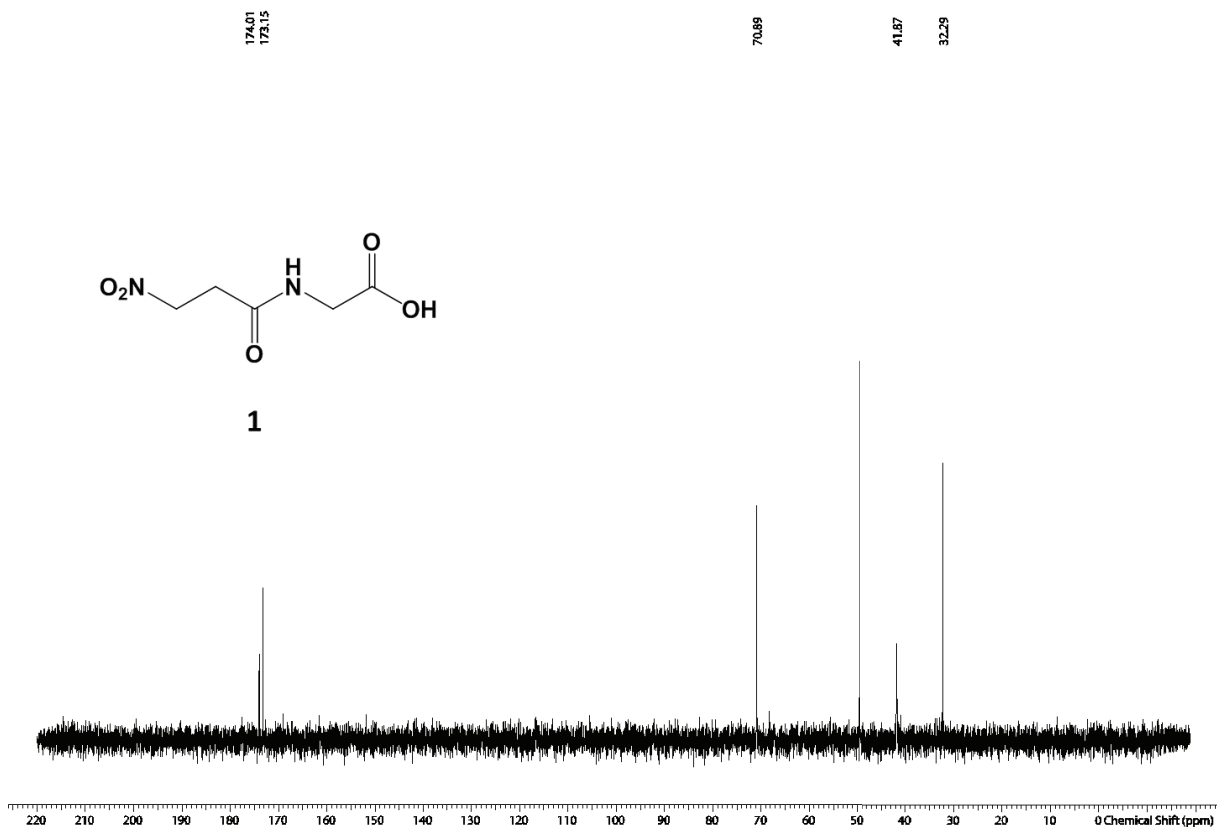
Fig. S4. ¹³C NMR compound 1.
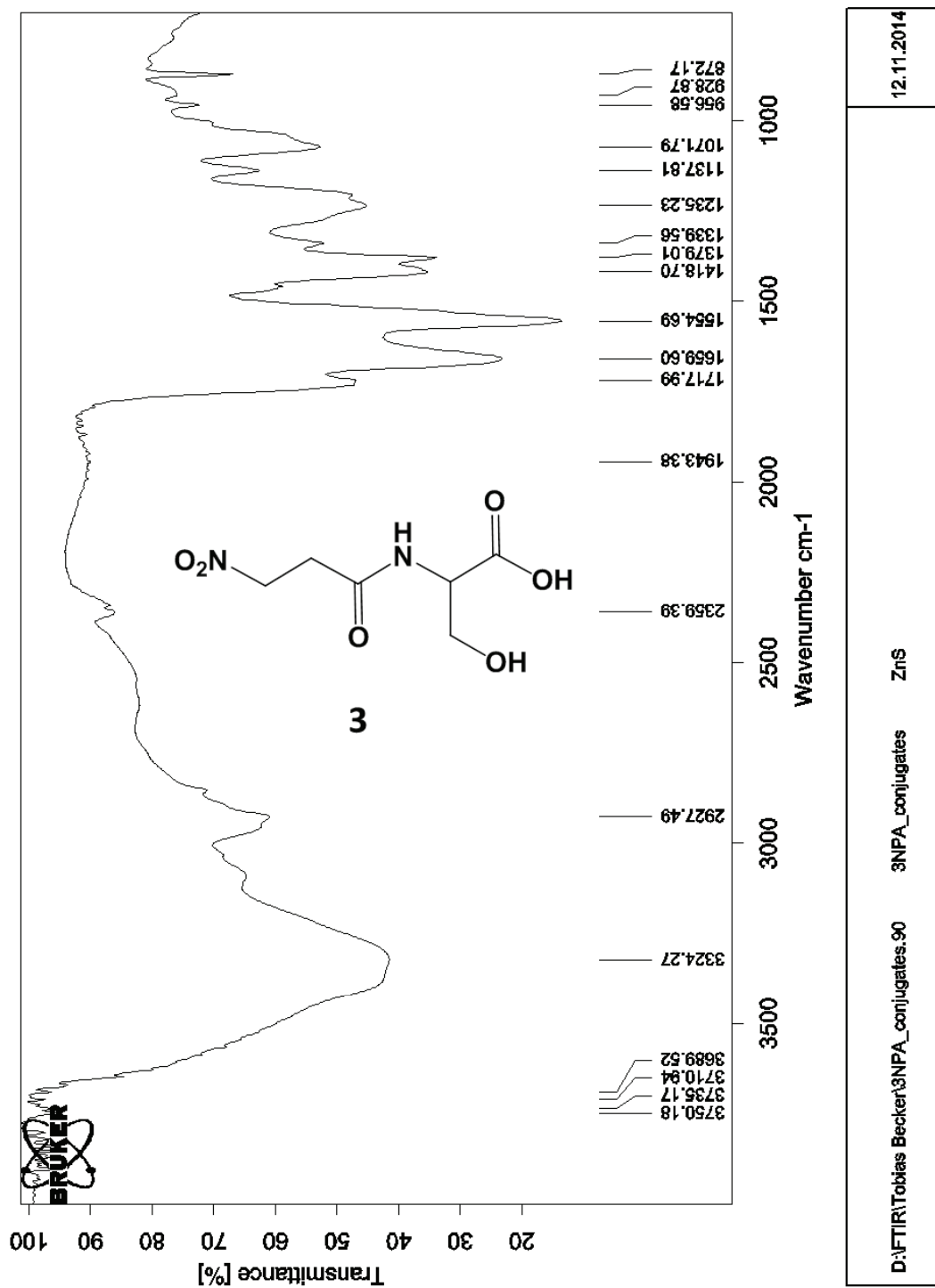
Fig. S5. IR spectrum of compound 1.

¹H NMR of compound **2** at 400 MHz in CD₃OD
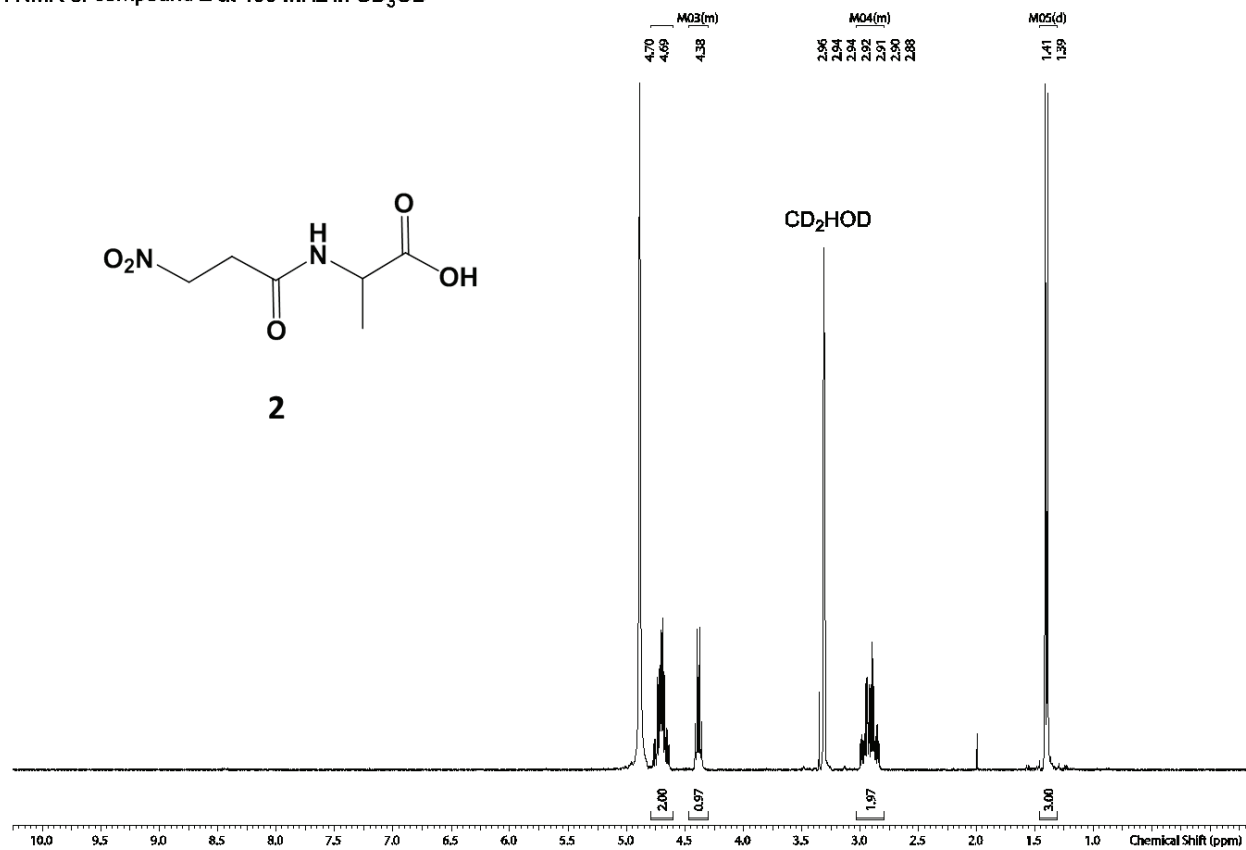
Fig. S6. ¹H NMR compound 2.

¹³C NMR of compound **2** at 100 MHz in D2O

177.25
172.40
70.91
49.50
32.26
16.73

2

220 210 200 190 180 170 160 150 140 130 120 110 100 90 80 70 60 50 40 30 20 10 0 Chemical Shift (ppm)
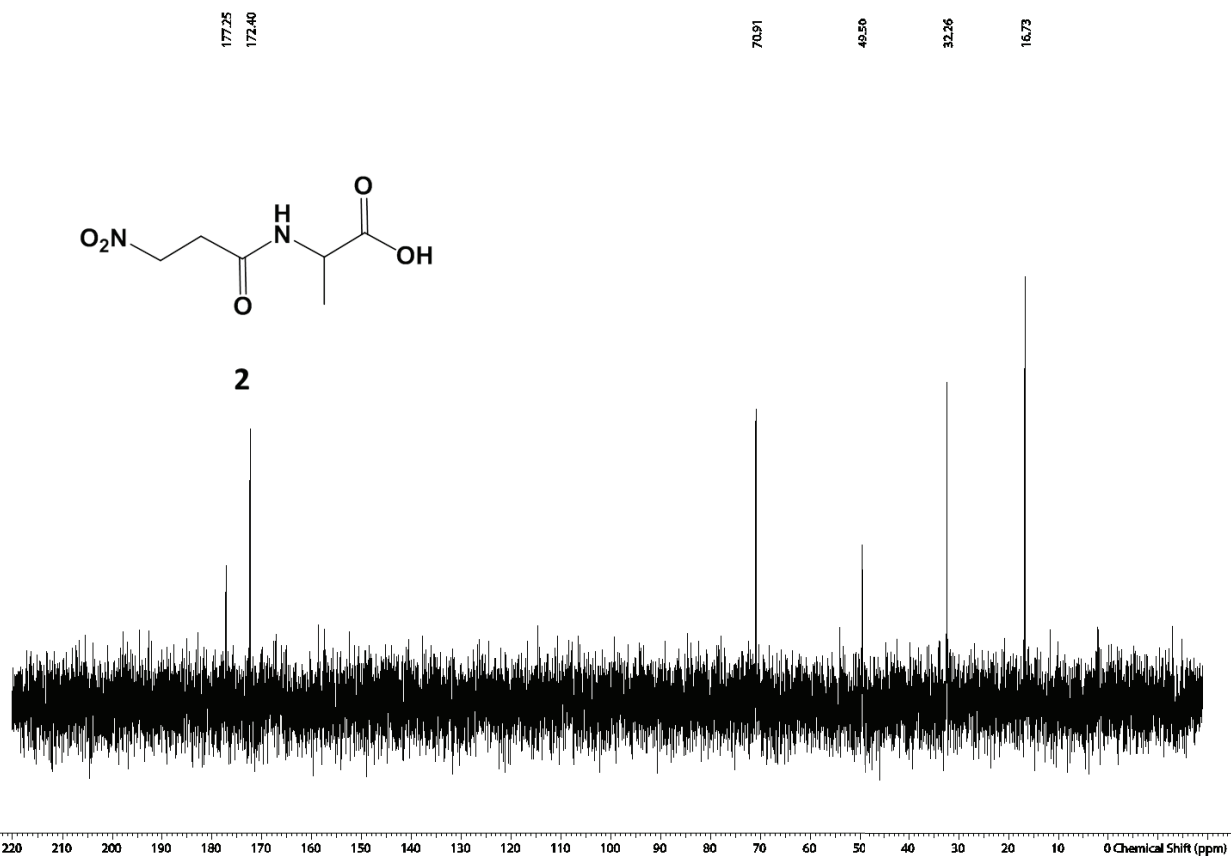
Fig. S7. ¹³C NMR compound 2.

IR spectrum of compound 2
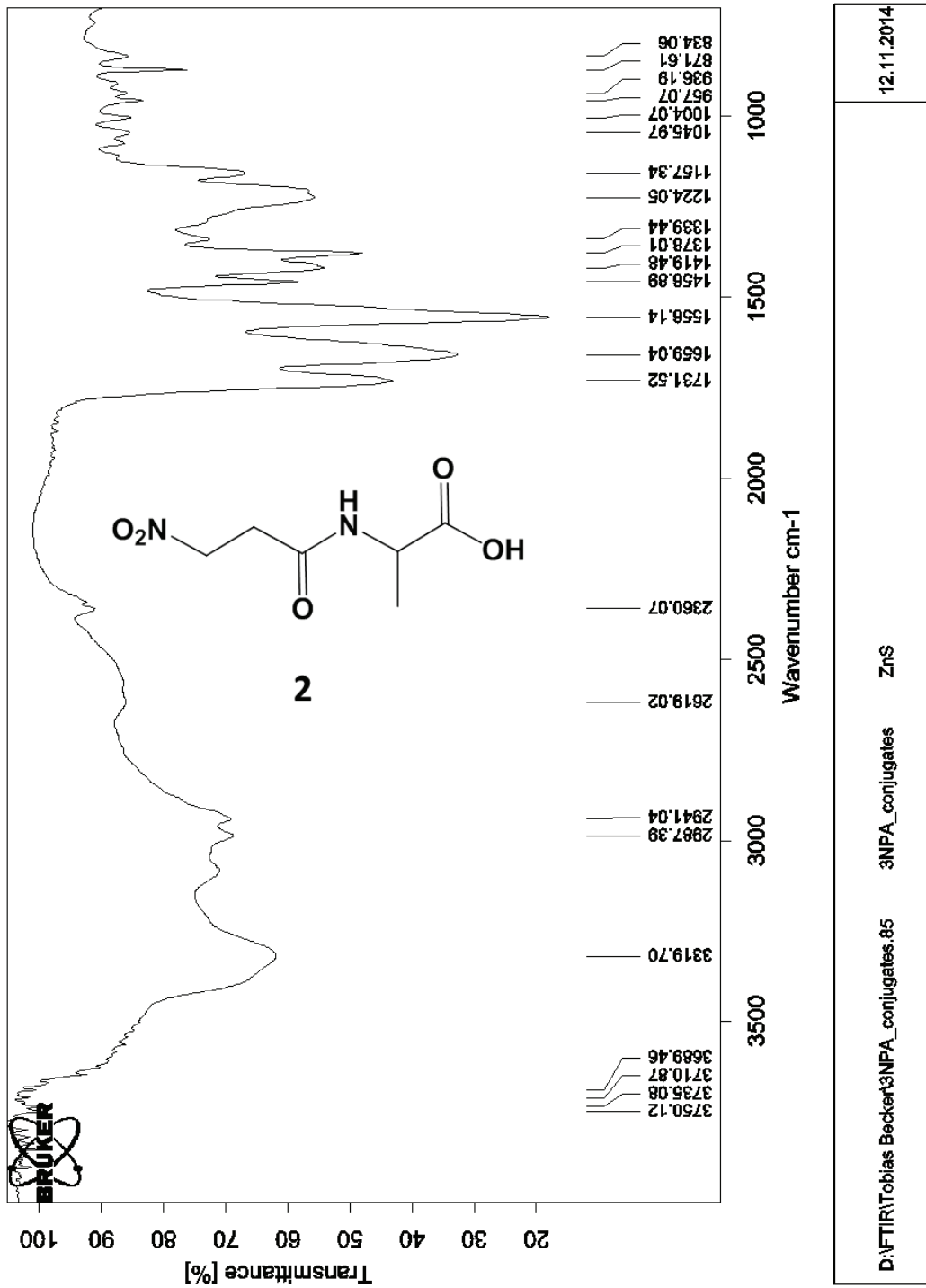
Fig. S8. IR spectrum of compound 2.

Fig. S9. ^{1}H NMR compound 3.
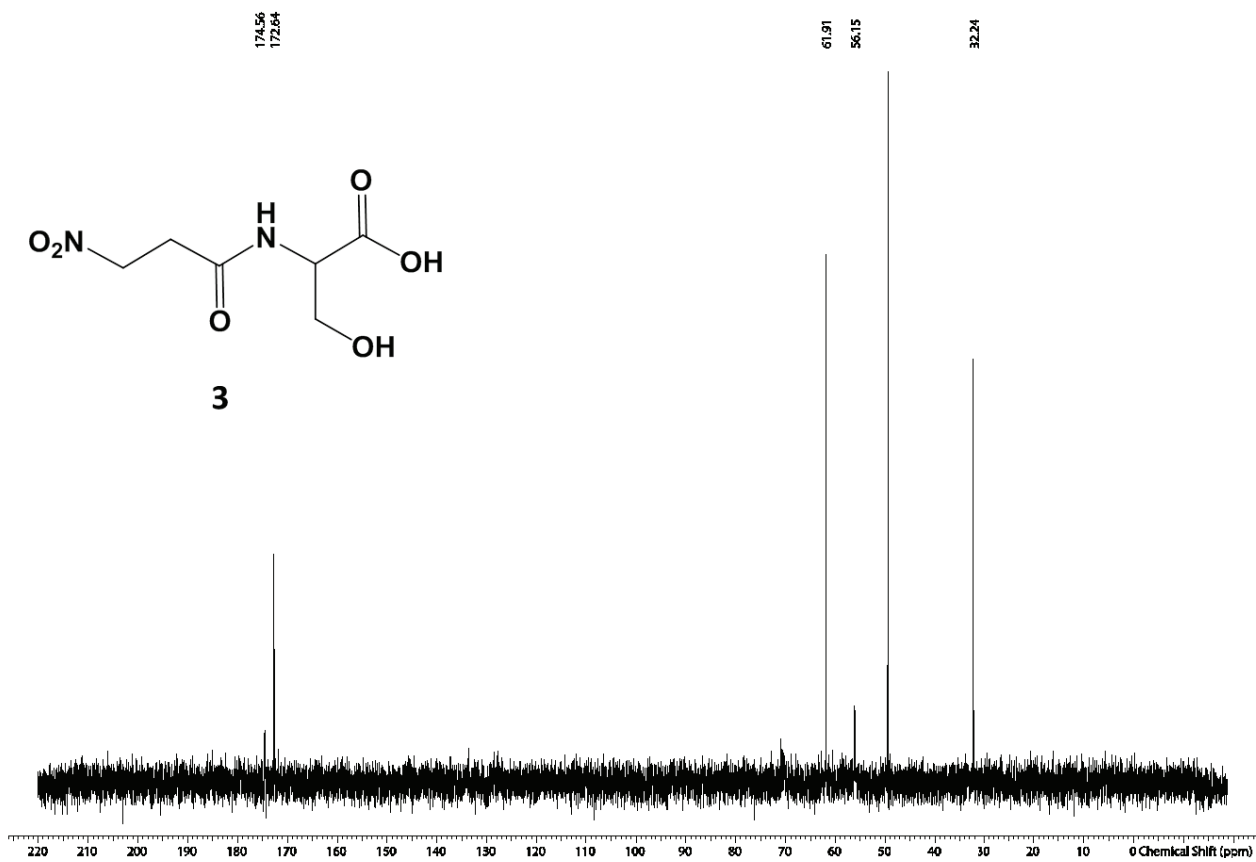
Fig. S10. ^{13}C NMR compound 3.

Fig. S11. IR spectrum of compound 3.

Fig. S12. ^{1}H NMR compound 4.

¹³C NMR of compound **4** at 100 MHz in D₂O + MeOH
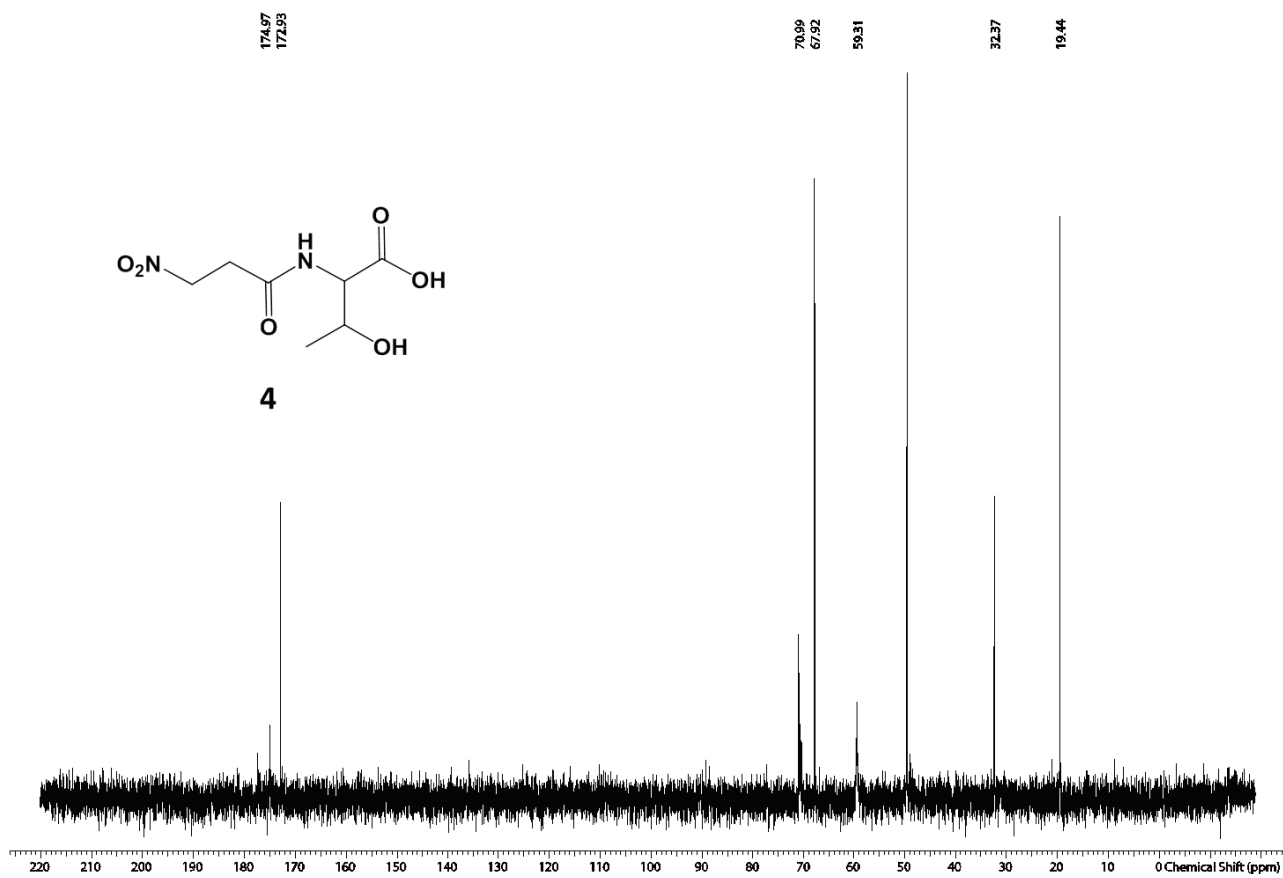

Fig. S13. ¹³C NMR compound 4.

Supplementary Material

Bacterial community and PHB-accumulating bacteria associated with the wall and specialized niches of the hindgut of the forest cockchafer (*Melolontha hippocastani*)

Pol Alonso-Pernas[*]**, Erika Arias-Cordero, Alexey Novoselov, Christina** Große**, Jürgen Rybak, Martin Kaltenpoth, Martin Westermann, Ute Neugebauer, Wilhelm Boland**[*]

* Correspondence: Pol Alonso-Pernas: palonso@ice.mpg.de, Wilhelm Boland: boland@ice.mpg.de
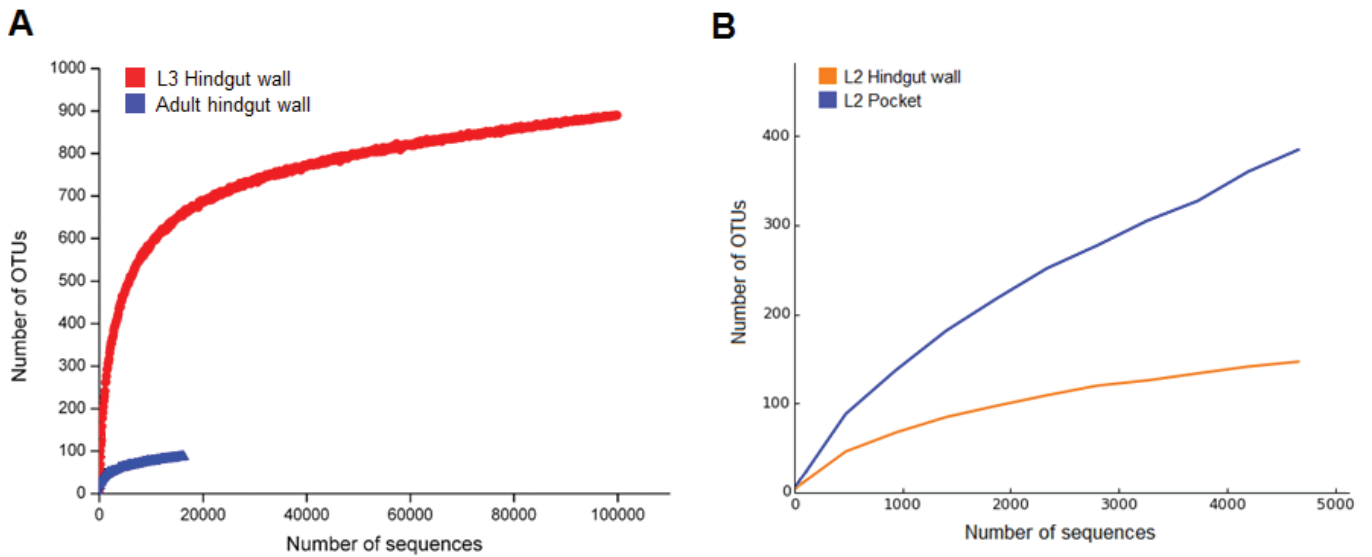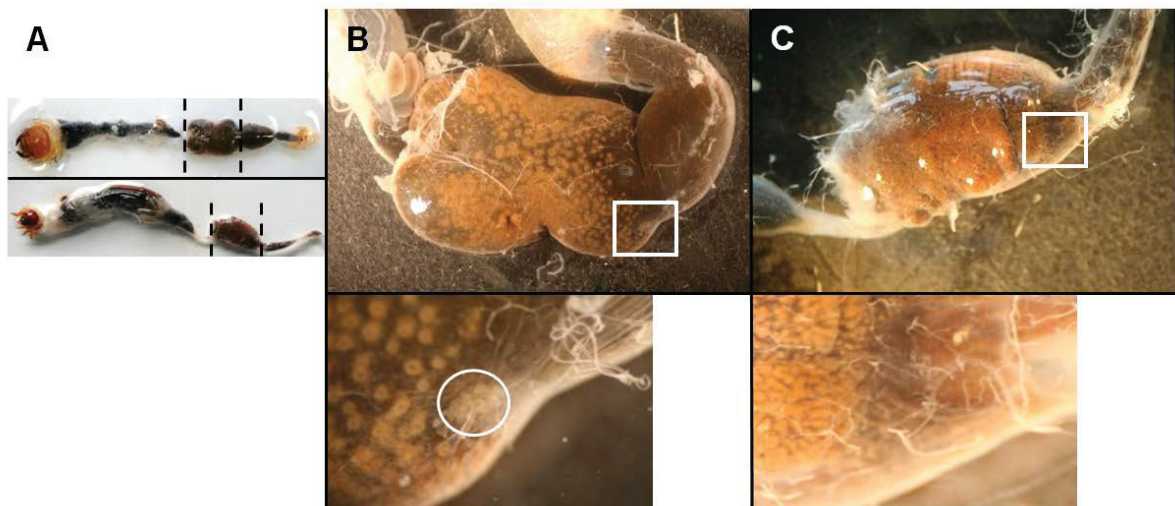
Supplementary Figures.
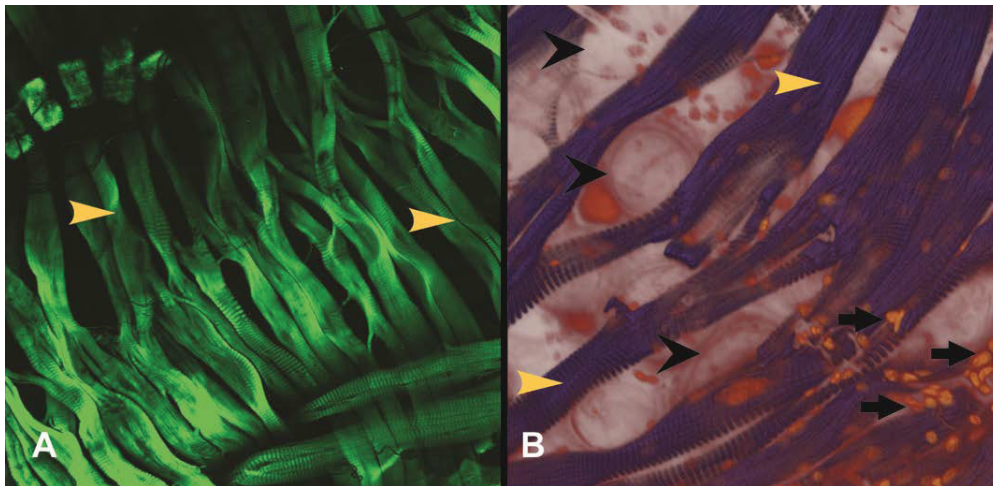
Supplementary Figure 1. Confocal images of the hindgut pocket tissue of a *Melolontha hippocastani* L2 larva. (A) Staining of the pocket tissue with Alexa Fluor 488 nm phalloidin stain (Phallotoxin, Invitrogen). (B) Double staining with Alexa Fluor 488 nm phalloidin stain and SYTOX Orange nucleic acid stain (Invitrogen), overlaid image. Yellow arrowheads point to muscle fibers that cover the pocket poles; black arrowheads indicate the position of the spheres at the distal point of the poles composing the pocket; black arrows point to the tracheoles that cover the pocket tissue.

Supplementary Figure 2. *Melolontha hippocastani* L2 larva hindgut and pocket microscopic detail. Cross section stained with Richards' solution. Black arrow point to the connection of one of the pocket poles to the hindgut lumen (L). Black arrowheads point to pocket poles. Scale bar 200 μm.

Supplemetary Figure 3. Rarefaction curves of the 454-pyro sequencing. (A) Comparison of L3 hindgut wall and adults hindgut wall. (B) Comparison of L2 hindgut wall and L2 pocket.

Supplementary Figure 4. Absence of pockets in *P. marginata* larvae compared to in *M. hippocastani*. The area within the white square is enlarged beneath. (A) Overview of a whole larval gut of *M.*

hippocastani (upper image) and *P. marginata* (lower image). The hindgut chamber is between the dashed lines. (B) Close-up of *M. hippocastani* hindgut chamber. The pocket is inside the white circle in the enlarged image. (C) Close-up of *P. marginata* hindgut chamber. Note the absence of pocket in the enlarged image.

Supplementary Tables.

Supplementary Table 1. Abundance of "Low abundance families" expressed as a percentage of total sequences. N.D.: not detected.

Family	Pocket L2	Hindgut wall L2	Hindgut wall L3	Hindgut wall Adult
Procabacteriaceae	0.0261	N.D.	0.1237	N.D.
Veillonellaceae	N.D.	N.D.	0.1396	N.D.
Proteobacteria phylum unk. fam.	0.1329	N.D.	N.D.	N.D.
Gammaproteobacteria class unk. fam.	N.D.	N.D.	0.1325	N.D.
Oxalobacteraceae	0.0057	0.0202	0.0721	0.0107
Microbacteriaceae	0.0403	N.D.	0.0545	N.D.
Nocardioidaceae	N.D.	0.0927	N.D.	N.D.
Bacteroidaceae	0.0591	0.0300	N.D.	N.D.
Opitutaceae	N.D.	N.D.	0.0708	N.D.
Chitinophagaceae	0.0641	N.D.	N.D.	N.D.
Methylobacteriaceae	0.0169	0.0395	N.D.	N.D.
Peptococcaceae	N.D.	N.D.	0.0514	N.D.
Turicibacteraceae	0.0438	N.D.	N.D.	N.D.
Bradyrhizobiaceae	0.0095	0.0202	N.D.	0.0027

Phyllobacteriaceae	0.0297	N.D.	N.D.	N.D.
Propionibacteriaceae	0.0019	0.0202	N.D.	N.D.
Moraxellaceae	0.0095	0.0102	N.D.	N.D.
Patulibacteraceae	0.0114	N.D.	N.D.	N.D.
Catabacteriaceae	0.0114	N.D.	N.D.	N.D.
Rhodobacteraceae	0.0114	N.D.	N.D.	N.D.
Staphylococcaceae	N.D.	0.0102	N.D.	N.D.
Coriobacteriaceae	0.0076	N.D.	N.D.	N.D.
Bacteroidia class unk. fam.	N.D.	N.D.	0.0005	0.0027

Supplementary Table 2. Genus-specific primers used.

Primer	Target	Sequence (5'-3')	Reference
Achro F	*Achromobacter* spp.	GCTAATACCGCATACGCCCT	This study
Achro R	*Achromobacter* spp.	AGCCGTTACCCCACCAACTA	This study
Bos F	*Bosea* spp.	TAAGTTGGGAACTCTAGGGGG	This study
Bos R	*Bosea* spp.	TTTCGCTGCCCATTGTCACCG	This study
Brev F	*Brevundimonas* spp.	TTAGTTGGGAACTCTAATGG	This study
Brev R	*Brevundimonas* spp.	AGGATTAACCCTCTGTAGTTG	This study
Citro F	*Citrobacter* spp.	ACGGGTGAGTAATGTCTGGG	This study
Citro R	*Citrobacter* spp.	AGGTCCCCCTCTTTGGTCTT	This study
Pseudo F	*Pseudomonas* spp.	TTCGATTCAGCGGCGGACGG	This study
Pseudo R	*Pseudomonas* spp.	AGGTCCCCTGCTTTCTCCCGT	This study

Supplementary Table 3. Raman bands assignment. Slashes (/) indicate different band positions with the same assignment. Hyphens (-) indicate interval. def.: deformation.

Observed band (cm⁻¹)	Band assignment	References
500 / 505	S-S stretch	(Tuma 2005),(Maquelin et al. 2002)
650	C-C twist Tyr	(Tuma 2005),(Maquelin et al. 2002),(Neugebauer et al. 2010)
837 / 841	C-C stretch	(Majed and Gu 2010),(Ciobotă et al. 2010)
854 / 859	Ring vibration Tyr	(Tuma 2005),(Maquelin et al. 2002)
1007	Phenylalanine	(Tuma 2005),(Maquelin et al. 2002),(Neugebauer et al. 2010)
1058 / 1063 / 1067	C-O and C-C stretches	(Majed and Gu 2010),(Ciobotă et al. 2010),(Wu et al. 2011)
1114	C-C stretch	(Wu et al. 2011)
1131	C-O-H def., C-O and C-C stretches.	(Wu et al. 2011)
1152	C-N and C-C stretches	(Neugebauer et al. 2010), (Notingher et al. 2003)
1240 - 1280	C-H$_2$ twist, amide III	(Wu et al. 2011),(Tuma 2005),(Maquelin et al. 2002),(Neugebauer et al. 2010),(Notingher et al. 2003)

1440 / 1470	C-H deformation	(Wu et al. 2011),(Tuma 2005),(Maquelin et al. 2002)
1622 / 1626	C=C stretch Tyr and Trp	(Maquelin et al. 2002),(Notingher et al. 2003)
1650 - 1680	amide I, C=C stretch	(Tuma 2005),(Maquelin et al. 2002),(Notingher et al. 2003),
1729 / 1741	C=O stretch	(Ciobotă et al. 2010),(Majed and Gu 2010),(Wu et al. 2011)
2800 - 3000	$C\text{-}H_2$ and $C\text{-}H_3$ sretches	(Majed and Gu 2010),(Ciobotă et al. 2010),(Wu et al. 2011),(Maquelin et al. 2002)

Supplementary Table 4. Richness and diversity indices calculated at the OTU level from the pyrosequencing data of samples of hindgut wall of *Melolontha hippocastani*. Simpson expressed as 1-D, the bigger the number, the greater the diversity.

Sample	Total number of high quality reads	OTUs	Richness index	Diversity indexes	
			Chao1	Shannon	Simpson
Adults hindgut wall	16 016	74	105.67	3.06	0.71
L3 hindgut wall	85 233	572	705.91	6.52	0.96
L2 hindgut wall	4 797	147	217.38	2.87	0.67
L2 pocket	4 726	889	1338.04	4.19	0.78

15.3. Unpublished results Part II

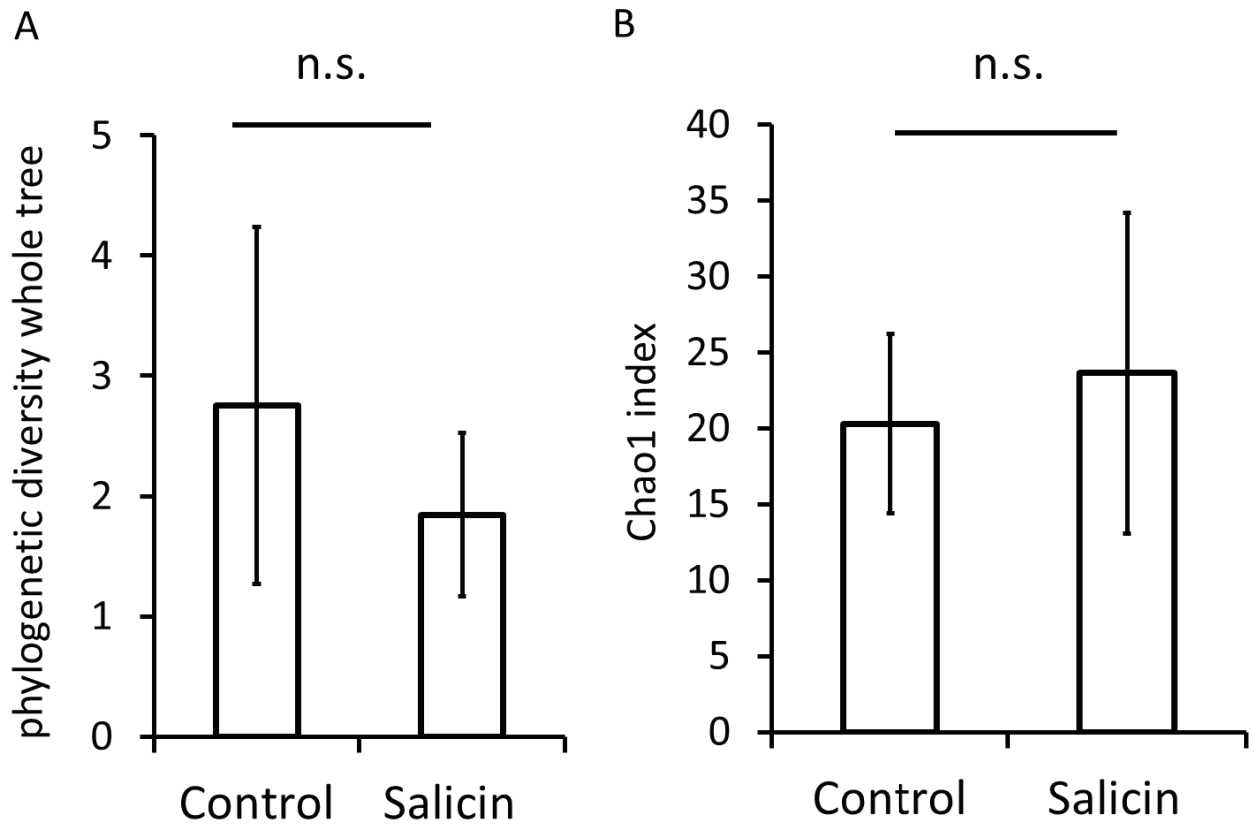Supplementary materials to unpublished results Part II

A

B

Figure 1. Phylogenetic diversity per whole tree (A) and Chao 1 index (B) of untreated and treated
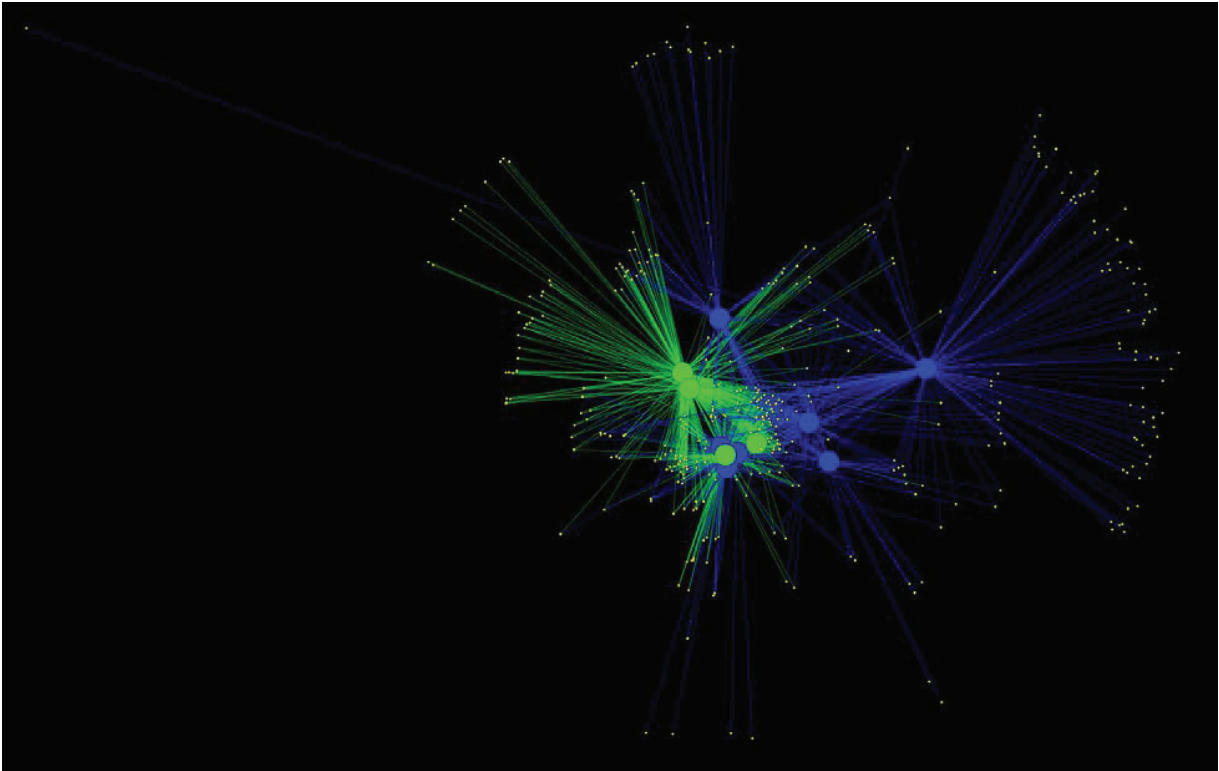*S.littoralis* gut microbiome (Monte Carlo permutations, n.s.- not significant, n=7, ± 1 SD).

Figure 2. OUT network of treated and untreated *S.littoralis* gut microbiome ▇▇▇ samples of treated with salicin gut microbiome, ▇▇▇ untreated gut microbiome, ▇▇ OTUs (Layout: Edge-Weighted Spring Embedded).
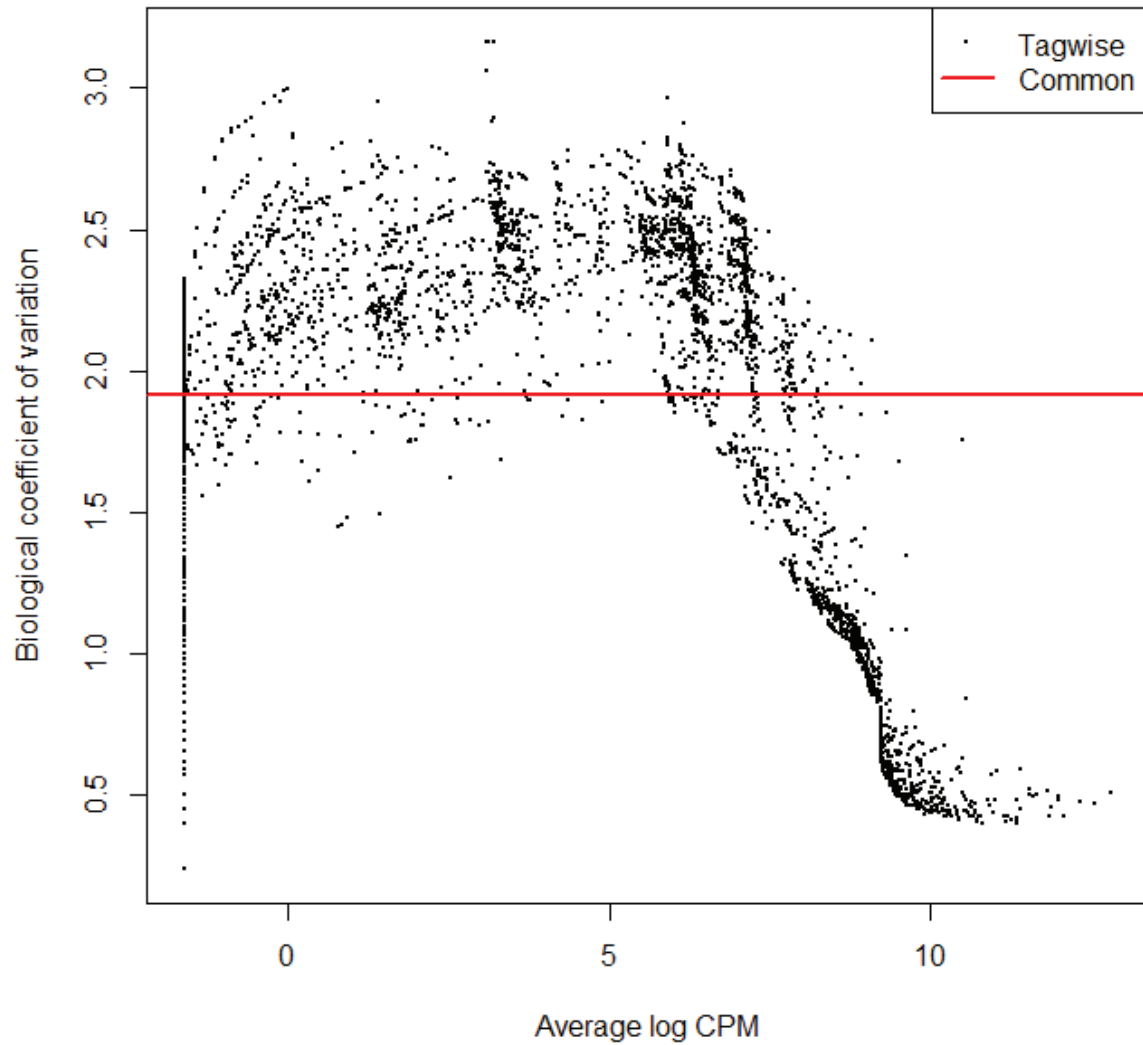
Figure 3. Biological coefficient of variation of gene predicted by PICRUSt and they relative abundance in count-per-million (CPM).
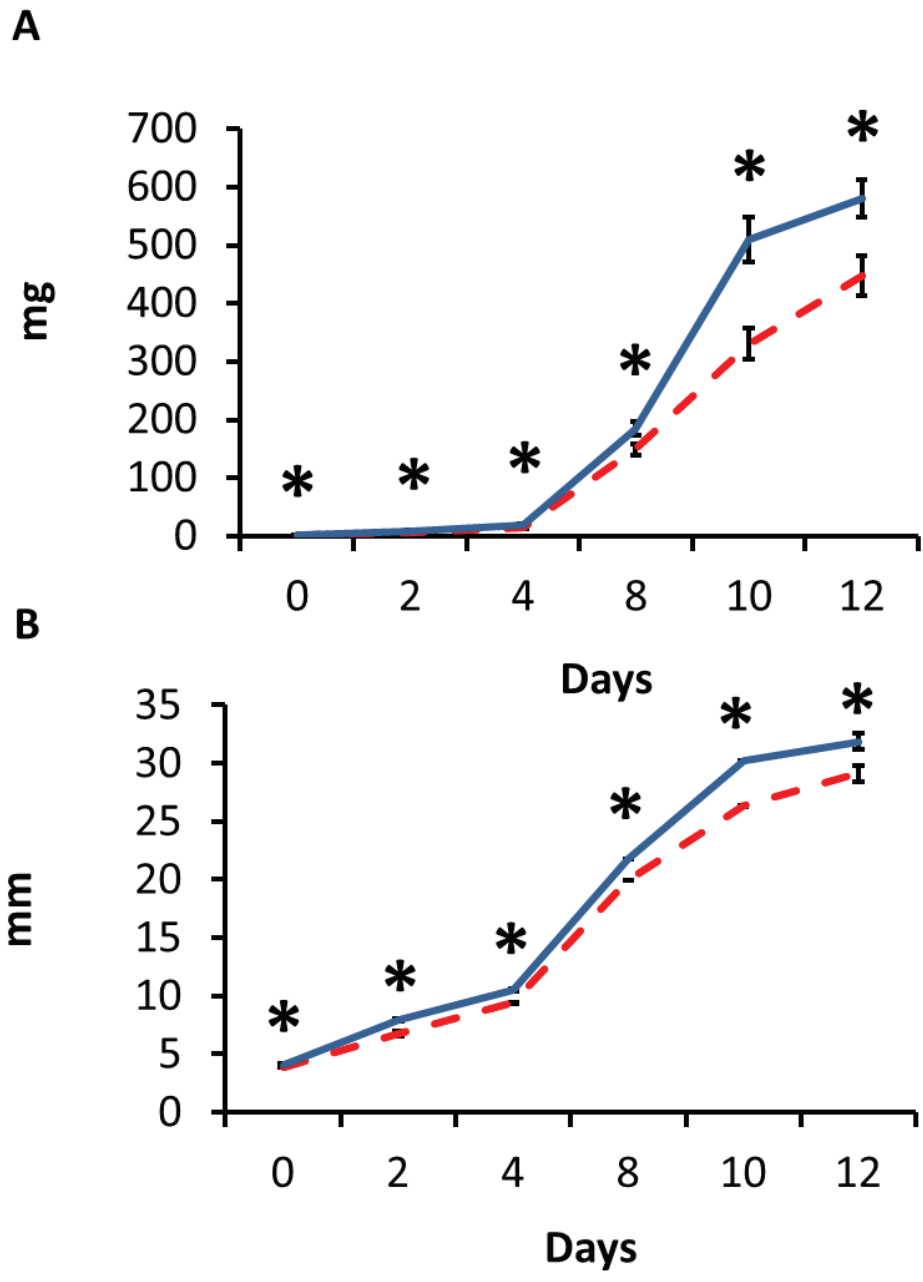
Figure 4. Effect of the plant secondary metabolite salicin 1.03% on the body weight (A) and length (B) of *S. littoralis* larvae over time (━ ━), compared to the control (━━), one-way Anova, Dunnett's post test, *p < 0.05; ±1 SD, n = 20.